RAPID, HIGH SENSITIVITY CAPILLARY SEPARATIONS FOR THE ANALYSIS OF BIOLOGICALLY ACTIVE SPECIES

by

Suminda Hapuarachchi

_____

A Dissertation Submitted to the Faculty of the

DEPARTMENT OF CHEMISTRY

In Partial Fulfillment of the Requirements
For the Degree of

DOCTOR OF PHILOSOPHY

In the Graduate College

THE UNIVERSITY OF ARIZONA

2 0 0 7

THE UNIVERSITY OF ARIZONA
GRADUATE COLLEGE

As members of the Dissertation Committee, we certify that we have read the dissertation prepared by Suminda Hapuarachchi

entitled Rapid, High Sensitivity Capillary Separations for the Analysis of Biologically Active Species

and recommend that it be accepted as fulfilling the dissertation requirement for the Degree of Doctor of Philosophy

_____Date: 4/27/07
Dr. Craig A. Aspinwall

_____ Date: 4/27/07
Dr. Bonner M. Denton

_____Date: 4/27/07
Dr. Mary J. Wirth

_____Date: 4/27/07
Dr. Dominic V. McGrath

_____Date: 4/27/07
Dr. Indraneel Ghosh

Final approval and acceptance of this dissertation is contingent upon the candidate's submission of the final copies of the dissertation to the Graduate College.

I hereby certify that I have read this dissertation prepared under my direction and recommend that it be accepted as fulfilling the dissertation requirement.

_____Date: 4/27/07
Dissertation Director: Dr. Craig A. Aspinwall

STATEMENT BY AUTHOR

This dissertation has been submitted in partial fulfillment of the requirements for an advanced degree at The University of Arizona and is deposited in the University Library to be made available to borrowers under rules of the Library.

Brief quotations from this dissertation are allowable without special permission, provided that accurate acknowledgement of source is made. Requests for permission for extended quotation from or reproduction of this manuscript in whole or in part may be granted by the head of the major department or the Dean of the Graduate College when in his or her judgment the proposed use of the material is in the interests of scholarship. In all other instances, however, permission must be obtained from the author.

SIGNED: Suminda Hapuarachchi

ACKNOWLEDGMENTS

I wish to express my appreciation and thanks to Dr. Craig A. Aspinwall, my graduate advisor, for his valuable guidance, support and advice and the great amounts of time given to me in this endeavor. I am truly thankful for him giving me the freedom to work in the lab and the giving me resources to achieve my research goals. I thank current and past Aspinwall group members for their support given to me during the past five years at the University of Arizona. I would also like to thank my dissertation committee members for their support and encouragement. I would like to thank the faculty who have taught me in the graduate school and the Department of Chemistry for giving me the chance to pursue my Ph.D. studies at U of A. I would like to express my sincere gratitude to the American Chemical Society, J & J Pharmaceuticals and Pfizer for funding.

I would like to thank Lee Macomber and Ed Autz in the Chemistry Machine Shop and Marcus Perry in the Chemistry Electronics Facility for their support. I appreciate the support from Nick Cellar at University of Michigan for his assistance with the sheath flow instrumentation. I thank Stephanie Gage for providing me with *Manduca sexta* samples.

Special thanks go to my parents and my family for their love, support and encouragement given to me and for bringing me to this level. Finally, I thank my wife for being so patient and supportive throughout my studies and my daughter for her love. Thanks to everyone who offered their support and the encouragement during my graduate work.

DEDICATION

To my parents and my wife for their unconditional love and support

TABLE OF CONTENTS

TABLE OF CONTENTS – *Continued*

TABLE OF CONTENTS – *Continued*

TABLE OF CONTENTS – *Continued*

TABLE OF CONTENTS – *Continued*

LIST OF FIGURES

LIST OF FIGURES – *Continued*

LIST OF FIGURES – *Continued*

LIST OF FIGURES – *Continued*

LIST OF FIGURES – *Continued*

LIST OF FIGURES – *Continued*

LIST OF FIGURES – *Continued*

LIST OF FIGURES – *Continued*

LIST OF TABLES

ABSTRACT

A series of rapid, high sensitivity capillary electrophoresis (CE) separation systems have been developed for the analysis of biological analytes and systems. A majority of the work has focused on development of novel instrumentation, in which new injection and detection strategies were investigated to improve the sensitivity of fast CE.

A novel optical injection interface for capillary zone electrophoresis based upon the photophysical activation of caged dye attached to the target analyte was developed. The primary advantage of this approach is the lower background and background-associated noise resulting from reduced caged-fluorescein emission in conjunction with the high quantum yield of the resulting fluorescein. Improved detection limits were obtained compared to those observed in photobleaching-based optical gating.

A primary drawback of photolytic optical gating CE is the lack of available caged-dye analogs with sufficiently fast reaction kinetics for online derivatization. To overcome this limitation, we have developed a chemical derivatization scheme for primary amines that couples the fast kinetic properties of o-phthaldialdehyde (OPA) with the photophysical properties of visible, high quantum yield, fluorescent dyes. The feasibility of this approach was evaluated by using an OPA/fluorescent thiol reaction, which was used to monitor neurotransmitter mixtures and proteins.

The utilization of a high power ultraviolet light emitting diode for fluorescence detection (UV-LED-IF) in CE separations has been introduced to analyze a range of environmentally and biologically important compounds, including polyaromatic hydrocarbons and biogenic amines, such as neurotransmitters, amino acids, proteins and

peptides, that have been derivatized with UV-excited fluorogenic labels, e.g. o-phthaldialdehyde/β-mercaptoethanol.

To understand cellular chemistry, it is imperative that single cells should be studied. This work was focused on developing CE based method to characterize the cellular uptake of TAT-EGFP. We demonstrated TAT mediated delivery of EGFP protein into HeLa cells and TAT-EGFP loaded single cell was analyzed by CE-LIF to determine the intracellular EGFP content.

An application of CE-LIF for the determination of biogenic amine levels in the antennal lobes of the *Manduca sexta* is also explored and methods were developed to analyze a single antennal lobe dissected from moths. The lobe was digested and contents were labeled with the fluorogenic dye prior to CZE analysis.

CHAPTER 1. INTRODUCTION

1.1 Introduction to Capillary Electrophoresis

Though Hjerten first utilized narrow diameter tubes (300 µm) to perform electrophoresis in 1967,[6;7] only a few reports[8-10] on open tubular electrophoresis were published until the 1981 ground breaking research by Lukacs and Jorgenson.[11] The application of narrow bore glass capillaries (<100 µm inner diameter) for high efficiency electrophoretic separations revolutionized the field of separation, giving birth to modern capillary electrophoresis (CE).[11;12] The use of < 100 µm i.d. capillaries allowed for utilization of high voltage, which markedly improved separation efficiencies. Also, the application of fluorescence detection significantly enhanced sensitivity. Since their initial publication, the sophistication and utilization of CE has grown exponentially, such that CE is now a commonly used separation technique for a wide range of investigations.[13] This growth has been fueled by the contribution of researchers from numerous backgrounds who have explored various aspects of CE methodology and instrumentation including novel detection strategies, injection methods and new applications.[14-24] In fact, CE has become the method of choice for low volume separations over the past 25 years. Due to the inherently high separation efficiency and mass sensitivity, CE is routinely used to analyze complex biological and environmental samples. The utilization of narrow bore capillary columns in CE facilitates separations using high voltages while maintaining effective heat dissipation from the capillary walls to minimize excessive band broadening. Various forms of CE such as free zone, micellar, gel, isotachophoresis and isoelectric focusing, have broadened the application of CE to analytes with a wide

range of properties, e.g. charged and uncharged molecules. A large body of literature, in which the application of CE has stretched from small ions to large molecules including proteins, peptides, and DNA has been published.[20;22;25] With the remarkable development of CE, it has gradually been accepted outside research laboratories, where HPLC and gel based techniques are frequently utilized for routine analytical separations. CE, however, has proved its worth by demonstrating separation quality superior to that of HPLC or gel electrophoresis due its high resolution and high speed.[11] Hence, it has emerged as one of the frequently used techniques for protein analysis in biotechnology.[26-28]

CE has revolutionized genomic research during the last 15 years with a primary application in large scale DNA sequencing.[11;29;30] Recently, CE has been studied in the field of proteomic analysis[11;31;32] as it has the potential to overcome some of the limitations of slab-gel electrophoresis, which is predominantly used for protein separations. Its ease of automation has been the key advantage over slab gel electrophoresis. In addition, repeated sample analysis using a capillary and the capability of online sample detection are also attractive features of CE. CE has also been used to analyze single cell contents,[33;34] sub cellular components,[35] biopolymers including carbohydrates,[36] fatty acids,[37;38] lipids[39;40] and in online monitoring[41-45] applications of biologically relevant analytes. In addition, the analysis of complex biological samples that contain a large number of analytes (> 30) is not trivial with single separation technique such as CE and HPLC.[46-49] Hence, use of two-dimensional techniques, in which two orthogonal separation techniques are integrated, is desired to obtain high resolution power. In these instruments, speed of the first dimension is usually slow

compared to the second dimension. Liquid chromatography is typically used in the first dimension while CE is utilized in the second dimension. As the modes of separation are different from each other, 2-D separation provides remarkable peak capacities. Multidimensional separations have been used to analyze glycoprotein factor in urine sample from cancer patients.[50]

Chemical monitoring applications demand real time sample analysis to map the dynamics within the system of interest. One of the main strengths of CE is the rapid separation capability while maintaining high resolution and efficiency.[18;51;52] Hence, separation-based sensors can provide a higher level of chemical information than the traditional single analyte optical or electrochemical sensors. The difficulty of dynamic chemical monitoring by CE is that temporal information is lost during conventional sample injection techniques where movement of the separation capillary from the buffer to the sample, is necessary. This limitation can be overcome by online sampling techniques such as optical gating and flow gating[47;51-53]. High temporal resolution is achieved using these online interfaces to couple the sample with the separation capillary. The goal of this research is to develop CE-based methodologies to analyze biologically important molecules with high sensitivity and high temporal resolution. In order to achieve this goal, a novel injection interface based on optical methods is developed, which is orthogonal to the existing photobleaching based optical gating technique. In addition, miniaturization of CE instrumentation and development of a novel fast labeling reaction for online chemical monitoring applications are also explored. The other area of

research is to develop instrumentation to study single cells using CE, the ultimate objective being to develop new approaches to understand cellular signaling processes.

1.2 Principles of Capillary Electrophoresis

1.2.1 Basic Instrument

Electrophoresis is a process by which charged molecules are separated under the influence of an applied electric field. The separation of two analytes requires that individual electrophoretic mobilities should be different for each analyte. Analyte mobility in an electric field is related to the charge to size ratio of the molecule. In general, electrophoresis has different modes of operation including gel electrophoresis, isoelectric focusing, isotachophoresis, and capillary electrophoresis. Some methods require running medium, which provides the mechanical support for the separation. The arrival of high performance CE provided a method for electrophoresis without a gel medium. CE offers many advantages over the gel-based techniques including ease of automation, repeatable sample introduction and analysis, and online detection that are lacking in gel electrophoresis. Since CE was developed, many variations to the technique have been introduced including capillary zone electrophoresis (CZE),[11;12] capillary gel electrophoresis (CGE),[54;55] capillary isoelectric focusing (CIF),[56-58] capillary isotachophoresis (CITP),[59-61] and micellar electrokinetic chromatography (MEKC)[62] (as describe below). Figure 1.1 illustrates the basic separation mechanisms associated with each variant of CE.

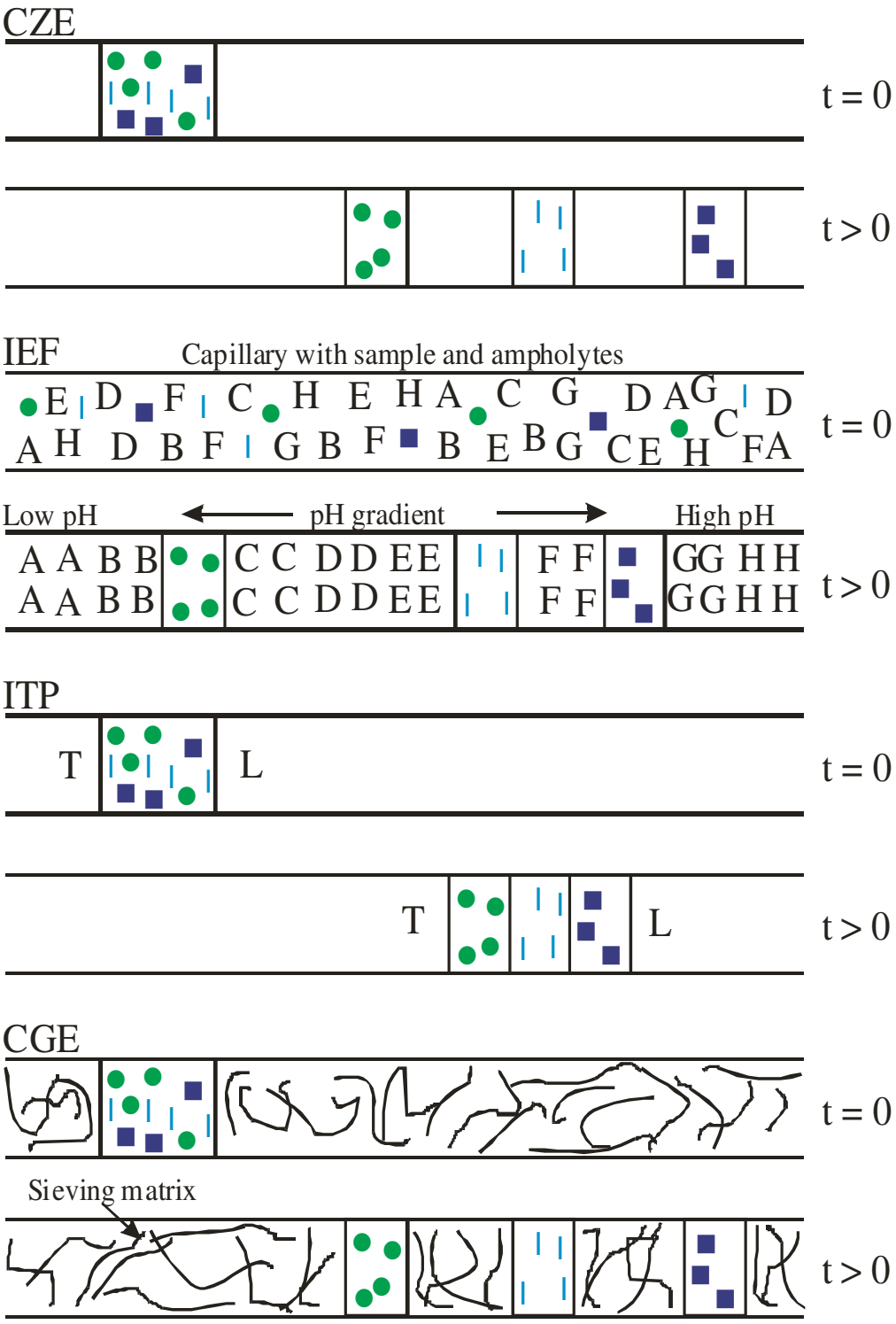

Figure 1.1. Schematic representation of modes of capillary electrophoresis.

1.3 Modes of Capillary Electrophoresis

1.3.1 Capillary Zone Electrophoresis (CZE)

CZE is the most popular mode of CE due to its simplicity and versatility. In this format, separation capillary is only filled with buffer and a potential is applied across the capillary after introducing a narrow plug of sample.[11] Different solutes migrate in discrete zones along the capillary due to differences in their mobilities, which are based on the charge to size ratios.[11;12] Analytes with different mobilities are separated from one another, and samples are detected at the other end of the separation capillary. Separation of both positively and negatively charged molecules is possible with CZE due to electroosmotic flow. However, CZE can not be used to separate neural solutes since neutral analytes elute with the EOF resulting in no separation. CZE is widely used in the analysis of amino acids, peptides, ions, drugs and enantiomers.[14;63;64] Basic theory behind CZE will be discussed in the following section in detail.[22;28]

1.3.2 Capillary Isoelectric Focusing (CIEF)

CIEF is a technique that is used to separate analytes based on their isoelectric point (pI value) similar to its gel counter part.[56] This is a high resolution separation technique and it is capable of separating protein and peptides with different pI units. The resolution of CIEF can be as low as 0.005 pI units. In CIEF, a pH gradient is formed along the capillary using ampholytes, which are zwitterionic molecules with a wide range of pI values.[65] The cathodic end of the capillary is kept in a basic solution while anodic end is kept in an acidic solution during the electrophoresis. After the sample injection, proteins or peptides migrate along the capillary in the presence of an electric field until

they reach the pH zone that matches the pI of the solute at which overall charge of the solute is zero. Once proteins stationed in their corresponding pI zones, zone focusing continues until the separation reaches steady state, at which no current flows through the capillary. Subsequently, analytes are mobilized and detected. Mobilization can be achieved by three methods: chemical mobilization, hydraulic mobilization and electroosmotic mobilization.[56;66;67] In chemical mobilization, chemical composition of one reservoir is changed by adding salt. For hydraulic mobilization, materials are moved by applying pressure, vacuum or siphon at one end of the capillary. EOF can also be used to move samples out of the capillary. To maintain the pH gradient steady during the focusing, EOF is needed to be minimized since it is possible to flush out the ampholytes inside the capillary before the completion of focusing. In CIEF, a large quantity of sample is loaded into the capillary and precipitation of the sample is a concern. One of the main applications of CIEF is to measure pI of different proteins and this technique is frequently used in industrial settings to separate different isoforms of proteins.[68]

1.3.3 Capillary Isotachophoresis (CITP)

In CITP, two buffers known as leading (L) and terminal (T) are used to create a voltage gradient during separation while constant current is maintained.[56] These buffers are selected in such a way that the leading buffer moves faster than the analytes and terminal buffer moves slower than the analytes. Therefore, the sample, which is not buffered, is sandwiched between the two buffers during the separation. Once the sample is injected, high voltage is applied. Then, analytes are separated into different zones but they remain between two buffers zones. In CITP, the separation is carried out at constant

current. Hence, zones stick together as they move along the capillary at the same terminal velocity. As the zone gets broader, resistance (R) increases, which makes the electric field for a given zone increases. This results in increased velocity and refocusing of the zone. As a result of this phenomenon, sharp boundaries between zones are always maintained. The sample is quantified by taking the length of the sample zone instead of the peak area or the peak height. CITP has been coupled to other analytic techniques such as CZE, MEKC and NMR as a preconcentration method.[69-71]

1.3.4 Capillary Gel Electrophoresis (CGE)

CGE is similar to the conventional slab gel electrophoresis since the both methods have identical separation mechanisms.[54] However, CGE offers a number of advantages over conventional method such as low joule heating, automation, on-column detection, small sample requirement, high mass sensitivity and high separation efficiencies. In CGE, the capillary is filled with a polymer, which functions as a molecular sieve. Hence, separation is mainly based on the size unlike in CZE. When the sample is injected into the gel filled capillary, analytes migrate through the polymer network, in which the movement of large analytes is hindered more than the small ones leading to the separation of analytes based on their mass. CGE is frequently used to analyze biomolecules such as DNA and SDS-saturated proteins.[72-75] The type of sieving polymer used for a given application depends on the solute.

1.3.5. Micellar Electrokinetic Capillary Chromatography (MEKC)

Neutral species in a sample can not be separated using CZE as they comigrate with EOF. MEKC, on the other hand, provides the mechanism to separate both charged

and neutral molecules in a sample. This method was introduced by Terabe in 1984 and it has become one of the most widely used electrophoresis techniques.[62] In MEKC, surfactants are added to running buffer to achieve the separation of neutrals. Surfactants form micelles above their critical micelle concentration (CMC) that can interact with neutral analytes while they migrate along the capillary. Neutral molecules interact with micelles with different dissociation constants, which facilitates their separation downstream. Solutes that interact more with the micelles retain longer during the separation while solutes that do not interact with the micelles elute faster. Sodium dodecyl sulfate (SDS, CMC = 8 mM) is a commonly used anionic surfactant in MEKC. Cationic surfactants have also been used in MEKC. Surfactants also interact with the capillary surface altering the EOF. Some of the applications of MEKC include the analysis of amino acids, nucleotides, aromatic hydrocarbons and polyaromatic hydrocarbons (PAHs).[76-79]

The instrumentation for both CZE and MEKC is simple. The main components are the separation capillary, a high voltage power supply, two buffer vials and a detector (Figure 1.2). CE systems can be easily built in the research laboratory setting and the instrumentation can be easily automated using commercially available interfaces. There are also various commercially available CE instruments. A polymer coated fused silica capillary (10 to 100 μm i.d.) provides the mechanical support and flexibility for the separation, with an optical window created by removing the polyimide coating for detection purposes. Depending on the application, the capillary is washed and subsequently filled with a running buffer prior to utilization for separations. The sample

is injected into the separation capillary at the opposite end relative to the detector either by hydrodynamic methods or by electrokinetic methods (described below). For the separation, both ends of the capillary are placed in buffer containers and high voltage is applied to two platinum electrodes in the buffer. Analytes are separated based on their electrophoretic mobilities and sample is detected at the end of the separation capillary. There are a number of frequently used detection methods including absorption, fluorescence, refractive index, conductivity and amperometric, which will be discussed later in the chapter.[80] The basic theory of CE will be discussed in the next section.

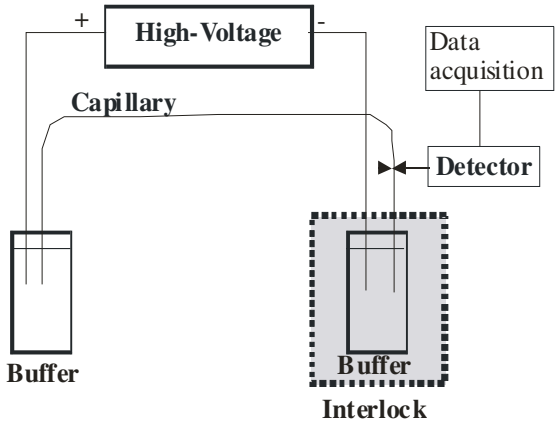

Figure 1.2. Schematic diagram of capillary electrophoresis instrument showing basic components.

1.4 Capillary Electrophoresis Theory

The difference in solute velocity in an applied electric field is used to separate charged analytes in electrophoresis. The movement of analytes in an electric field is determined by the electrophoretic mobility (μ_{ep}) of an ion, which is related to the linear velocity of analytes during electrophoresis. The theory can be more clearly presented considering the case of capillary zone electrophoresis, where analyte molecules are

separated in a buffer filled solution base solely on the electrophoretic mobility of the analytes. Analyte mobility is related to the balance between applied electric field (F_{EF}) and the frictional force (F_{FR}). F_{ER} is defined by the charge of the ion (q) and the electric filed strength (E, V/cm) as given by Equation 1.1.[11;81]

$$F_{EF} = qE \quad (1.1)$$

F_{FR} is the resistance that molecules experience as they move through solution during electrophoresis as given by Equation 1.2.

$$F_{FR} = 6\pi\eta r\nu \quad (1.2)$$

where η is the viscosity of the buffer, r is the radius of the solvated molecule and ν is the linear velocity of the analyte (cm/s).

At equilibrium, the applied electric force and the frictional force are equal and this results in migration of ions at a constant terminal velocity. The following shows the relationship between the electrophoretic velocity (ν_{ep}) of ions and the applied electric field (Equation 1.3).

$$\nu_{ep} = \left(\frac{q}{6\pi\eta r}\right)E \quad (1.3)$$

Hence, $\left(\frac{q}{6\pi\eta r}\right)$ is defined as the electrophoretic mobility (μ_{ep}, $cm^2/V.\ s$) and it is specific for a given molecule of charge (q) and size (r).

$$\nu_{ep} = \mu_{ep} E \quad (1.4)$$

The velocity of the separation (Equation 1.4) can be enhanced linearly by application of high E defining a primary advantage of CE. It is important to note that μ_{ep}

is directly proportional to the charge of the analyte and inversely proportional to both the viscosity of the buffer and the radius of the analyte.

In addition to μ_{ep}, another factor is present in aqueous solution and effects the overall separation speed, quality, efficiency, etc. It is electroosmotic flow (EOF). Unlike HPLC, CE does not have applied pressure, but rather "pumping" is provided by EOF. Bulk movement of the buffer is caused by the zeta potential (ζ) at the silica/water interface.

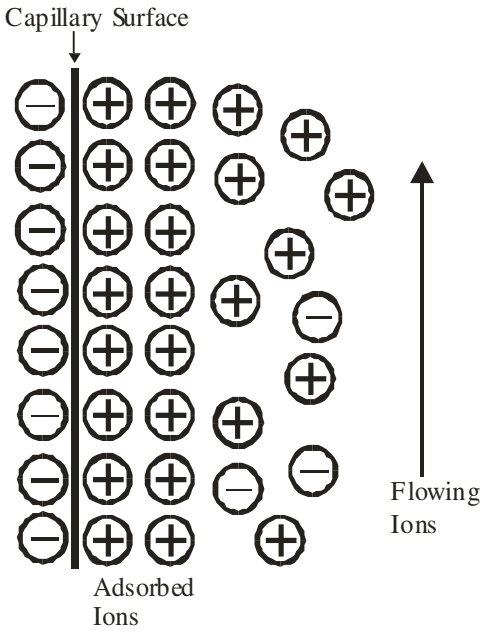

Figure 1.3. Representation of electroosmotic flow due to Stern double layer at the capillary surface.

The silanol (Si-OH) groups that line the inner surface of fused silica capillaries can be ionized at pH above 2. When the surface is washed with a basic solution, ionized silanol groups attract positively charged ions, forming an electrical double layer know as the Stern layer (Figure 1.3),[82] which is typically several hundred nanometers in thickness.

The formation of an electric double layer creates a potential difference at the silica/water interface. The magnitude of the zeta potential dictates electroosmotic flow velocity (v_{EOF}).

At an applied electric field, the cations at the silica surface start to migrate to the cathode. Solvated cations drag the bulk solution creating a net flow toward the cathode. The velocity of EOF follows,

$$v_{EOF} = \left(\frac{\varepsilon_0 \varsigma}{4\pi\eta} \right) E \quad (1.5)$$

where ε_0 is the dielectric constant, η is the solution viscosity, E is the electric field strength and ζ is the zeta potential. Hence, μ_{EOF} can be expressed by Equation 1.6 and it is directly related to the zeta potential.[7;11;83]

$$\mu_{EOF} = \left(\frac{\varepsilon_0 \varsigma}{4\pi\eta} \right) \quad (1.6)$$

EOF, the main driving force in CE, generates a plug-like flow originating from the interaction of solvent with the capillary surface as opposed to the parabolic flow profile generated by a pressure driven system due to the shear force at the column wall (Figure 1.4 and Figure 1.5).[2;84] The plug flow has a flat velocity distribution across the capillary cross-section with a very small deviation of only a few nanometers. The unique flat flow profile contributes to low band broadening and aids in the remarkable separation efficiencies associated with CE.

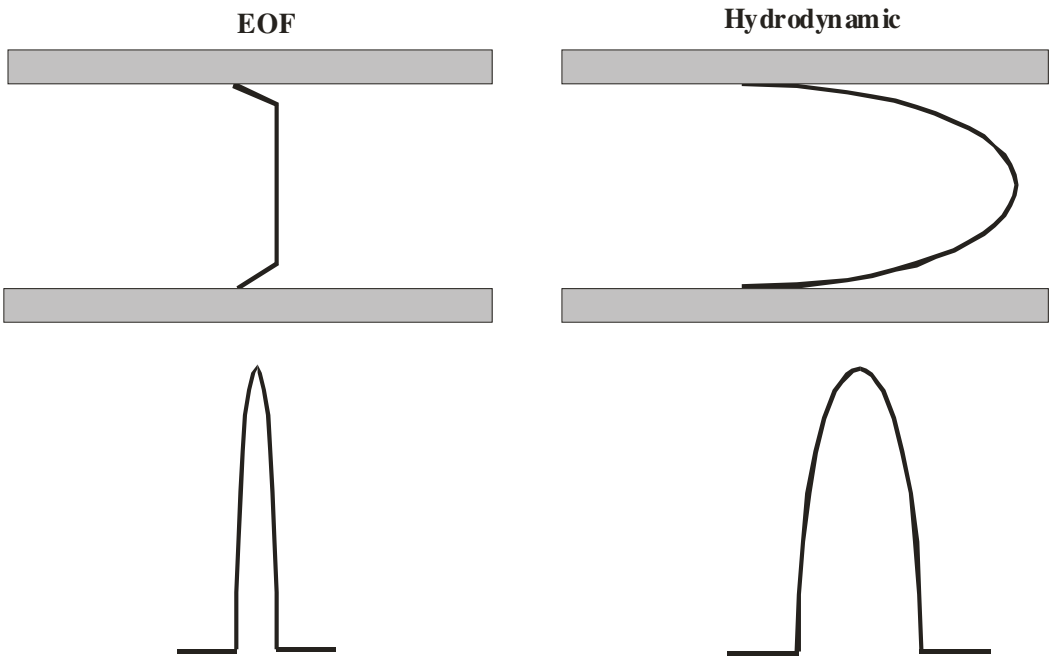

Figure 1.4. Representation of capillary flow profile and corresponding solute zone for electroosmotic and hydrodynamic flow.

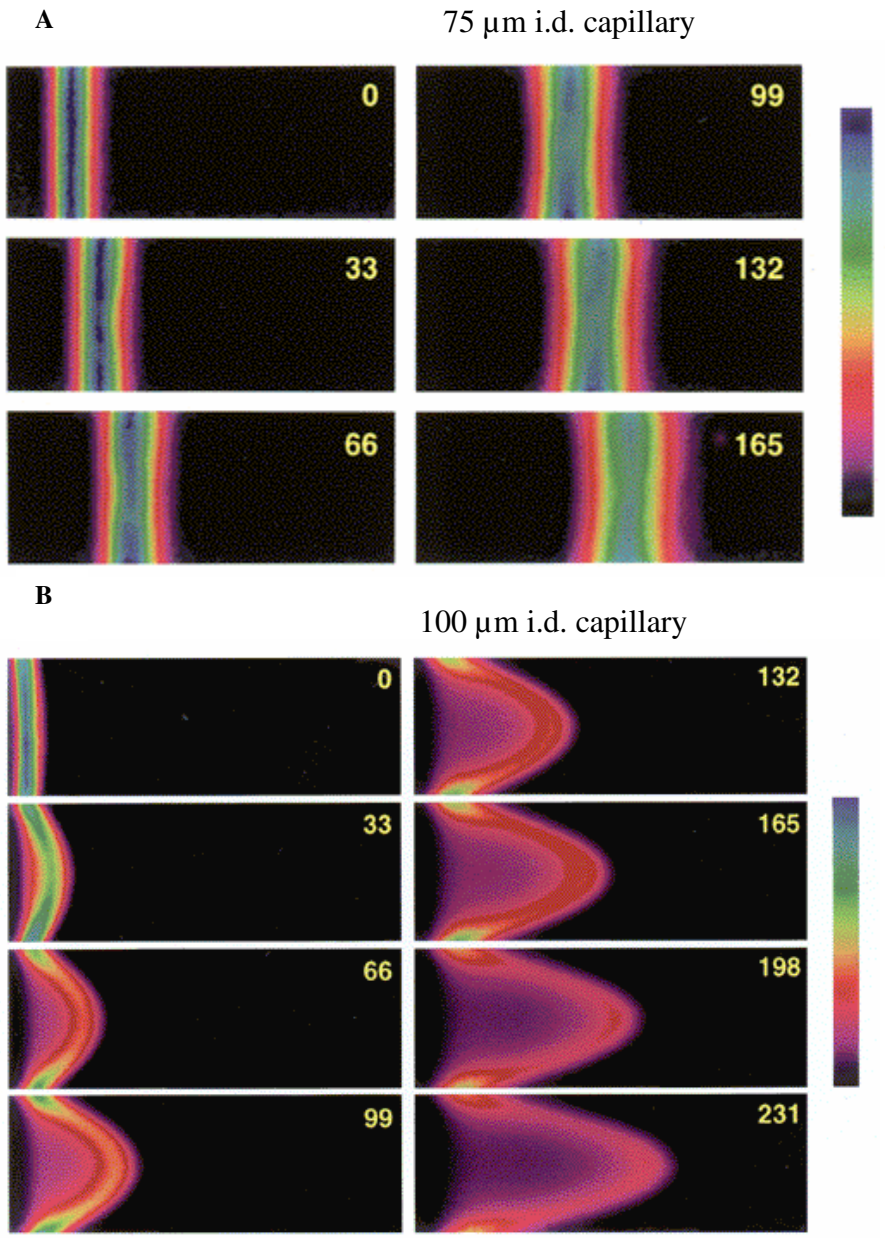

Figure 1.5. Images of electroosmotic (A) and hydrodynamic (B) flow. A fluorescent dye (caged-rhodamine) was imaged inside a capillary at different times during the migration to monitor the change in velocity profiles for electrokinetically driven and pressure-driven flow through an open tubular capillary column. Number on images is the time (ms) at which images were taken after the uncaging event. Reproduced with permission from the publisher. [2]

Given the two velocities associated with CE, the effective velocity, ν_{Total} of a given molecule is a vector sum of the electrophoretic mobility, ν and the velocity generated by the electroosmotic flow, ν_{EOF} (Equation 1.7). Similarly, effective electrophoretic mobility of a given molecule is the sum of both electrophoretic mobility and electroosmotic mobility as given by Equation 1.8 and Figure 1.6.

$$\nu_{Total} = \nu_{ep} + \nu_{EOF} \quad (1.7)$$

$$\mu_{Total} = \mu_{ep} + \mu_{EOF} \quad (1.8)$$

where μ_{Total} is effective electrophoretic mobility, μ_{ep} is the electrophoretic mobility and μ_{EOF} is the mobility due to electroosmotic flow. In order to detect molecules at the end of the capillary, it is imperative that the direction of an analyte's total mobility be toward the cathode. According to Figure 1.6, μ_{ep} for a cation is positive and for an anion is negative, while both experience the same μ_{EOF} regardless of charge. As μ_{EOF} is typically > μ_{ep}, both cations and anions migrate toward detector. This enables the detection of both species in the same separation as depicted in Figure 1.7.

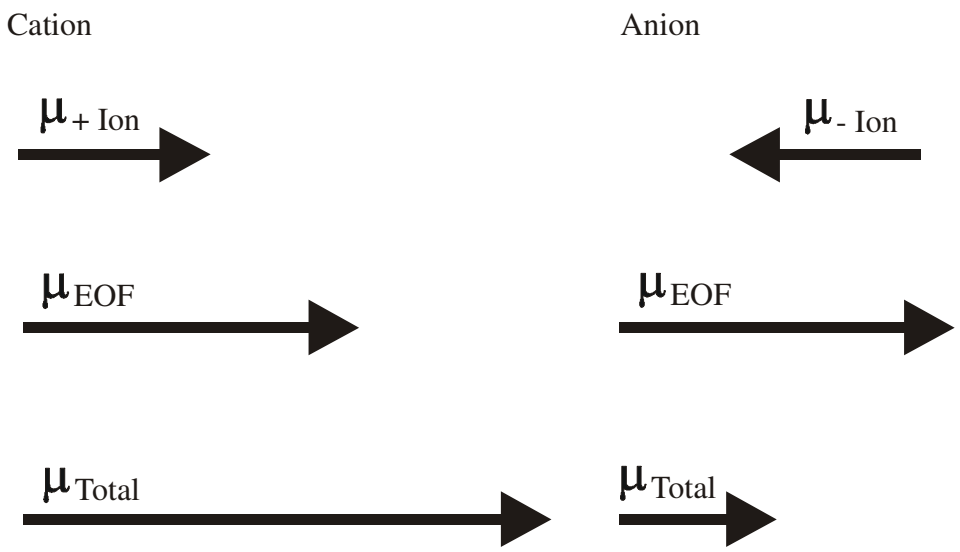

Figure 1.6. Total electrophoretic mobility. Total mobility (μ_{Total}) is the vector sum of electroosmotic mobility (μ_{EOF}) and electrophoretic mobility (μ_{ep}) for a given analyte.

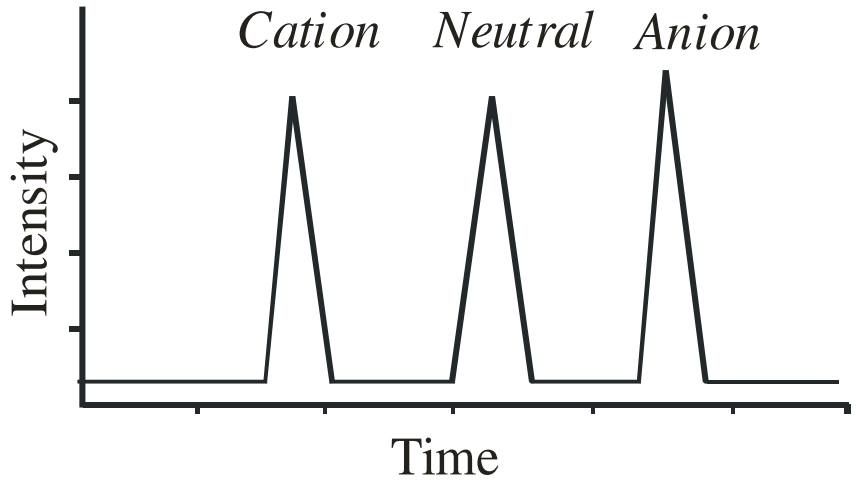

Figure 1.7 Typical migration order of solutes in capillary zone electrophoresis.

$$H \approx A + \left(\frac{B}{u_x}\right) + Cu_x \quad (1.9)$$

where H is the plate height, u_x is the linear flow rate and A, B, and C are constants.

CE provides very high efficiency and resolution. As predicted by the van Deemter equation (Equation 1.9),[85;86] there are three ways that peaks broaden in chromatography including multiple flow path (A term), longitudinal diffusion (B term) and mass transfer (C term). CE uses open tubular capillaries without packing material, thereby band broadening associated with A and C terms can be disregarded making the diffusion (B term) the main source of band broadening. As for all separations, the efficiency of CE separations is defined by the number of theoretical plates (N). As for CE, the number of theoretical plates is mainly related to the longitudinal diffusion as discussed by Jorgenson and Lukacs (Equation 1.10).[11]

$$N = \frac{\mu_{Total} V_1}{2D} = \frac{(\mu_{ep} + \mu_{EOF}) V_1}{2D} \quad (1.10)$$

where N is the number of theoretical plates, μ_{Total} is the total effective electrophoretic mobility, V_1 is the fraction of voltage (V) drop between point of sample injection and detection and D the diffusion coefficient of the molecule ($cm^2\ s^{-1}$). Equation 1.10 implies that high efficiency is directly proportional to the μ_{Total} of the analyte, i.e. the faster the molecules migrate, the better the separation efficiency. As Equation 1.10 suggests, increasing μ_{EOF} is one way to achieve a high number of theoretical plates. V_1 can be expressed as

$$V_1 = V\left(\frac{l}{L}\right) \quad (1.11)$$

where l is the distance to the detector and L is the total capillary length. By combining Equation 1.11 with Equation 1.10, we can write N as

$$N = \frac{\mu_{Total} l}{2D}\left(\frac{V}{L}\right) (1.12)$$

This indicates that high filed strength must be maintained to obtain maximum efficiencies. Monnig and Jorgenson have shown that high efficiency separation can be achieved with CE by using high voltage (Equation 1.12). Consequently, high voltages result in high speed separation. Hence, it is apparent that high voltage is important in getting maximum efficiency in a short time. On the other hand, very high efficiencies (> 10^6 plates/m) are possible by using shorter capillary with very high field strengths (> 1-2 kV/cm) as demonstrated by Jorgenson and coworkers.[51;52]

The number of theoretical plates can be calculated using the peak migration time (t) and the full width at half maximum ($w_{1/2}$) as given in Equation 1.13. This Equation is only valid for peaks with a Gaussian peak profile, otherwise asymmetry associated with peak should be taken into account in the calculation.

$$N = 5.545\left(\frac{t_m}{w_{1/2}}\right)^2 \quad (1.13)$$

If the calculated plate number from Equation 1.12 and Equation 1.13 is compared, N obtained from Equation 1.13 is more descriptive than the numbers obtained using Equation 1.12. Thus, it is clear that factors associated with band broadening other than longitudinal diffusion, are important for CE separation. Other factors affecting the efficiency are discussed in the next section, in which minimizing band broadening due to various sources is discussed in order to achieve diffusion limited separations (Equation 1.12). In conventional CE, separation of a sample can be achieved between 5 and 30 min,

but for chemical monitoring applications, rapid separation is required as the chemical processes occur rapidly. Hence, the theory and other requirements, achieving highly efficient and fast separations are discussed here, since part of this research was focused on developing high speed capillary techniques for biological analysis. According to Equations (1.12, 1.13), separation efficiency is independent of column length and proportional to voltage while migration time is inversely proportional to the voltage. Consequently, shorter capillaries can be used without increasing the applied voltage, allowing for short separation times while maintaining the same efficiency. Separation time of a charged analyte can be determined by simply dividing the length of the capillary (L) by the linear velocity (ν_{Total}). By replacing linear velocity with total μ_{Total} of the molecule, the relationship between migration time and the applied voltage can be drawn (Equation 1.14).

$$t = \frac{L}{\nu_{Total}} = \frac{L^2}{\mu_{Total} V} \quad (1.14)$$

Even though basic CE theory predicts that the only source of band broadening is from longitudinal diffusion, there are other dispersive processes associated with CE. In order to achieve diffusion limited separation, all the other processes have to be minimized. Efficiency of separation (N) can be expressed (Equation 1.15) in terms of all the other band broadening processes.

$$N = \frac{t_{Mig}^2}{\sigma_{Tot}^2} \quad (1.15)$$

where σ^2_{Tot} is the total zone variance associated with all the sources of band broadening and t^2_{Mig} is the migration time. The total zone variance can be defined as

$$\sigma^2_{Tot} = \sigma^2_{Diff} + \sigma^2_{Inj} + \sigma^2_{Det} + \sigma^2_{Heat} + \sigma^2_{Ads} \quad (1.16)$$

where σ^2_{Diff} is the variance due to longitudinal diffusion, σ^2_{Inj} is the variance due to injection, σ^2_{Det} is the variance due to detection, σ^2_{Heat} is the variance due to joule heating and σ^2_{Ads} is the variance due to adsorption. For fast separations with very short migration times, it is difficult to achieve diffusion limited separations. Although the variance due to diffusion decreases with fast migration times, contributions from other sources of band broadening can increase with high voltage. One of the significant sources of band broadening in fast separations is joule heating. Individual sources of band broadening and current practices to minimize their effects will be discussed in the following section in detail.

One consequence of high voltage is heating known as Joule heating. Heating results from a constant current, which passes through the capillary during the separation and can create a temperature gradient across the capillary diameter if the heat is not properly dissipated by the capillary wall. Joule heating increases with increasing current flow through the capillary, which is proportional to the applied voltage. This could affect the separation efficiency in various ways, including convective mixing, zone broadening, viscosity changes in the buffer and variation in migration time. The temperature difference between the center of the capillary and the surrounding media depends on the inner diameter, wall thickness of the capillary, and the efficiency of the heat transfer. The

magnitude of the thermal gradient is directly proportional to the square of the capillary radius (r^2).[87] By using small inner diameter capillaries with thick walls for separation, Joule heating can be minimized due to improved heat dissipation from capillary walls. On the other hand, utilization of small capillaries limits the amount of current through the capillary due to high resistivity minimizing the heat generation. Hence, for fast capillary separations, high voltage (1.5 kV/cm - 3 kV/cm) and 5 - 10 µm i.d. capillaries are used. One of the disadvantages of utilizing small diameter capillaries is the requirement of highly efficient injection schemes and detection systems. Having low conductive buffers can also reduce the amount of current generated during separation minimizing Joule heating effectively.[88] Low conductive buffers are particularly attractive in the case of utilizing large diameter capillaries for fast separations.

Wall adsorption of analytes also degrades the separation efficiency and leads to irreproducible migration times.[89] The negative surface of the separation capillary interacts with positive charged analytes or analytes with positively charged domains leading to non-equilibrium effects during electrophoresis. Analyte adsorption leads to retention during the separation, which is considered to be a major source of band broadening during the separation of large analytes such as proteins and peptides. As mentioned above, capillary coating methods are utilized to minimize interaction between the capillary wall and molecules.[90-92]

When the separation is performed at high pH, high EOF may contribute to migration of analytes before they are separated resulting in low resolution. High charge density on the capillary surface can ultimately degrade the separation efficiency in which

case wall interaction between cationic molecules and cationic analyte leads to irreproducible migration times. This phenomenon is a major issue in the separation of basic proteins using CE. Analyte adsorption onto the capillary wall changes the EOF resulting in inconsistency in separation.[93;94] EOF can be controlled by changing the capillary surface to alter the zeta potential or altering the buffer viscosity. There are various methods of altering the EOF including reducing the double layer thickness by using high ionic strength buffers, or adding organic solvents to increase pK_a values of the silanol groups at the surface thereby decreasing the EOF.[95;96] In addition to changing the buffer viscosity, cationic surfactants have extensively been used to alter the zeta potential between the capillary surface and water interface. This approach, which is known as a dynamic capillary coating method, creates a layer of cationic surfactants on the capillary surface.[97;98] This can change the composition of the interface creating reversed EOF. Some commonly used additives are cetyltrimethyl-ammonium bromide (CTAB) and tetradecyl-trimethyl-ammonium bromide (TTAB).[99;100] There are other types of chemicals that are used for capillary coatings both in the form of permanent or dynamic type coatings.[90;91;101;102]

The variance due to injection has the potential to be a key source of band broadening in fast separations. Utilization of short capillaries for fast separations puts a great demand on the injection step where high reproducible injection methods that are capable of delivering a very small plug (pL to fL volumes) of samples are required. To achieve such small injection volumes, new online injection methods have been investigated and will be discussed in the following section.[18;51;52]

The variance due to detection is minimized using high sensitive detection methods. High mass sensitivity is necessary for fast separation applications because very small sample plugs are injected. Fluorescence is the detection method of choice in such applications due to its inherently high sensitivity. Specific details on detection methods are discussed in the following section.

The quality of the separation can be expressed in terms of the resolution of the system. Resolution (R) is a measure of the ability to separate analytes that migrate closely (Equation 1.13)[11;81]. When the separation is diffusion limited, which is the best case scenario, the maximum resolution in the separation is defined by

$$R = 0.177\left(\mu_{i1} - \mu_{i2}\right)\left[\frac{V}{D(\mu_{ave} + \mu_{EOF}}\right]^{1/2} \quad (1.17)$$

where μ_{i1},μ_{i2} are the mobilities of closely eluting analytes, μ_{ave} is the average electrophoretic mobility, μ_{EOF} is the electroosmotic mobility and V is the applied voltage. According to Equation 1.17, resolution is directly related to differences in the mobilities of closely eluting analytes and is inversely proportional to their total mobilities, which indicates that resolution can be affected by high analyte mobility. For fast separations, high voltage is required to decrease the migration time but at the same time, an increase in the μ_{Total} limits how fast the separation can be performed without sacrificing resolution (Equation 1.17). A high EOF might not be advantageous in such situations. Hence, while a high EOF is beneficial in obtaining high separation efficiency, control of EOF is necessary to attain optimal resolution during separation.

1.5 Injection Methods

Sample introduction to the separation capillary can be performed by many different methods. However, care must be taken to inject the sample in a reproducible way to maintain the quality of the separation. Otherwise, irreproducibility of injection can have deleterious effects on the limits of detection, efficiency and resolution. Injection methods can be categorized into two main groups such as off-line and on-line injections. A summary of the injection methods is given in the following section.

1.5.1 Off-line Injection

In off-line injection, the sample is injected by moving capillary from the running buffer and subsequently placing it in the sample to perform the injection by different techniques such as hydrodynamic or electrokinetic as discussed in the following section.

1.5.1.1 Hydrodynamic Injection

Hydrodynamic sample injection can be achieved by three different methods: gravity, pressure, and vacuum (Figure 1.8).[103;104] The volume of the sample (V_t, nL/s) injected per unit time by the hydrodynamic method is defined by the Poiseuille Equation (Equation 1.18).[103] In pressure injection, the capillary is kept in a pressurized sample vial to inject a plug of the sample into the separation capillary. Sample injection is controlled by manipulating applied pressure. For the vacuum injection, a vacuum is applied to the detection end of the capillary while the other end of the capillary is kept in the sample vial. In the gravity injection, the sample is held above the detection end of the capillary to be injected. By varying the height and the time, the amount of sample injected can be controlled. For all hydrodynamic injection approaches, the capillary must be moved from

the buffer reservoir in which electrophoretic separations are performed to the sampling vial to initiate sample injection. With hydrodynamic injection, the volume of sample loaded does not depend on the type of the sample, but rather is defined by the parameters in Equation 1.18.

$$V_t = \frac{\Delta P d^4 \pi}{128 \eta L} \quad (1.18)$$

where ΔP is the pressure drop, d is the capillary i.d, η is the solution viscosity, and L is the capillary length. For gravity injection, the pressure drop can be calculated by

$$\Delta P = \rho g \Delta h \quad (1.19)$$

where ρ is the density of the analyte solution, g is the gravity constant, and Δh is the height difference between the sample vial and the buffer container at the detection end.

1.5.1.2 Electrokinetic Injection

For electrokinetic injection, high voltage is used to facilitate sample introduction.[103;104] The injection end of the separation capillary is placed in the sample vial while the detection end of the capillary remains in the running buffer vial. A high voltage is then applied for a short time to load the sample. The volume of injection can be controlled by varying the field strength and the time of injection (Equation 1.20). In electrokinetic injection, sample bias can occur since the sample can be injected into the capillary both by EOF and by electrophoretic mobility.[105] It has been shown that mass of analyte injected directly depends on the electrophoretic mobility of the analyte (Equation 1.20).

$$Q = \frac{(\mu_{ep} + \mu_{EOF}) \pi r^2 V C t}{L} \quad (1.20)$$

where Q is the quantity injected (g or moles), r is the capillary radius, C is the analyte concentration, t is the injection time, L is the capillary total length and V is the voltage. The volume of sample injected (V_{inject}) can also be estimate by

$$V_{inject} = \frac{E_{inject}}{E_{separate}} \times \frac{t_{inject}}{t_{retention}} \times V_{capillary} \quad (1.21)$$

where E_{inject} and $E_{separate}$ are the injection voltage and separation voltage, respectively, t_{inject} and $t_{retention}$ are the injection time and migration time of the analyte, respectively, and $V_{capillary}$ is the volume of the capillary.

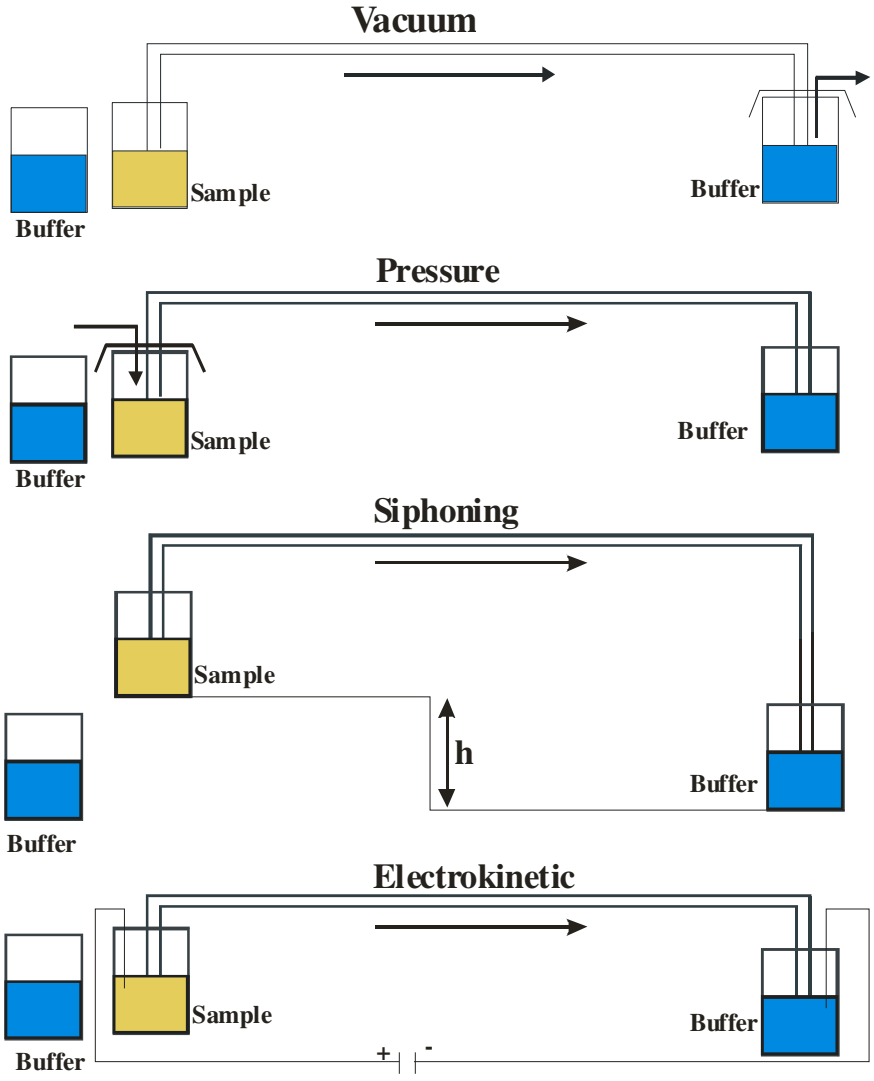

Figure 1.8. Conventional methods of sample injection in capillary electrophoresis.

1.5.2 On-line Injection (or Continuous Injection)

Conventional injection methods do not facilitate online injection, which is essential in chemical monitoring applications where fast separation is utilized to obtain time resolved measurements. As discussed previously, conventional methods require switching the capillary between the sample and the buffer, which leads to sample damage and severe temporal constraints. For fast separations, online injection methods are

preferred. When short and small i.d. capillaries are used, the total volume of the capillary is small (nL to pL) and the amount of analyte injected must be controlled to minimize excessive band broadening in the separation. Otherwise, a band broadening form injection can be significant.[51;106] The minimum allowable injection volume[107] is limited by the total column volume and the efficiency of separation (N) as shown by

$$V_{inject} = \frac{\Theta V_{column}}{\sqrt{N}} = \frac{\Theta}{\sqrt{N}}\left(\frac{\pi d^2 L}{4}\right) \quad (1.22)$$

where V_{inject} is the allowable injection volume, Θ^2 is the fraction of allowable peak broadening, V_{column} is the volume of the capillary and N is the number of theoretical plates. V_{column} is defined by inner diameter of the capillary (d) and length (L).[107]

For example, allowable volume of injection for a separation performed using a 10 cm long 10 µm i.d. capillary can be calculated by taking efficiency as 100 000 theoretical plates and allowable peak broadening by injection as 10 %, i.e. $\Theta = \sqrt{0.1} = 0.32$ and V_{column} as 7.8 nL. Hence, V_{inject} is calculated to be 8 pL. In fast CE separations, a short capillaries with small i.d are used, which puts a great demand in injection, leading to the development of a number of sampling and interface technologies, including: optical gating,[51;52] flow gating,[47;53] micromechanical valving,[108] capillary introduction[109] and integrated microfluidic gating[110;111] and flow-through microfluidic sampling[112;113].[114] Three main on-line injection methods are discussed in the following section.

1.5.2.1 Flow Gating

One of the most commonly used interfacing techniques is the flow gate interface (Figure 1.8), which allows continuous, low volume sample introduction.[41;42;47;53;115]

Briefly, the outlet of the reaction capillary and the inlet of the separation capillary are aligned adjacent to one another, 30-75 μm apart, in a Plexiglas block. A cross-flow comprised of separation buffer is continuously applied across the gap at the rate of 1 mL/min using a syringe pump to prevent analyte transfer between the two capillaries as depicted by Figure 1.9(a). Sample injection into the separation capillary is accomplished by temporary disruption of the cross-flow using a solenoid valve typically for < 1 s as shown by Figure 1.9(b). During the entire process, the separation capillary is maintained at constant high voltage, allowing electrokinetic injection of the sample when the cross-flow is stopped. One of the main advantages of this method is the ability to deliver a small plug of sample into the separation capillary without physically moving the capillary. Flow-gating-CZE has been used extensively for online monitoring, particularly when longer (> 100 ms) injection times are utilized.[44;100;116-118] Shorter injection times are limited by deviations in the switching valves used to stop the cross flow.[119] Further, increased band broadening is often observed in flow-gating due to the cross-flow at the sampling and injection capillaries.[119;120]

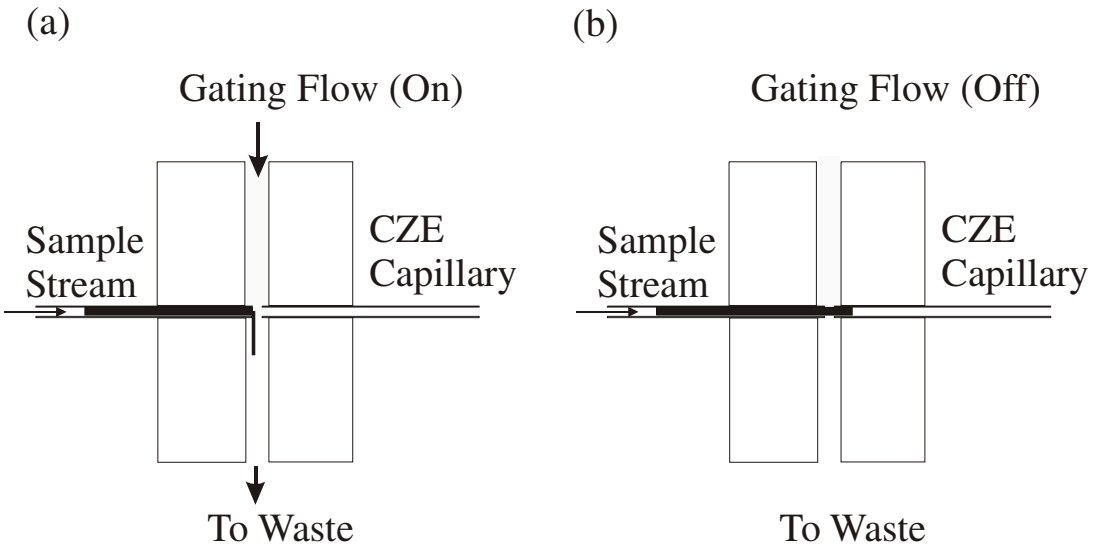

Figure 1.9. Schematic diagram of a flow gate. (a) When the gating flow is on, sample is prevented from entering the separation capillary and (b) sample is injected by closing the gating flow off thus allowing a plug of sample into the capillary, while applying high voltage to the separation capillary.

1.5.2.2 Optical Gating

For very fast injections and separations, optically-gated (OG) CZE is often employed. Developed by Jorgenson and co-workers,[43;45;51;52;115] OG sample injections provide the basis for the fastest and highest efficiency CZE separations reported to date.[51;52;106;121;122] In OG-CZE interfaces, the sample and separation capillaries are directly coupled or are constructed of one continuous capillary (Figure 1.10). Sampling is accomplished by continuously drawing fluorescently-labeled analyte into the separation capillary via EOF generated by application of a constant high voltage.[51;52;106] A high power laser beam (gating beam) focused near the entrance of the separation capillary is used to photobleach the sample rendering it optically transparent at an LIF detector positioned downstream as shown in Figure 1.10(a). Injection of small analyte plugs is accomplished by blocking the gating beam using a shutter for a short time as

depicted by Figure 1.10(b). The separation distance is defined by the distance between the gating beam and probing beam at the LIF detector, allowing short separation distances and thereby rapid separations.[51;52;106;121;123] Since OG-CZE provides on-column injections, narrow sample plugs can be continuously injected with high reproducibility .[51]

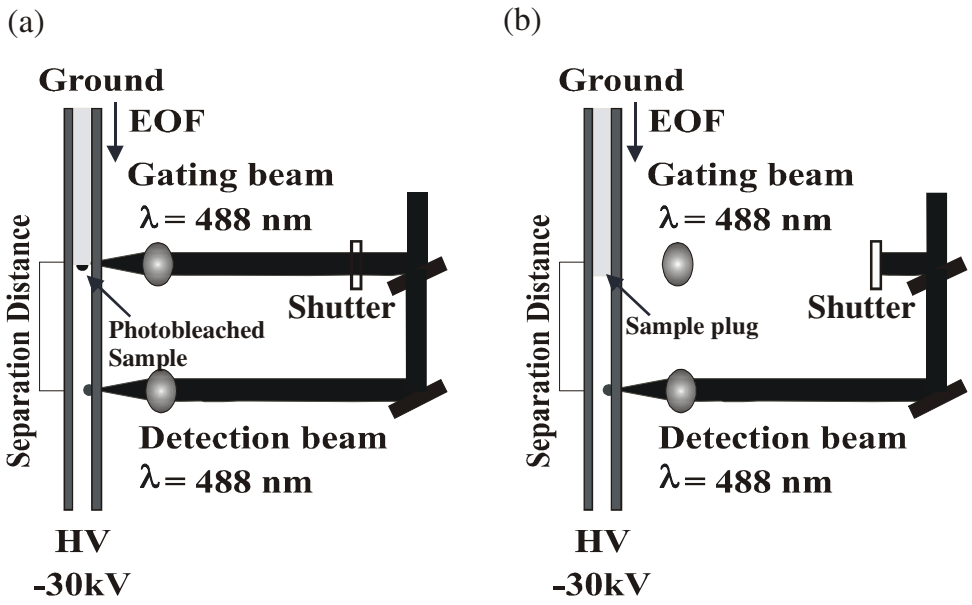

Figure 1.10. Schematic diagram of laser beam orientation for online photobleaching injection (OG-CE). (a) When the gating beam is focused onto the capillary, sample is photobleached making analytes undetectable at the detector and (b) sample is injected by blocking the gating beam for few ms allowing a plug of analyte into the capillary.

A primary drawback of photobleaching-based optical gating in CZE is the inefficient photodegradation of most common fluorescent probes, e.g. fluorescein,[51;52] and NBD,[123;124]even with very high power gating beams. This results in an increased fluorescence background, increased noise and reduced sensitivity. The resultant fluorescent background can be reduced by employing more easily photodegraded probes or by utilizing a fluorogenic probe that can be photoactivated from a non-fluorescent state

rather than photodegraded. The first of these approaches was utilized by Tao et al. for o-phthalaldehyde (OPA)/β-mercaptoethanol (β-ME) labeled amino acids with 351 nm injection and detection.[106;125] The resulting increase in sensitivity was achieved without an accompanying decrease in efficiency or resolution.[106] To reduce the background associated with OG-CZE and still utilize visible LIF detection, we have developed an approach based on the photochemical activation of caged-fluorescein (CF) derivatives. Sample injection was achieved using the combined 351-364 nm lines of an Ar^+ laser (Figure 1.11) to photoactivate the fluorogenic caged-fluorescein derivatized sample. High voltage was applied to the separation capillary continuously during the analysis allowing sequential sample introduction. When the CF is in the caged (non-fluorescent) form, derivatized samples were not detected by LIF although the samples continue to migrate past the detector as shown in Figure 1.11(a). To inject a sample plug by photophysical activation, the gating beam was focused into the capillary for a short time (5-20 ms) by opening a mechanical shutter as depicted by Figure 1.11(b). The uncaged, fluorescent analytes proceed to separate during the migration between the gating (photolysis) beam and the detection beam. In this geometry, the separation distance is dictated by the distance between the photolytic beam and the detection beam as shown in Figure 1.11.[126]

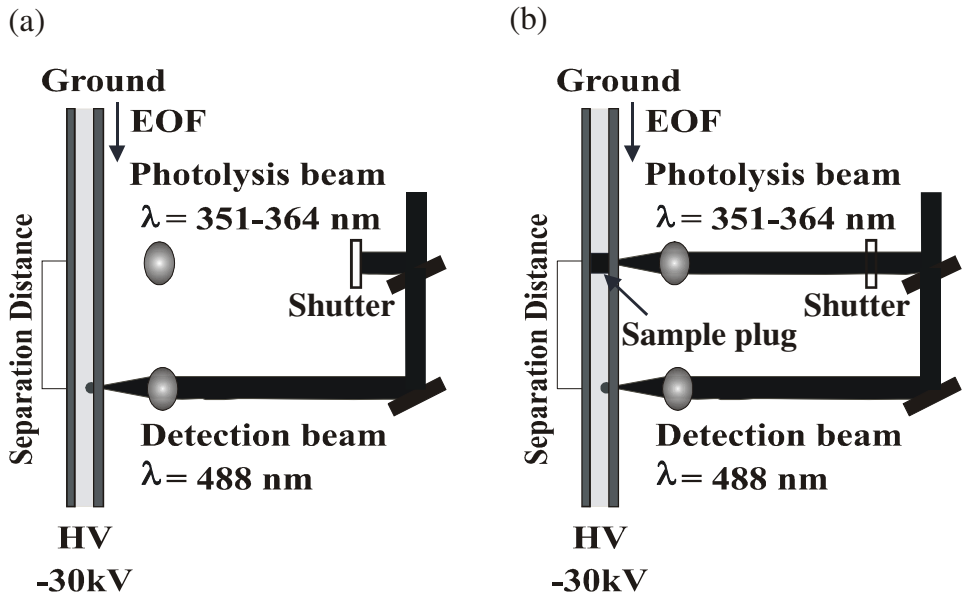

Figure 1.11. Schematic diagram of laser beam orientation for online photolytic injection in CE. (a) When the photolysis beam is blocked from the capillary, sample is undetectable downstream at the detector and (b) the sample is injected by photophysically activating caged probe by exposing it to the photolysis beam for a few ms introducing a fluorescence plug of analytes into the capillary.

1.5.2.3 Cross Injection

Microfabricated devices are also used for fast CE separations. These devices are produced using lithographic techniques in which a network of channels is formed on a substrate e.g. glass. These channels are utilized for separations and for sample handling purposes. In microchip-based devices, on-chip injection schemes have been developed to introduce sample into the separation channel since channels can not be moved physically like in CE to perform injection. Most commonly used method is the cross injection technique, which is done using T-type channel geometry as show in Figure 1.12. In cross injection, sample is electrokinetically pumped across the separation channel by applying high voltage between sample reservoir and the sample waste reservoir. After filling the intersection of channels, voltage is switched to the buffer reservoir and waste to inject the

sample plug trapped in the channel intersection. It has been shown that T-type injection valves can be used for rapid sample injection in fast chip capillary separations.[127]

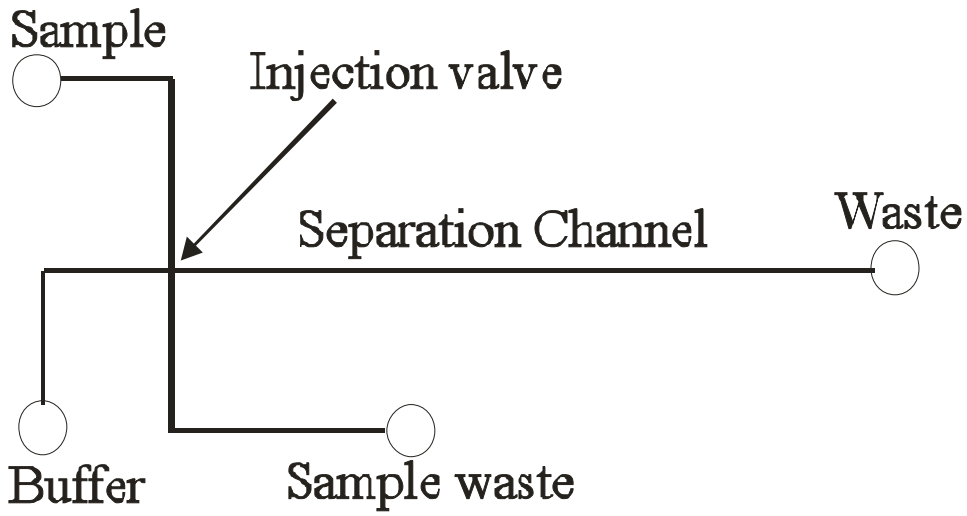

Figure 1.12. Schematic diagram of a microchip electrophoresis with T-type injection interface. When the voltage is applied across the sample reservoir and sample waste reservoir, sample is loaded into the intersection of channels. Then, voltage is switched to buffer and waste reservoirs to draw the sample plug trapped in the across.

1.6 Detection Methods

Detection in CE is demanding due to the capillary column dimensions and the small sample plug volumes e.g nanoliters to picoliters. CE also utilizes similar detection methods to those used in liquid column chromatography. The commonly used methods are absorbance detection, fluorescence detection, refractive index, conductivity detection, and amperometric detection.[13;80;128] Mass spectrometry is also emerging as a CE detection technique. Both off-column and on-column detection are used in CE. On-column detection is the most commonly used mode. Off-column laser induced fluorescence

detection is achieved by using a sheath flow cuvette while mass spectrometric detection is also achieved off-column.[13]

1.6.1 Absorption Detection

Absorption detection is a nearly universal detection method and both UV and visible light can be used due to the favorable spectral properties of fused silica capillaries, which have a transmission cut-off at 170 nm. This technique is predominantly used in commercial CE instrumentation. Light for the detection is obtained by a lamp, a light emitting diode (LED) or by a laser. The selected light is focused into the separation capillary and the difference in the absorbance coefficient between the analyte and the running buffer is utilized for detection. Absorbance measurements depend on the path length, which is defined by the capillary i.d., and usually less than 100 μm in CE. Hence, several efforts have been made to extend the path length without affecting the resolution. Those methods include utilization of a bubble capillary, utilization of a "Z" bend in capillary, and multiple reflections in capillary and absorbance measurements along the capillary axis.[129] The concentration detection limits using UV-Vis-CE for protein and small organic molecules is approximately 10^{-6} M, which is mainly limited by the size of the capillary.[128] However, UV-Vis-CE is not a universal detection method since inorganic salts and ions can not be directly detected. These ions do not possess high absorption coefficients. Indirect absorption detection in CE has been introduced as to overcome such limitations making UV-Vis detection universal. In indirect absorption, buffer additives with a high absorption coefficient are used. Therefore, high absorption from the buffer is always present during the analysis. When the sample is introduced, analyte zone dilutes

the concentration of the buffer additive in the background, which changes the background signal enabling the detection of the solute. LODs for indirect absorption detection CE is reported to be in the range of 10^{-6} to 10^{-5} M.[87;130] This method has been used to analyze inorganic ions[131;132], carbohydrates[133] and carboxylates[134].

1.6.2 Refractive Index Detection

Refractive index (RI), which is a bulk property, can be used in CE to detect analytes. RI detectors are universal and sample derivatization is not required. Since analytes can have different RI from the running buffer, RI detection is applicable for a wide range of analytes. Sensitivity of RI detection methods is also limited with the small optical path and also the small analyte volume. Capillary heating can create potential problems as RI is sensitive to temperature fluctuations.[135] Several efforts have been made to improve the sensitivity of this technique such as utilization of interferometric techniques and use of a holographic grating to detect RI.[136;137] Limits of detection for RI detectors in CE are still in the 10^{-6} M and this method has not been widely used due to its non-selective nature.

1.6.3 Conductivity Detection

Conductivity detection is typically used for ion analysis in CE as inorganic ions do not have intrinsic spectral properties, e.g. absorbance or fluorescence, but it can be used as a universal detector.[138] Sample analysis is performed indirectly by applying an electric potential between two electrodes in contact with the electrolyte solution (buffer) and the current flow through electrodes is a measure of the conductivity of the solution. As the analytes pass through the detector, the change in conductivity between the two

electrodes is used to quantify the sample. High voltage can create potential problems in conductivity detection generating a large DC potential between the electrodes. This could be combated by placing electrodes directly opposite from one another along the capillary.[139] Limits of detection for conductivity measurements can be in the range of 10^{-6} and 10^{-7} M and are primarily limited by the conductivity of the background electrolyte and the capillary size. When the conductivity of the background electrolyte is high, it is hard to measure the change in conductivity caused by the analytes. To enhance the conductivity difference between the analyte and the buffer, low conductivity buffers are used to reduce the high conductivity of the running buffer. With suppressed conductivity from the background, LODs can be improved by one order of magnitude. Recently, a new approach for conductivity measurements in CE has emerged to minimize interferences from the sample matrix. This approach is know as contactless conductivity detection (CCD), which was reported for the first time in two seminal papers by Bonn and coworkers and de Lago and coworkers in 1998.[140;141] In this method, two cylindrical electrodes are place along the capillary and the gap between the electrodes was around 2 mm. The two electrodes act as cylindrical capacitors, which are used to measure the conductivity of the solution in the space between the electrodes. As the analytes pass through the detection cell defined by the space between the electrodes, the change in conductivity due to the change in resistance in the background electrolyte is measured in order to quantify the sample during the separation. This method is becoming popular as it provides an alterative way to perform conductivity detection in CE without running into

potential problems associated with interferences from the background electrolyte. CE-CCD has been applied to detect inorganic ions with sensitivity in 200 ppb.

1.6.4 Amperometric Detection

Amperometric detection is used to analyze electrochemically active species in CE. Electrochemical methods are highly selective and sensitive. In amperometric detection, electron transfer occurs between the analyte and the electrode under the influence of DC voltage. This electron transfer is caused by a redox reaction at the electrode surface, which generates a current proportional to the analyte concentration. The current generated from the high voltage applied during separation can create potential interference with electrochemical detection though this can be prevented by proper electrical isolation of the electrode. Typically, this problem is overcome through the use a fractured capillary covered with porous glass at the ground potential creating a field-free section of the capillary while maintaining EOF.[142;143] In this arrangement, EOF is used to pump the analytes coming off the column toward the detector. Recently, electrochemical measurements have been made by positioning the working electrode immediately after the separation capillary to avoid the fabrication of a porous glass junction. Ewing and coworkers have extensively worked on amperometric detection in CE to analyze biologically relevant analytes.[144;145] They have reported single cell analysis by using CE with amperometric detection. These applications were mainly possible due to the high sensitivity of this method, which has detection limits in the range of sub-nM.

1.6.5 Mass Spectral Detection

Mass spectrometry provides structural information of analytes, which is not possible with other detection methods. Hence, significant efforts have been made to couple MS techniques to capillary electrophoresis (CE-MS) in recent years. One area of interest was to develop reliable interfaces that can effectively couple MS to CE since MS is an off-column detection technique which includes ion source, mass analyzer and the ion detector. One of the major concerns of using MS detection in CE was the non-volatile buffers used during the separation, which can potentially create background problems. There are three main approaches of coupling MS including coaxial configuration, liquid junction and sheathless.[23;146] Using these methods, ionization techniques such as electrospray ionization (ESI) and fast atom bombardment (FAB) have been used in CE-MS applications. CE-MS techniques are used to analyze a wide variety of sample containing inorganic ions, proteins, peptides, nucleic acids, drugs and metabolites.[23;146;147] On the other hand, problems associated with on-line coupling of MS can be alleviated by off-line methods, in which analytes are collected at the end of analysis and subsequently analyzed by MS. Off-line sample handling provides means to utilize other ionization techniques e.g. matrix-assisted laser desorption (MALDI).[148]

1.6.7 Fluorescence Detection

Fluorescence detection is used for measurements with high sensitivity and high selectivity. Since Jorgenson and Luckacs first reported fluorescence detection in CE in 1981, this technique has evolved into a frequently used detection method.[11] Later in 1985, laser induced fluorescence detection (LIF) was introduced by Zare and coworkers, in

which they utilized a helium-cadmium laser line to excite the sample instead of incoherent light sources.[149] Lasers are extensively used in fluorescence detection due to the quality of light, which can easily be focused to a spot the size of the capillary i.d.. LIF detection is predominantly used in the analysis of biological samples since it can provide zmol detection limits at pM concentrations or below.[150] With CE-LIF, single molecule detection and routine sub-aM detection limits are possible.[21] LIF detection is the only detection method used in this research. Hence, some of the basic components of LIF-CE systems are discussed in detail in the following section.

1.7 CE-LIF

The key to assembling a sensitive fluorescence detector for monitoring analytes in CE is the ability to optimize fluorescence signal while reducing the background to improve S/N ratio. Analyte fluorescence is generated by the absorption of excitation light followed by the emission of photons while traveling along the separation capillary. Typical CE systems with LIF have a light source for excitation, focusing optics, collection optics, and a photodetector. Various fluorescence detection approaches have been reported in the literature including on-column fluorescence detection[149], post-column sheath flow detection using sheath flow cuvette[150-153], and indirect on-column fluorescence detection [154;155]. On-column fluorescence detection is the most frequently used method though it suffers from background problems associated with scattering from the capillary walls. Post-column fluorescence detection has provided a way to reduce scatter and allows detection of single molecules due to its extreme mass sensitivity.

1.7.1 Light Sources

1.7.1.1 Lasers

For fluorescence detection, analytes should either possess a natural fluorophore or should be labeled with a dye to make it fluorescent. Choice of the laser depends on several criteria including the analyte absorption spectrum, Raman scattering, spectral quality of the laser light, laser power and noise. To obtain the maximum signal from the analyte, the absorption spectrum of the analyte or its derivatization reagent must be matched. If all analytes have similar absorption spectra, the choice of laser is trivial, but for analytes having different absorption maximum, laser selection should be made to accommodate optimal excitation for all analytes to achieve better detection limits.

There are several sources of background in LIF detection including scatter of the laser light from the capillary walls and Rayleigh & Raman scatter from the background electrolyte. Among those sources of scattering, the contribution from Raman scattering is the most significant compared to the other sources as the major Raman bands of H_2O typically fall close to the emission wavelength of the analyte. There are two primary Raman bands for water: 1640 cm^{-1} and 3400 cm^{-1}. For 488 nm laser excitation, these lines correspond to 585 nm for the 3400 cm^{-1} line and 530 nm for the 1640 cm^{-1} line.[17;156] Under ideal conditions, it is preferred that the analyte have a large Stoke's shift beyond 585 nm for 488 excitation, though for most dyes e.g. fluorescein isothiocyanate and a wide range of derivatization reagents, this is not the case. Hence, it is practical to select an excitation wavelength for which the emission wavelengths fall between two major Raman bands to avoid as much background scatter as possible. However, in the case of

the fluorescein based reagents, this problem is not completely minimized as the maximum emission of fluorescein derivatives is around 525 nm, at which Raman scatter from water is substantial with 488 nm excitation.

Other criterion for selecting a laser is the spatial mode quality, which is important in focusing the laser beam to a small spot in size similar to the capillary i.d.. With a tightly focused laser beam, separated sample can effectively be excited. Most continuous lasers e.g. Ar^+ and HeCd have high coherent beam profiles and can easily be focused down to a spot with a few micrometers beam waist while light from pulsed lasers can not be focused the same way due to their poor beam quality.

To obtain optimal S/N, laser power should be increased until S/N of the fluorescence signal is optimized. The fluorescence emission intensity is proportional to the intensity of the light absorbed by the analyte. According to a first approximation, high laser power for excitation is required to obtain Emission intensity. However, as the laser power for excitation is increased, background noise also increases. One of the reasons that lasers are used in fluorescence detection in CE is the shot noise limitation. When the system is running under shot-noise conditions the background noise rises with the square root of the laser power while detection limits vary inversely with the square root of laser power. In terms of optimizing laser power, the simplest strategy is to vary the excitation power until the highest S/N ratio is obtained.

For ultrasensitive fluorescence measurements, the power of the laser should be controlled to obtain efficient excitation. Otherwise, at high power levels, signal roll-off

begins due to optical saturation and photobleaching. Hence, care must be taken to minimize such problems. The condition for saturation is given by:[17]

$$1.632 \times 10^{-9} . \frac{r^2}{\tau_m \varepsilon \lambda P} \langle\langle 1 \quad (1.23)$$

where, r is the focused excitation beam radius (μm), τ_m is the measured fluorescence lifetime (ns), ε is the molar absorptivity, λ is the excitation wavelength (nm) and P is the incident power (mW).

For highly absorbing dyes, laser radiation should be kept below 10^5 W/cm^2 to avoid reaching saturation. Photodegradation can be minimized using low laser power or short exposure times. The latter can be reduced by adjusting the linear velocity of the molecule during the separation. Pulsed lasers are not frequently used in LIF-CE detection since high power can create both saturation and photobleaching.

To maintain shot-noise limited conditions in LIF-CE detection, a laser with high stability is necessary. Commercially available lasers can produce a range of power depending on the application i.e. a few mW to 10 W. The most commonly used laser in CE-LIF are KrF (248 nm), HeCd (325 nm and 442 nm), Ar^+, (244 nm, 280 nm, 351 nm, 364 nm, 488 nm and 514.5 nm), and HeNe laser (543.5 nm, 594 nm, and 633 nm).

1.7.1.2 Light Emitting Diodes

The drive towards portable, miniaturized CE separation systems is limited by the size of the detection sources and optics as well as the power consumption of the laser. Hence, alternative light sources that are small, inexpensive, and possess the appropriate spectral characteristics are desirable and studied in this work. Light emitting diodes

(LED) are attractive as alternative light sources for CE due to their high stability, low cost, long life time, compact size, low power consumption and availability over a wide spectral range.[78;157-161] One of the concerns with LED sources however, is the quality of the beam. Unlike lasers, LED's emits incoherent light, but nonetheless it is still possible to attain small spot sizes allowing fluorescence detection in capillaries with > 25 µm i.d. These sources will be discussed later.

1.7.2 Focusing Optics

Focusing laser light tightly to a small spot size is important in order to excite analytes efficiently. Having well focused light, stray light can also be reduced. Laser light can be focused easily using a biconvex lens with a short focal length or using a microscope objective, which are inexpensive and are corrected for aberrations. These devices are capable of producing a beam waist less than the capillary i.d..[162]

1.7.3 Detection Cells

On-column fluorescence detection is the most frequently used method in routine analysis. Polyimide on the capillary wall is removed to create an optically transparent window to focus the laser light. On-column detection can sometimes be problematic due to the reflection, refraction and luminescence background light from the capillary. One way to alleviate the background problems associated with on-column fluorescence detection is to use post column fluorescence detection with a sheath flow cuvette (Figure 1.13).[150-153] In a post column sheath flow detection system, the detection end of the capillary is inserted into a 200 µm square flow chamber made up of high optical quality quartz with a 2 mm thick window. A sheath flow, which flow around the exit end of the

capillary, is gravimetrically pumped through the cuvette at a rate higher than the sample flow. The sample flow is hydrodynamically focused creating a stable, narrow sample stream at the tip of the capillary. The fluorescence signal is collected by focusing the laser through the sample stream. To minimize the scatter from the interface between the sample stream and the sheath stream, the same buffer is used for both the running buffer and the sheath buffer. Depending on the sheath flow rate and the migration velocity of the sample, the size of the sample stream can vary.

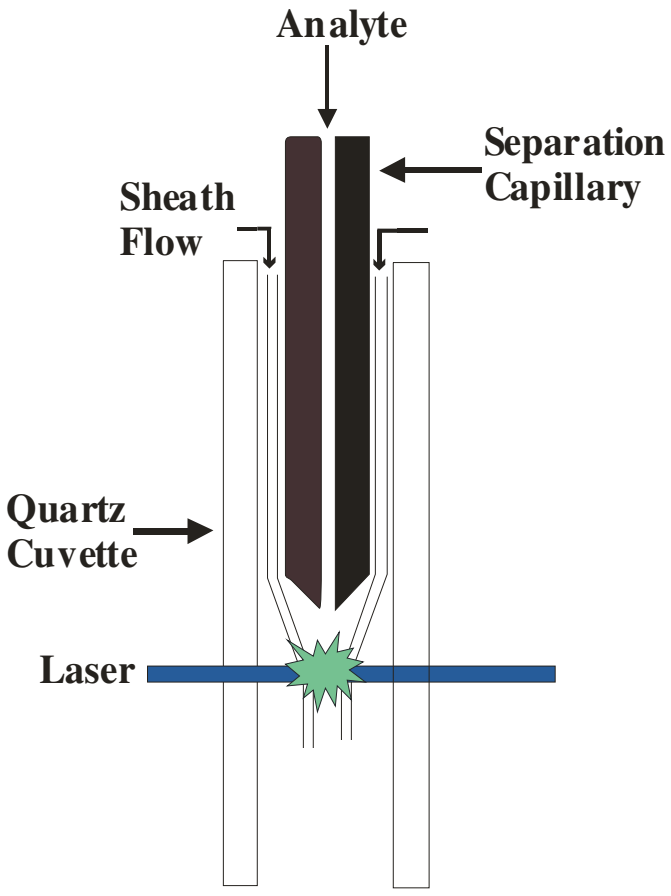

Figure 1.13 The Sheath flow cuvette arrangement in CE-LIF detection.

1.7.4 Collection Optics

The fluorescence signal from the sample is collected at a right angle to the incident beam to minimize the background light, microscope objectives are used. In order to collect maximum fluorescence signal, a high numerical aperture (N.A.) microscope objective can be used as the collection efficiency is related to the N.A. and the refractive index of the media, n (Equation 1.22). To achieve high collection efficiency, an objective with very a high N.A. is needed. For example, an objective with a N.A = 1 collects ca. 50 % of emitted light. One concern with the high N.A. objectives is that they have a very short working distance, which can not be used in the sheath flow arrangement due to thick chamber walls (2 mm). Hence, for post-column detection systems, a long working distance objective with a high N.A. is necessary, whereas for on-column methods short working distance objectives with high N.A can be used.[150] Objectives with a high N.A. with a long working distance of typically 2-3 mm are commercially available.

$$\text{collection efficiency} = \sin^2\left[\frac{\arcsin(N.A./n)}{2}\right] \quad (1.24)^{150}$$

1.7.5 Spatial Filtering

The spatial filter is used to eliminate the scattering from the cuvette wall or from the capillary walls. In general, a pin hole or a slit is used in front of the photodetector. The size of the spatial filter is determined by the image size, which is in turn determined by the collection objective. The spatial filter limits the amount of scatter light collected from the capillary walls and also defines the collection volume. Hence, it is important to

match the size of the aperture to the size of the image to maintain maximum collection volume.[150]

1.7.6 Spectral Filters

Spectral filtering is widely used to minimize the background signal. Optical filters must be chosen to obtain maximum emission intensity (I_m) while rejecting Raman scattering from the background electrolyte and stray light, etc.. One of the advantages of using spectral filters instead of a monochromator is that high transmission. Band-pass filters can provide > 90 % transmission at the emission band pass, while reducing excitation wavelength transmission to << 1% where as monochromators reduce emission intensity to 40-60 % to incident radiation. On the other hand, optical filters are economical compared to monochromators. For on-column fluorescence detection, laser scattering intensity from the capillary walls can be very high even in the presence of a band-pass filter. Hence, a holographic notch filter can be used to remove Rayleigh scattering. Most of the time, holographic notch filters reduce the I_m signal by 30-40 %. By placing the optical components inside a Plexiglass box, stray light and room light can be prevented from reaching the photodetector.

1.7.7 Photodetector

The fluorescence signal gathered by the collection objective is converted to an electrical signal using photodetectors. To obtain high sensitivity, highly efficient conversion of photons to current is necessary. Photomultiplier (PMT) tubes are most commonly used in CE instruments. For applications around 500 nm, PMT's with GaAs or multialkali photocathodes offer quantum efficiency of more than 10 %. GaAs tubes

possess higher efficiency than multi-alkali tubes but are more easily destroyed by high light intensity due to the high sensitivity of the photocathode. Hence, relatively inexpensive and rugged multi-alkali PMT's such as Hamamatsu R1477, which has a quantum efficiency range from 22 % to 15 % in the wavelength range of 450 nm to 550 nm, can provide sufficient sensitivity in LIF-CE applications.[150] For fluorescence applications, the PMT should be covered to block scattered light from entering the detector. Otherwise, dark current of the PMT can be an issue in the analysis. For high sensitivity detection, the PMT is cooled to reduce the detector noise, which depends on the type of the device.

There are other photodetectors available for fluorescence detection such as avalanche photodiodes, photodiode array, charge couple devices, and charge injection devices and these devices are used for miniaturizing applications. Among those devices, avalanche photodiodes are becoming an alternative device for PMTs due to its characteristic high-gain and relatively high quantum yield at 550 nm. Array detectors are useful in applications such as multi-channel and whole column detections.[163]

1.7.8 Derivatization for Fluorescence Detection

To achieve fluorescence detection of analytes in CE, analytes should contain a natural fluorophore or be derivatized with a fluorescent reagent. In terms of analyzing biologically active molecules such as amino acids, peptides and proteins, native fluorescence detection can be applied if the analytes contain tryptophan or tyrosine residues, which can be excited with a high power Ar^+ laser using the 280 nm line.[164;165] This approach is not particularly attractive, however, due to several disadvantages i.e.

limited availability of UV lasers in that region, cost, limited laser lifetime, expensive optics and lack of tryptophan present in some biological molecules. Alternatively, the analyte is labeled with a known fluorophore for high sensitivity fluorescence detection. Derivatization reagents are designed to react with some of the active groups in the analyte molecule including primary amine, thiols, and acidic groups.

Numerous fluorescent labeling reactions have been reported for use in CE, the most common of which involve either the fluorescent or fluorogenic derivatization of primary amines.[166;167] Fluorescent reagents contain a highly fluorescent fluorophore whereas fluorogenic reagents are intrinsically nonfluorescent until they react with a primary amine. There are various modes of derivatization depending on the application and the type of reagents used in the labeling reaction, mainly pre-column, post-column and on-line derivatization. The pre-column mode is the most commonly used method, in which any type of labeling reagents including fluorogenic and fluorescent can be used. For online derivatization often coupled with online sampling methods, stringent demands are placed on the reaction rate of the dye such that fluorogenic dyes with high reaction kinetics are commonly utilized in such instances. Derivatization can alter the mobility of the analyte significantly, sometimes in negative ways, but can be eliminated by post column labeling. For post column labeling, fluorogenic labels are required, introducing several advantages over other approaches. In general, higher sensitivity is obtained in CE with highly absorbing, high quantum yield fluorescence labels, e.g. fluorescein or rhodamine, that are excited with commonly available visible laser and laser diode lines. Among these labeling reagents, isothiocyanate (ITC) and succinimidyl ester (SE)

derivatives of fluorescein and rhodamine are the most commonly used in CE.[150;168-171] Though higher sensitivity is attained, the slow reaction kinetics are not favorable for on-line derivatization required for dynamic chemical monitoring using CE and other situations where fast labeling reactions are desired. Recently, 5-(4,6-dichloro-s-triazin-2-ylamino) fluorescein (DTAF)[169;172-174] and (6-oxy-(N-succinimidyl acetate)-9-(2-methoxycarbonyl)fluorescein (SAMF))[175] have emerged as alternatives to ITC and SE fluorescein derivatives as they react quickly with primary amines. While desirable for a number of applications, the reaction conditions and/or kinetics remain incompatible for others, most notably with on-line labeling required in DCM-CE. For fast derivatization, Naphthalene-2,3-dicarboaldehyde (NDA) and *o*-phthalicdicarboxaldehyde (OPA)/β-mercaptoethanol (β-ME), -(4-carboxybenzoyl)quinoline-2-carboxaldehyde (CBQCA), FQ (5-furoylquinoline-3-carboxaldehyde) are frequently used to label biologically important amines due to their superior reaction kinetics.[43;45;115;176-180] There are various other derivatization reagents depending on the analyte available through Molecular Probes Inc, Oregon, which provides a wide range of fluorescent and fluorogenic regents.

1.8 Bioanalytical Applications of Capillary Electrophoresis

CE has transformed into an analytical tool that has a wide range of applications. One of the primary utility of capillary electrophoresis was DNA analysis,[11;29;30] and its contribution to genome sequence has been remarkable. Since CE based DNA sequence data was submitted to GenBank in 1997, it has been the primary tool of DNA sequencing.

In addition, CE has been also studied in analysis of biopolymers such as protein, peptides and polypeptides. One of the main disadvantages of protein separation using

CZE is the adsorption of analytes on the capillary surface resulting in band broadening and reduced sensitivity.[92]. Hence, protein separation using CZE may produce unsatisfactory results unless appropriate measures are taken such as coating capillaries, buffer additives and separation at extreme pHs. For protein separations, other separation modes e.g. MEKC, SDS-CGE, CIF and submicellar CE are frequently used instead of CZE.

CE based methods have been reported for the analysis of single cells due to its inherent mass sensitivity. Dovichi and coworkers initiated this line of study where they developed highly sensitive CE instrumentation based on a sheath flow cuvette to study single cell protein content and single cell enzyme assays.[181-183] Protein kinase activities in single cells were also studied using laser micropipette techniques coupled with CE-LIF, in which enzyme substrates were loaded into cells and single cells were analyzed to monitor enzyme activity of individual cells.[184-187] Detection of biogenic amines in a single cell was also reported by Ewing and coworkers and they used amperometric detection to analyze dopamine from a single nerve cell of *Planorbis corneus*.[188] Immunoassays (IA) are predominantly used in biological analysis, in which reaction between an antibody (Ab) and an antigen (Ag) is utilized to analyze solutes in a complex sample. Immunoassays are routinely used in clinical and pharmaceutical areas due to its extreme sensitivity and selectivity. Recently, immunoassays have been combined with CE (CEIA) to perform bioassays, where separation of the reaction mixture is performed using CE. When CEIA is combined with LIF detection, it can have several potential advantages over conventional immunoassay such as high throughput, short analysis time,

small volume requirements, multiple analyte detection and automation. CEIA have been developed to analyze biological molecules such as insulin, glucagons and human growth hormone.[189-191] CEIA can typically provide detection limits in the range of 0.1-1.0 nM depending on the Ab used in the assay. CE has been extensively used in neurochemistry and neurobiology due to its capabilities such as fast separation, minimum sample requirements, and high mass sensitivity. When CE is coupled with on-line sampling techniques such as microdialysis and push-pull, it provides high temporal and spatial resolution required in studying neurochemically important analytes. CE-LIF has been reported for the analysis of neurological samples *in vitro* and *in vivo*, in which the analysis of biogenic amines, amino acids, neuropeptides in samples such as tissue, extracellular fluid and single neuron have been reported. Kennedy and coworkers have worked extensively on coupling microdialysis sampling techniques to CE directly using flow-gated interface to monitor dynamic chemical changes in rat brains.[43;115] In this study, they were able separate more than 15 biogenic amines with 20 s temporal resolution. Analysis of single neurons by CE-LIF was also reported by Sweedler group and they reported detection of D-amino acid containing peptides, serotonin and serotonin metabolites in single neurons from *Aplysia californica*.[34;192;193] CE has also been used to analyze sub cellular components[35] as well. Overall, the contribution from CE toward the development of bioanalytical chemistry has been outstanding. A large number of papers published during the last 25 years in this field is a clear indication of the wide acceptance of CE as an analytical tool.

1.9 Outline of Dissertation

Chapter 2 describes an on-line, optical injection interface for CZE based upon the photophysical activation of a caged, fluorogenic label that has been covalently attached to the target analyte. This interface allows online analysis of biomolecular systems with high temporal resolution and high sensitivity. Samples are injected onto the separation capillary by photolysis of a caged-fluorescein label using the 351-364 nm irradiation of an Ar^+ laser. Following injection, the sample is separated and detected via laser-induced fluorescence detection at 488 nm. Detection limits for on-line analysis of arginine, glutamic acid and aspartic acid were less than 1 nM with separation times less than 5 s and separation efficiencies exceeding 1,000,000 plates/m. Rapid injection of proteins was demonstrated with migration times less than 500 ms and 0.5 nM detection limits. On-line monitoring was performed with response times less than 20 s suggesting the feasibility of this approach for online, *in vivo* analysis for a range of biologically relevant analytes.

Chapter 3 describes the development of a chemical derivatization scheme for primary amines that couples the fast kinetic properties of o-phthaldialdehyde (OPA) with the photophysical properties of visible, high quantum yield, fluorescent dyes. In this reaction, OPA is used as a cross linking reagent in the labeling reaction of primary amines in the presence of a fluorescent thiol (SAMSA fluorescein), thereby incorporating fluorescein (ε=78 000 M^{-1}, quantum yield of 0.98) into the isoindole product. Detection is based on excitation and emission of the incorporated fluorescein using the 488 nm laser line of an Ar^+ laser rather than the UV-excited isoindole, thereby eliminating the UV

light sources for detection. Using this method, we have quantitatively labeled biologically important primary amines in less than 10 s. Detection limits for analysis of glutamate, glycine, GABA and taurine were less than 1.5 nM. The results from the characterization of this reaction suggest that the new reaction has inherent fast reaction properties from OPA while possessing the spectral properties similar to fluorescein.

Chapter 4 presents the utilization of a high power ultraviolet light emitting diode for fluorescence detection (UV-LED-IF) in capillary electrophoresis (CE) separations. CE-UV-LED-IF allows analysis of a range of environmentally and biologically important compounds, including polyaromatic hydrocarbons (PAHs) and biogenic amines, such as neurotransmitters, amino acids, proteins and peptides, that have been derivatized with UV-excited fluorogenic labels, e.g. o-phthaldialdehyde/β-mercaptoethanol (OPA/β-ME). The 365 nm UV-LED was used as a stable, low cost source for detection of UV-excited fluorescent compounds. UV-LED-IF was used with both zonal CE separations and micellar electrokinetic chromatography (MEKC). Native fluorescence detection of PAHs was accomplished with detection limits ranging from 10 nM to 1.3 μM. Detection limits for OPA/β-ME-labeled glutamic acid and aspartic acid were 11 nM and 10 nM, respectively for off-line labeling and 47 and 47 nM, respectively for on-line labeling, limits comparable to UV-laser based systems. Analysis of OPA/β-ME-labeled proteins and peptides was performed with 28 nM and 47 nM detection limits for bovine serum albumin (BSA) and myoglobin (Myo), respectively.

Chapter 5 discusses novel strategies for single cell analysis. It is important to analyze single primary cells to understand their function and signaling mechanisms.

Molecular reagents are predominantly used to monitor signaling pathways. However, the cell membrane acts as a barrier for chemical reagents making chemical analysis more challenging. It has been shown that microinjection of reagents into cells can overcome this difficulty but one potential problem of the technique is the cell membrane damage. We have developed a series of cell penetrating, fluorescent, protein reagents that can be readily loaded into cells without using microinjection methods. In our approach, we expressed and purified recombinant proteins that possess the general structure: 6xHis-TAT-peptide substrate-EGFP. The key components of this peptide geometry are as follows: a) the 6xHis tag allows high yield purification; b) the TAT protein, of HIV origin, serves to translocate proteins across the cell membrane; c) the peptide substrate serves as the phosphorylation site; and d) EGFP serves as the fluorescent label. We have constructed 6xHis-TAT-EGFP and loaded it into a number of cell types with high efficiency simply through addition of the protein to the cellular medium, thus avoiding physical disruption of the membrane. CE-LIF with sheath flow cuvette detector was used to monitor intracellular protein contents.

Chapter 6 describes application of CE-LIF for the determination of biogenic amine levels in the antennal lobes of the *Manduca Sexta*. In this work, methods were developed to analyze a single antennal lobe dissected from Manduca Sexta. The lobe was digested and contents were labeled with the fluorogenic dye 5-furoylquinoline-3-carboxaldehyde (FQ) before the CE analysis. The sample was then analyzed by CE and peaks were identified by co-migrating with FQ-labeled standards amino acids. GABA levels in antennal lobes (AL) were quantified, which are in agreement with the GABA

levels reported by utilizing other techniques. This work reports the utility of CE-LIF to monitor biogenic amines in complex biological systems.

CHAPTER 2. HIGH SPEED CAPILLARY ZONE ELECTROPHORESIS WITH ONLINE PHOTOLYTIC OPTICAL INJECTION

2.1 Introduction

Real time analysis of complex chemical and biochemical mixtures is important in a number of environmental and biomedical applications. Electrochemical detection with microelectrodes has recently been used to monitor electroactive species in biological samples and they provide very high temporal resolutions typically 2 s.[194] However, many biologically important analytes can not be detected by electrochemical methods and also chemical interference can limit their durability. Hence, Rapid separation of analyte mixtures offers a higher level of chemical information than traditional single analyte optical or electrochemical sensors.[18] With fast separations, sufficient temporal resolution may be obtained to map the chemical dynamics within the sample, thus providing an information rich, separation-based sensor.[18;41;44;177] Separation-based chemical monitoring has primarily utilized capillary zone electrophoresis (CZE) due to the rapid separation capabilities, high resolution and high mass sensitivity. Utilization of CZE for online chemical monitoring requires the analytical separation be interfaced to the sample, leading to the development of a number of sampling and interface technologies, including: optical gating,[51;52;106;125] flow gating,[42;47;53;115] micromechanical valving[108], capillary introduction[109;195], integrated microfluidic gating[108;111;196;197] and flow-through microfluidic sampling.[112;113] CE systems utilizing online injection schemes have been used for a variety of applications, e.g. reaction dynamics studies,[111;198] multi-dimensional

separations,[46-49;122;199] online chemical monitoring,[41;44;116-118] combinatorial and pharmaceutical screening,[200;201] multiplexed CE[202;203] and high throughput assays.[117]

On-line chemical monitoring requires interfacing of sample with the analytical separation, a task that is most commonly performed using a flow gate interface,[47;53] which allows continuous, low volume sample introduction. Flow-gating CZE has been used extensively for online monitoring, particularly when longer (> 50 ms) injection times are utilized.[44;100;116-118] Shorter injection times are limited by deviations in the switching valves used to stop the cross flow.[119] For online chemical monitoring applications, microdialysis probes are frequently used to collect samples. When CE is coupled to a microdialysis probe using a flow gated interface, overall time to perform an injection can be dictated by the flow rate at which probe is perfused to collect the sample. In order to collect samples effectively using a microdialysis probes, low flow rates (1-10 μL/min) are used and this can be the limiting factor in filling the interface between the sampling and the separation capillary. If the interface is not completely filled before the injection, effective material transfer into the separation capillary can not be achieved. Beside, increased band broadening is often observed in flow-gating due to the cross-flow at the sampling and injection capillaries (Chapter 1).[119;120] More recently, flow-through sampling interfaces have integrated with microchip electrophoresis to provide on-chip flow-gating and separation capabilities[108;112], as well as coupling to a variety of sampling interfaces, e.g. microdialysis and push-full[113].

For fast injections and separations, optically-gated (OG) CZE is often employed to minimize band broadening due to injection. When short and small i.d. capillaries are

used for fast separations, the total volume of the capillary is small (nL to pL) and the amount of analytes injected should be controlled to minimize excessive band broadening in the separation. Otherwise, a band broadening form injection can be significant.[51;106] Hence, on-column OG injection is preferred in which injection times < 50 ms can be maintained to control the amount of sample introduced into the separation capillary unlike in flow gated injections. In OG-CZE interfaces, the sample and separation capillaries are directly coupled or are constructed of one continuous capillary and sample is continuously introduced into the separation capillary via EOF.[51;52;106;123] In traditional OG-CZE interfaces, fluorescently-labeled sample is photobleached using a high power laser beam (gating beam), rendering the sample inactive at an LIF detector positioned downstream. Injection of small analyte plugs is accomplished by blocking the gating beam for a short time allowing fluorescent analyte to enter the separation path. The separation distance is defined by the distance between the gating beam and LIF detection beam, allowing short separation distances and thereby rapid separations.[51;52;106;121;123] Since OG-CZE utilizes on-column injections, narrow sample plugs can be continuously injected with high reproducibility.[51] OG sample injections provide the basis for the fastest and highest efficiency CZE separations, with separation efficiencies exceeding 10^6 plates/m in as short as 1 s for fluorescently-labeled amino acids, peptides, oligonucleotides and other small molecules.[51;52;106;123;124] Using a derivative of OG-CZE where photoactive products are created, separated and subsequently detected using multiphoton photochemistry, separation speeds of 10 μs have been achieved.[121]

When fluorescein-labeled analytes are used in OG-CZE, less than 90% of the probe is photobleached, even with substantial laser power.[52] Thus, inefficient photobleaching results in continuous introduction of optically active label leading to high fluorescent backgrounds and reduced sensitivity with LODs for fluorescein-based applications ranging from high nM to low μM. OG sampling approach has been extended for microchips by Ewing and co-workers and they have used OG-CZE in parallel microchannels to analyze several important biological compounds, including amino acids,[123;124] oligonucleotides,[204] and enzyme activity,[205] though the low μM detection limits obtained were due, in part, to low photobleaching efficiency (~65%). These studies suggest the importance of alternative methodologies for reducing the fluorescent background associated with OG-CZE.

To reduce the background associated with OG-CZE and still utilize visible LIF detection, we have developed an approach based on photochemical activation of caged-fluorescein (CF) derivatives. CF is a fluorogenic dye that is photoactivated upon irradiation with light below 365 nm.[206] Upon exposure to UV radiation, the caging groups are photolyzed and released to generate a fluorescent species that can be detected with the 488 line of an Ar^+ laser.[206] The resulting injection approach is orthogonal to photobleaching based injections. In photolytic optical gating (POG), a UV beam is used as a gating beam to photoactivate the sample, which is then separated and detected by LIF of the resultant fluorescein derivative. The primary advantage of this approach is the lower background and background associated noise resulting from reduced CF emission in conjunction with the high quantum yield of the resulting fluorescein. Further, the large

Stokes' shift between the injection beam and the detection beam may allow shorter separation distances to be used providing the possibility of faster separations. Improved detection limits were obtained compared to those observed in photobleaching-based optical gating, while maintaining the high separation efficiencies typical of OG-CZE. In this chapter, we present the design, characterization and application of POG-CZE for continuous analysis of biologically important molecules.

2.2 Experimental

2.2.1 Material and Reagents

Amino acids were from Sigma. Cellulose acetate and dimethyl sulfoxide (DMSO) were from Aldrich. Fluorescein bis-(5-carboxymethoxy-2-nitrobenzyl) ether (CF), 5-carboxyfluorescein-bis-(5-carboxymethoxy-2-nitrobenzyl) ether, β-alanine-carboxamide, succinimidyl ester (CF-SE) and CMNB-caged conjugated streptavidin were from Molecular Probes (Eugene, OR). All the other chemicals were from VWR and used as received. Capillaries were from Polymicro Technologies (Phoenix, AZ). All solutions were prepared using 18 MΩ deionized water (Barnstead).

2.2.2 Sample Preparation

Samples were derivatized off line with CF-SE prior to analysis (Figure 2.1A). For amino acid derivatizations, 1 μL of 10 mM amino acid (Figure 2.1B) dissolved in 0.1 M bicarbonate buffer at pH 9.0 was mixed with 10 μL of 2 mM CF-SE dissolved in DMSO followed by dilution to 100 μL with bicarbonate buffer. The mixture was allowed to react for 3 hrs in the dark, and stirred every 15 min. The original sample was diluted in run buffer prior to analysis. For analyte mixtures, derivatization was

performed by adding 1 µL aliquots of mixture components (up to 3 µL total primary amine) and 30 µL CF-SE to 67 µL of 0.1 M bicarbonate buffer.

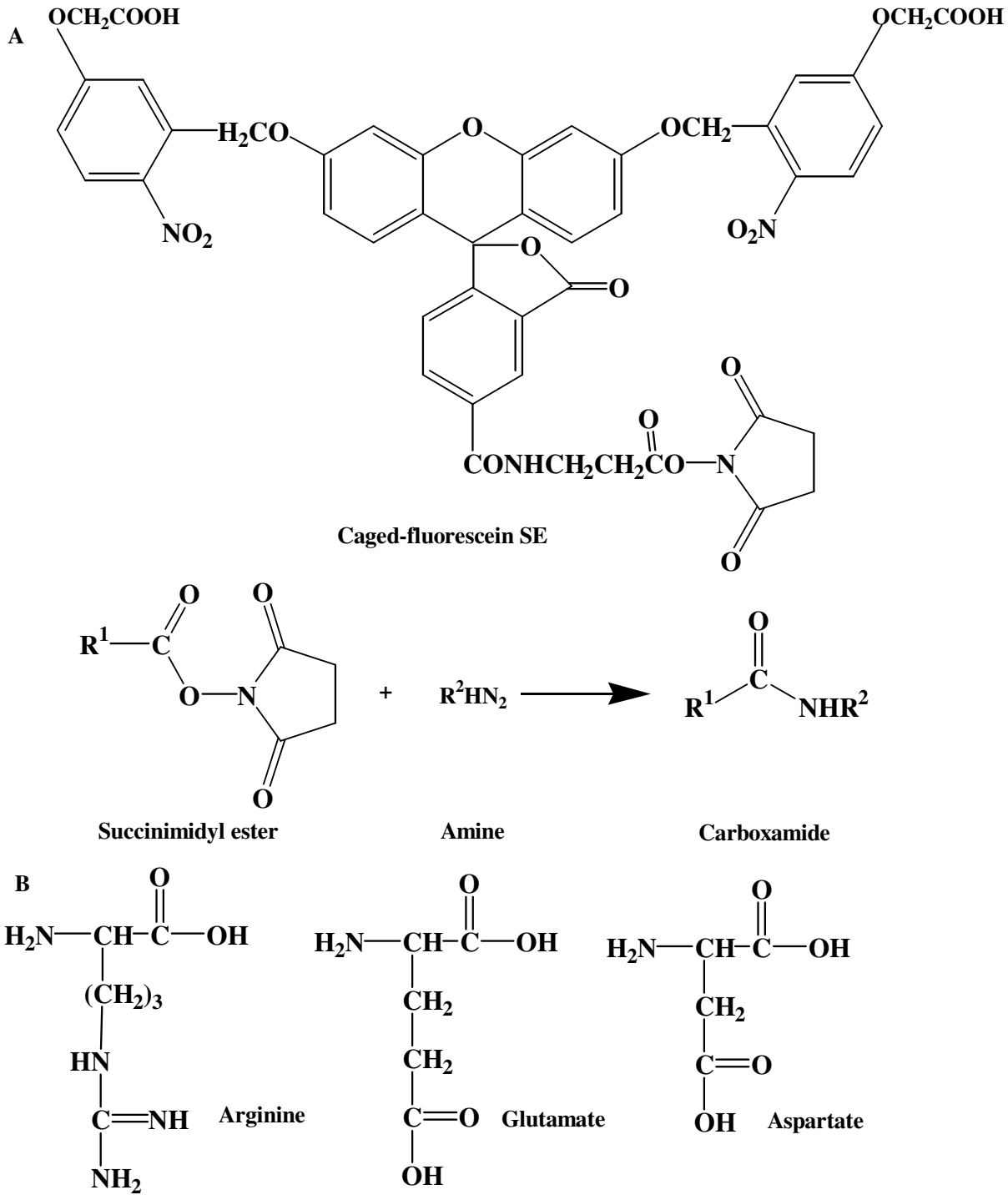

Figure 2.1. (A) Structure of caged-fluorescein SE and its reaction with a primary amine. (B) Chemical structures of amino acids used in the separation.

2.2.3 Capillary Preparation

The capillary was washed with 1 mM NaOH for 5 min followed by a 10 min wash with 10 mM phosphate buffer at pH 7.4 before use. For protein separations, the capillary was coated with cellulose acetate as described.[102] Briefly, the separation capillary was rinsed for 15 min with acetone followed by a 15 min wash with 12.5 mM cellulose acetate dissolved in acetone. The capillary was dried with low pressure He, cut to length and conditioned with running buffer for 30 min.

2.2.4 POG-CE-LIF Instrumentation

POG-CE-LIF instrument was built in house. A schematic is shown in Figure 2.2. The output of an Ar^+ laser (Innova 70C series, Coherent, Inc., Santa Clara, CA) operating at 3 W total power was split into UV and visible wavelengths using a dichroic mirror (LWP-45-RS 355-TS 488-PW-1025-UV, CVI Laser, Albuquerque, NM). The UV lines were passed through two UV band pass filters (U-330, Edmund Industrial Optics, Barrington, NJ) to further remove visible light in the photolysis beam. The photolysis beam, comprised of the combined 351-364 nm lines, was focused into the center of the separation capillary using a fused silica biconvex lens (f = 25 mm, Melles Griot, Irvine, CA). The beam orientation of the photolytic gating beam and the detection beam is depicted in Figure 2.2. Sample injection is accomplished by photolysis beam, which was controlled using a LS3 mechanical shutter with VMM-T1 control (Unibitz LS3, Vincent Associates, Rochester, NY). For detection, the visible wavelengths of the laser were dispersed using a prism (Melles Griot) and the 488 nm laser-line was isolated using spatial filters, passed through a neutral density filter (O.D. = 1.0, Thorlabs Inc, Newtown,

NJ) and focused into the center of the separation capillary using a biconvex lens (f = 25 mm, Melles Griot). The fluorescence signal was collected using a microscope objective (20x, 0.4 N.A., Melles Griot) and passed through a spatial filter, a band pass filter (D525/25 M, Chroma Technology, Rockingham, VT), and a 488 nm holographic notch filter (HNF-488.0-1.0, Kaiser Optical Systems Inc., Ann Arbor, MI). The signal was detected by a PMT (H957, Hamamatsu Photonics, Bridgewater, NJ), the current from which was amplified (Model 428, Keithley Instruments, Cleveland, OH), low pass filtered (950, Frequency Devices, Haverhill, MA) and collected with an A/D converter (PCI-MIO-16E-4, National Instruments, Austin, TX) using in-house software written in LabView (National Instruments). Electric fields were applied using a 60 kV power supply (Glassman High Voltage Inc., High Bridge, NJ).

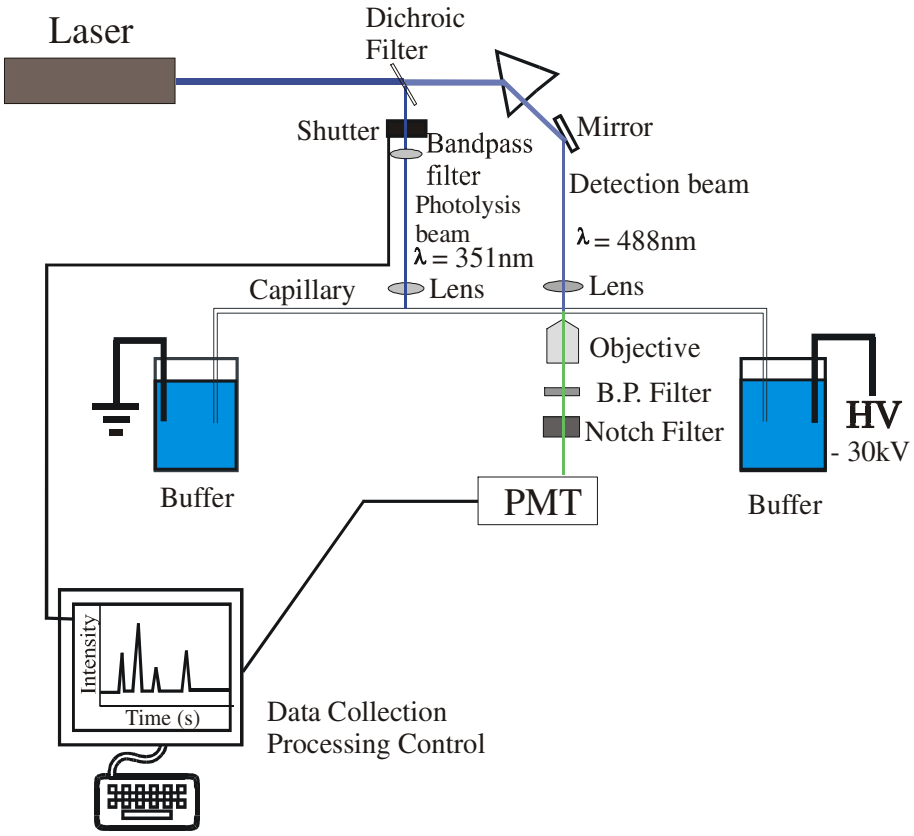

Figure 2.2. Experimental setup for POG-CE-LIF.

2.2.5 Sample Injection with Photolytic Optical Gating

Sample injection was achieved using the combined 351-364 nm lines of an Ar^+ laser (Figure 2.2) to photoactivate the fluorogenic caged-fluorescein derivatized sample. High voltage was applied to the separation capillary continuously during the analysis. When CF is in the caged (non-fluorescent) form, derivatized samples were not detected by LIF although the samples continue to migrate past the detector. To inject sample, the gating beam was focused into the capillary for a short time (5-20 ms) upon opening a mechanical shutter. The uncaged, fluorescent analytes proceed to separate during the migration between the gating (photolysis) beam and the detection beam. In this

geometry, the separation distance is dictated by the distance between the photolytic beam and the detection beam as shown in Figure 2.2. A separation distance of 1.4 cm was used here, though this is readily adjusted by varying the beam positions.

2.2.6 Temporal Measurements with Optical Injection

To characterize the feasibility of the POG-CZE approach for monitoring temporal dynamics, we interfaced the POG-CZE instrument described above to an HPLC injection valve that served as a stream selector (Figure 2.3). Sample from one of two 1 mL air tight syringes (Hamilton, Reno, NE) controlled by a Harvard syringe pump (Harvard Apparatus, Inc. Holliston, MA) was continuously introduced into the POG-CZE capillary. The syringes were connected to a six port injection valve (6UW, Valco Instruments, Houston, TX) through an 18 cm long, 50 µm i.d. capillary. The valve output (50 µm i.d. capillary) was snugly coupled to the separation capillary (10 µm i.d., 360 µm o.d.) using 1/16 in. i.d Teflon tubing that contains a hole at the junction of the two capillaries to release pressure at the interface[207;208] and to provide a grounding point for the separation capillary.

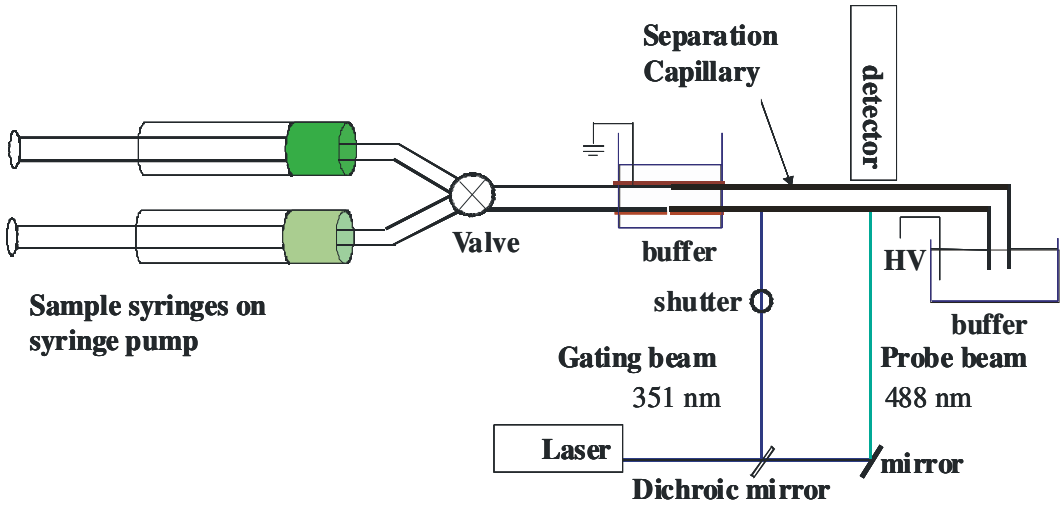

Figure 2.3. Schematic diagram of the system used in monitoring temporal dynamics.

2.3 Results and Discussion

A primary drawback of photobleaching based OG-CZE is the inefficient photodegradation of most common fluorescent probes, e.g. fluorescein[51;52] and NBD,[123;124] resulting in increased fluorescence background, increased noise and reduced sensitivity. The resultant fluorescent background can be reduced by employing more easily photodegraded probes or by utilizing a fluorogenic probe that can be photoactivated from a non-fluorescent state rather than photodegraded. The first of these approaches was utilized by Tao et al. for o-phthalaldehyde (OPA)/β-mercaptoethanol (β-ME) labeled amino acids with 351 nm injection and detection.[106;125] The resulting increase in sensitivity (detection limits ranging from 2.4 to 15 nM) was achieved without an accompanying decrease in efficiency or resolution.[106] The second approach was used by Plenert and Shear to achieve 10 μs separations of transient hydroxyindole photoproducts though the sensitivity reported was in the μM range.[121] Here, we further

explore this approach through the use of caged-fluorescent dyes with intrinsically low fluorescent backgrounds.

A number of caged-compounds have been developed to deliver enzyme substrates, metal ions, secondary messengers, nucleotides, fluorescent agents, etc.[209-212] Caged-fluorescein and caged-rhodamine have been used for a number of flow dynamic investigations, including on-line measurement of EOF in CE.[2;212-217] Upon photoactivation, the electron-withdrawing caging groups are removed from the optically dormant fluorophore restoring fluorescence.[206] Typical quenching efficiencies exceed 99.99% leading to an essentially non-fluorescent background. As illustrated in Figure 2.2, sample injection is performed by focusing the combined near UV lines of an Ar^+ laser into the separation capillary to photoactivate the caged-fluorescein labeled sample. Since the UV lines are used only for photoactivation, it is not necessary to isolate individual lines. Following photolysis, de-caged analytes proceed to separate during the migration between the gating (photolysis) beam and the detection beam (Figure 2.2). Detection of the resulting fluorescein-labeled product using the 488 nm line of the Ar^+ laser provides increased sensitivity and reduced fluorescence background compared to photobleaching-based OG. The large Stokes' shift between photolysis and detection wavelengths reduces the effects of excitation scatter in the capillary on detection during a gating event, possibly allowing closer proximities between the laser beams and shorter separation paths.

2.3.1 Reproducibility of Photolytic Injection

Utilization of CZE for online chemical monitoring requires highly reproducible injections. To assess the potential utility of POG-CE for online monitoring, we have investigated the reproducibility of the photolytic injection using caged-fluorescein (CF) (Figure 2.4). Electropherograms were collected serially utilizing 10 ms on-line photolytic injections of 200 nM CF every 10 s over a 300 s time period (Figure 2.4). Photolytic injection of CF yields multiple peaks (Figure 2.4B), due to formation of multiple photolytic products; however, for a given laser power, the ratio of the peak intensities remains constant. The average ratio of peaks was 1.8 and the relative standard deviation for peak ratio was 1.6 % for 60 sample injections. This suggests that we can effectively photolyze caged-fluorescein in a reproducible manner. Further, the analysis of CF by mass spectrometry (MS) suggests that the original sample contained both CF-SE and CF-SE hydrolyzed product (acid portion). Analysis of different CF-SE samples with a different shelf life i.e. newly prepared sample (Figure 2.5B) and old sample (6 months) (Figure 2.5A), by MS, suggests that the ratio between CF-SE and CF-SE hydrolyzed product varied over time. As given in Figure 2.5, CF-SE hydrolyzed product was the main component in the old sample of CF-SE compared to the newly prepared solution. Hence, it is important to use newly prepared CF-SE in analysis to minimize hydrolyzed products. This is especially important in the labeling reaction. In Figure 2.4B, the peak at 3.95 s corresponds to the CF-SE hydrolysis product, while the peak at 2.55 s is the intact CF-SE. Figure 2.4C shows composite peak parameter data calculated using the peak at 3.95 s migration time. Relative standard deviations were 1.3 %, 2% and 0.9% for peak

height, peak area, and migration time respectively. Data for the other primary peak showed similar reproducibility. The high reproducibility observed with POG-CZE is maintained with injection times of 10 ms compared to flow-gated methods that require a minimum injection time of 50 ms to obtain reproducible injections. Current implementations of POG-CZE allow injection times as short as 5 ms, below which imprecision in the mechanical shutter limits the injection reproducibility.[218] Thus use of shorter injection times in optical gating compared to flow gating yields increased peak capacities and higher efficiency separations as the variance due to injection is reduced as illustrated by Figure 2.6.[63;123;219]The effect of the injection time on efficiency on caged-fluorescein analysis was investigated (Figure 2.6). The exponential decrease in peak efficiency was observed as the injection time was increased. This is mainly due peak broadening due to injection and this has been reported by other groups.

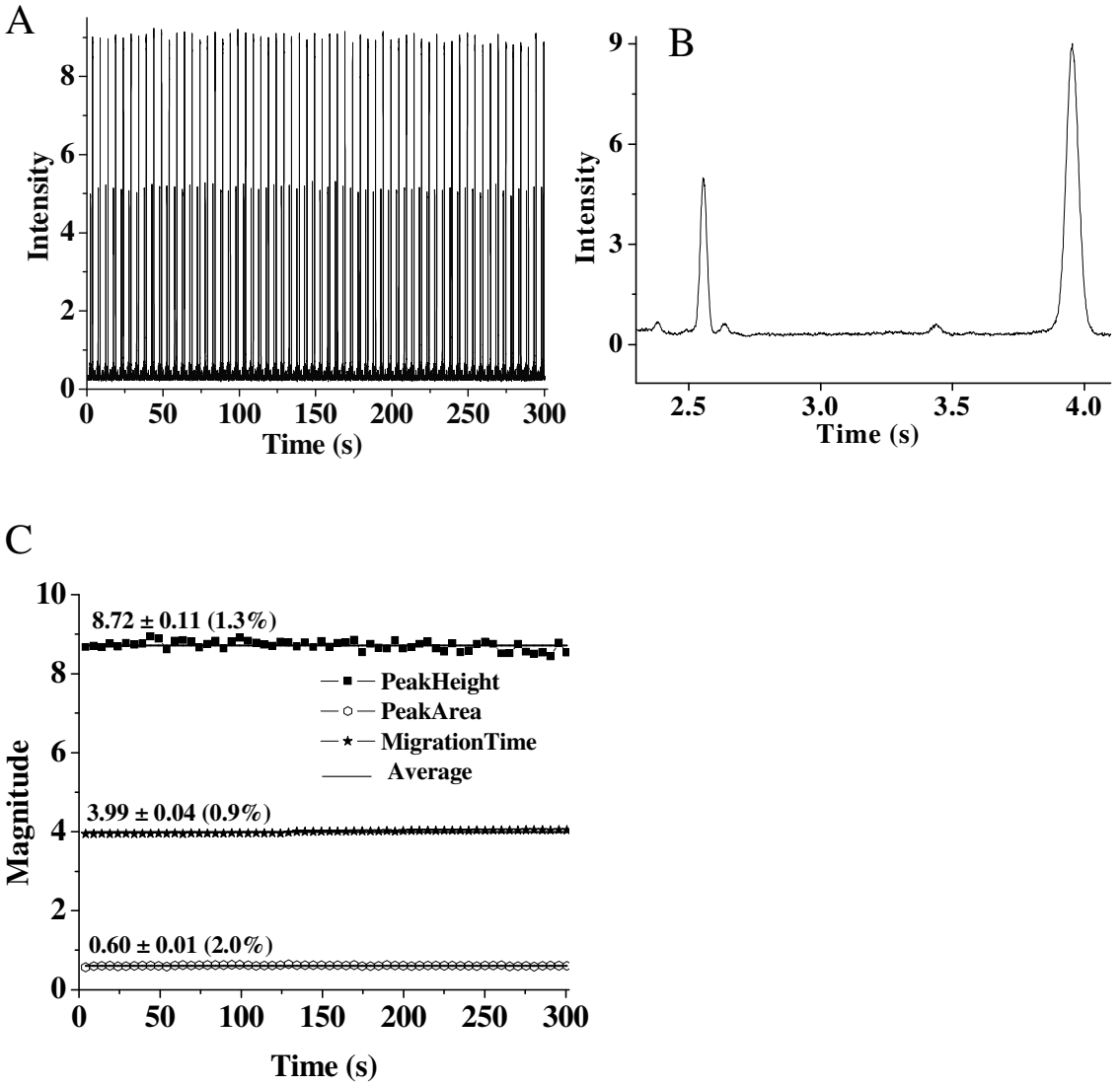

Figure 2.4. Reproducibility of photolytic optical injections. A) Plot of 60 continuous electropherograms obtained for 200 nM caged-fluorescein over 300 s. B) Expanded view of one electropherogram extracted from A. C) Plot of peak parameters calculated from the individual electropherograms in A. Data represents analysis of peak at ~ 4 s. E = 1.67 kV/cm, injection time = 10 ms.

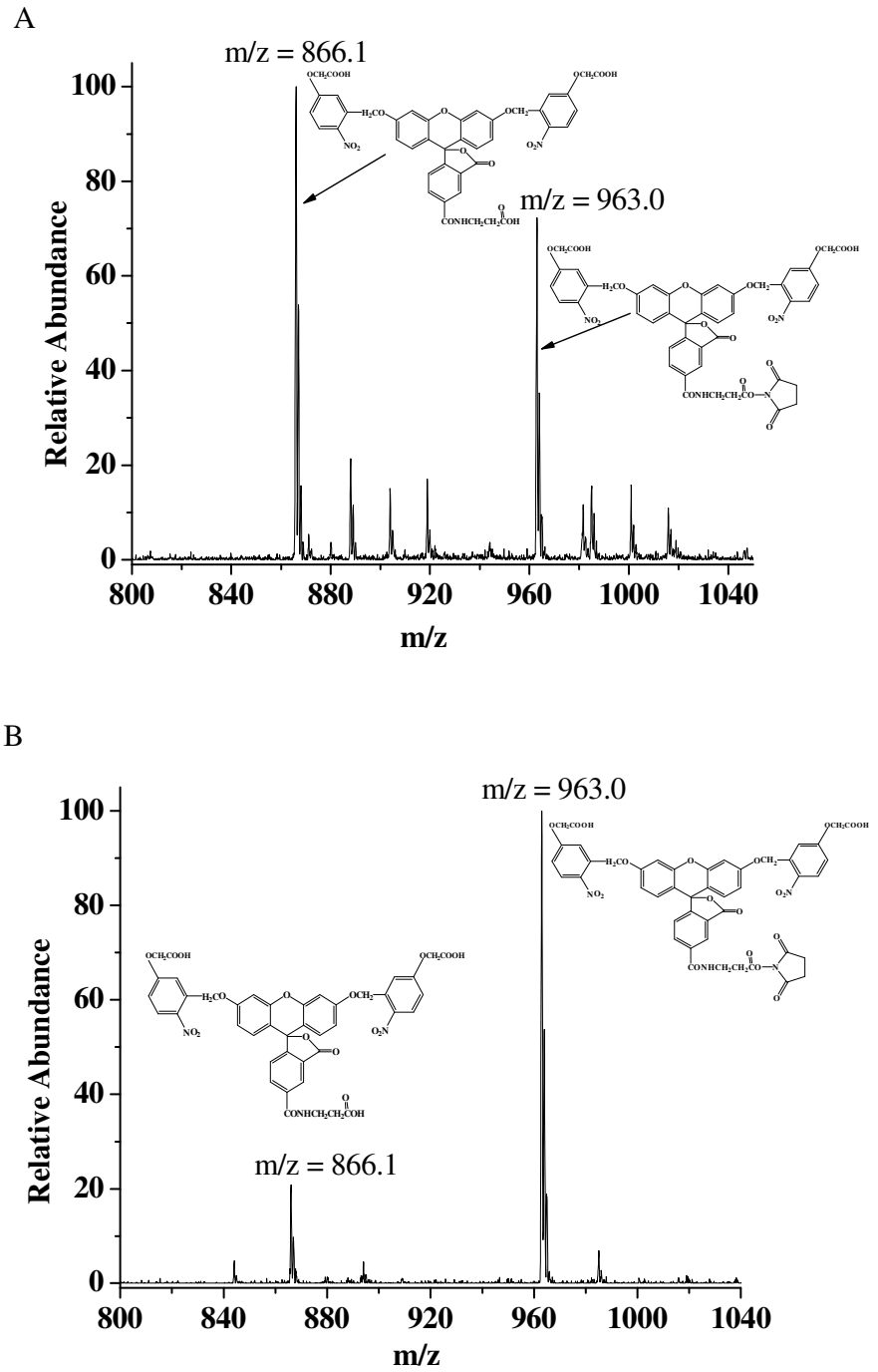

Figure 2.5. MS analysis of caged-fluorescein succinimidyl ester. (A) six months old cage-fluorescein sample, and (B) new caged-fluorescein sample.

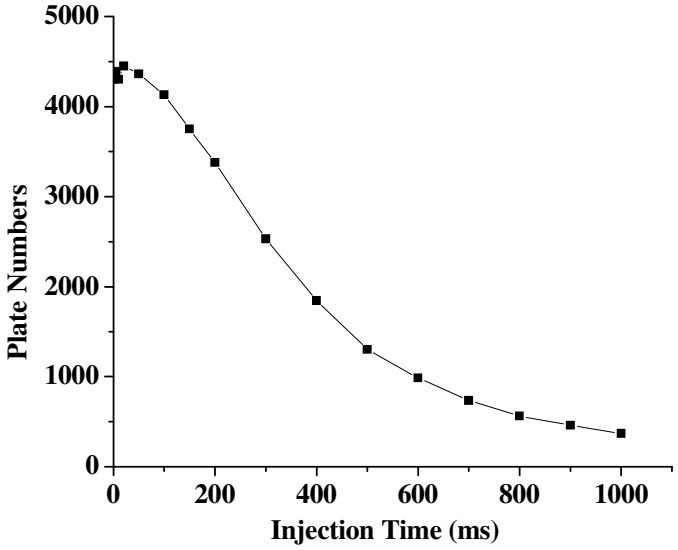

Figure 2.6. Effect of injection time on peak efficiency for 1 µM caged-fluorescein. Sample injection time range from 1 ms to 1000 ms and 26 µm i.d. capillary was used in this analysis.

2.3.2 Amino Acid Analysis CZE with Photolytic Injection

Figure 2.7 shows a series of electropherograms obtained for amino acids labeled with CF-SE. Figure 2.8A shows two consecutive, on-line separations of a CF-labeled amino acid mixture containing 10 nM arginine, glutamatic acid and aspartatic acid. Electropherograms were obtained at 10 s intervals with 20 ms photolytic injections. As seen in Figure 2.8A, the mixture is separated in under 5 s with baseline resolution between glutamic acid and aspartic acid. The unlabeled peaks in the electropherogram result from photolytic and hydrolysis products of excess CF-SE. Though the presence of excess peaks is undesirable, the photolytic side products generally result in an increase in products migrating with the neutral band in the electropherogram, an area where analytes are unresolved. The presence of peaks from excess CF-SE results from the pre-column fluorescent derivatization and maybe eliminated if faster, caged-fluorogenic reagents

were used. Migration times for Arg, Glu, and Asp were 1.72, 4.69 and 4.88 s respectively. Additionally, online analysis of this mixture over a 300 s period provides highly reproducible injections (Figure 2.8B).

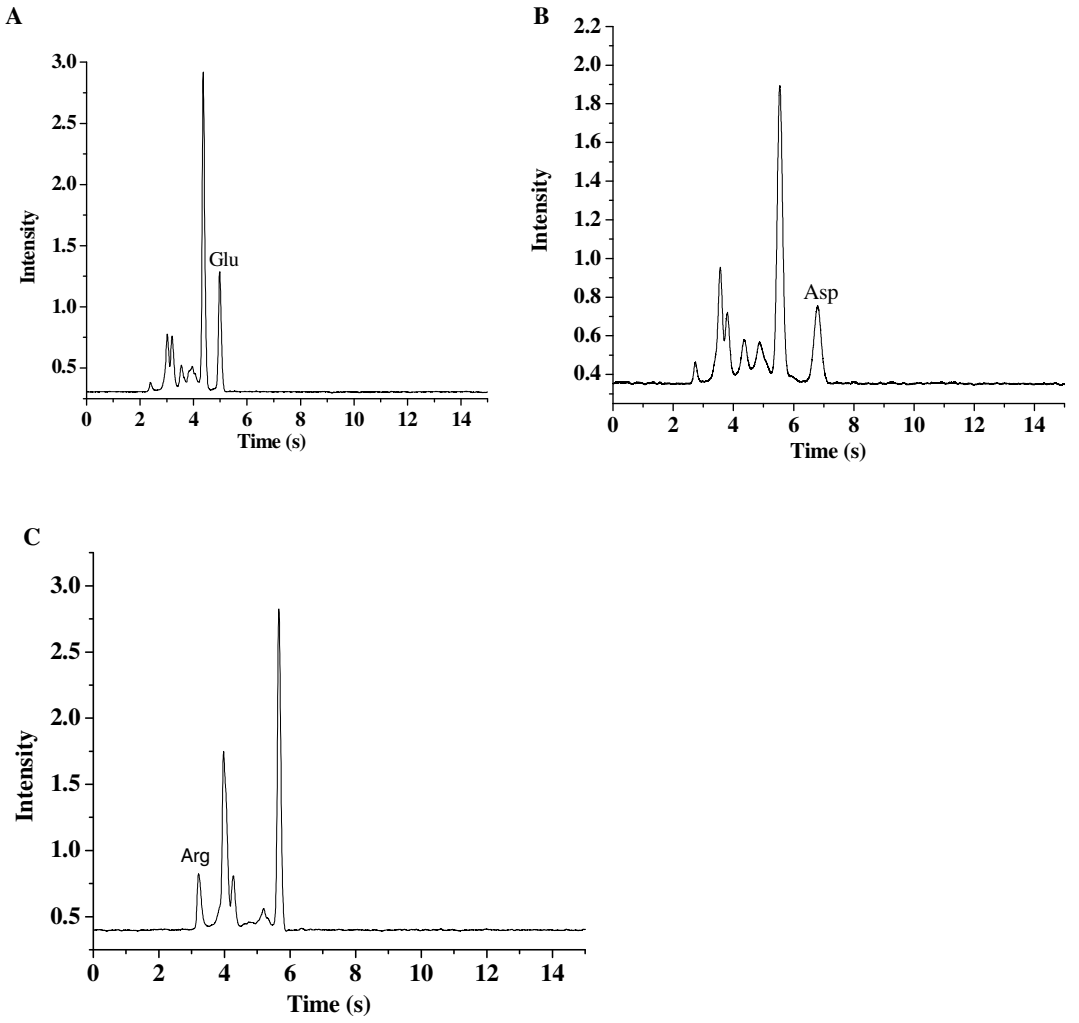

Figure 2.7. Separation of CF-labeled amino acids using POG-CZE. A) CF-labeled glutamic acid. (B) CF-labeled aspartic acid, and (C) CF-labeled arginine. E = 1.77 kV/cm, injection time = 20 ms.

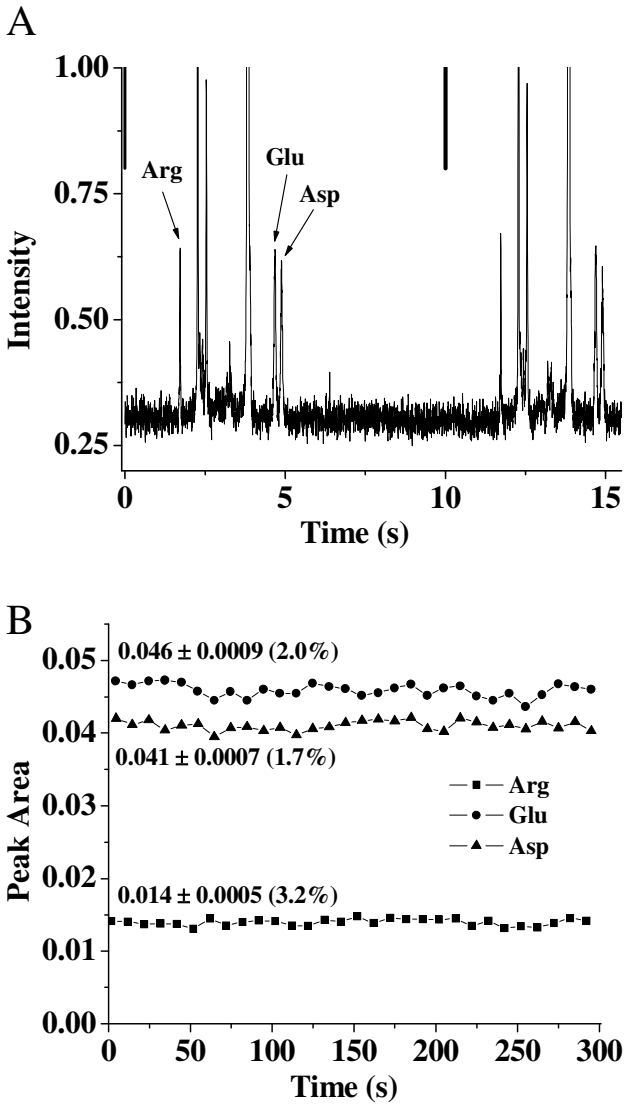

Figure 2.8. Separation of CF-labeled amino acids using POG-CZE. A) Consecutive, online injections were performed on a sample mixture containing 10 nM CF-labeled arginine (arg), glutamic acid (glu) and aspartic acid (asp). Lines in upper trace indicate times of injection. B) Plot of peak area calculated for 30 continuous electropherograms obtained for CF-labeled arg, glu and asp over 300 s. E = 1.77 kV/cm, injection time = 20 ms.

Table 2.1 shows the peak efficiencies obtained for Arg, Glu and Asp. The efficiencies observed in this approach are comparable to those reported using photobleaching-based optical gating using fluorescein derivatives[51;52] or OPA

derivatives,[106;125] and are approximately one order of magnitude higher than those obtained using NDB derivatives.[123] Further, these efficiencies are obtained using a 1.4 cm separation length. One limitation of the current POG-CZE instrumentation is the long capillary length required (20 cm total length) based on spatial limitations in the instrumentation, though the separation length defined by the spatial orientation of the injection and detection beams, is 1.4 cm. The net result is a reduced field strength and increased lag time for temporal measurements (see below). Thus with continued instrumental improvements and the application of shorter separation capillaries or microchips, it may be possible to further increase the separation efficiency.

Peak	Migration Time (s)	LOD (nM)	N	N/m
Arg	1.72	0.7	15,400 ± 200	1,100,000/m
Glu	4.69	0.7	51,000 ± 100	3,600,000/m
Asp	4.88	0.8	51,000 ± 900	3,600,000/m

Table 2.1. Summary of experimentally measured values for amino acid analysis with POG-CZE

2.3.3 Sensitivity and Calibration

Though the separation efficiency of POG-CZE is comparable to photobleaching approaches, the sensitivity is much higher in POG-CZE. Calibration curves were constructed for amino acids including glu, asp and arg, using the peak height for each derivative (n=3), and showed excellent linearity ($R^2 \geq 0.99$) (Figure 2.9). The calibration range for arg was 5 nM to 200 nM while the calibration range for glu and asp was 5 nM

to 800 nM. Limits of detection for the three component amino acid mixture used in Figure 2.8 are shown in Table 2.1 LOD's were measured to be 0.7, 0.7, and 0.8 nM for arg, glut, and asp, respectively, for S/N = 3. These detection limits are two to three orders of magnitude lower than previously obtained using fluorescein and NBD and are comparable to OPA based applications.[123;125] Mass detection limits for arg, glu, and asp were 11 zmol, 11 zmol and 13 zmol, respectively. Additionally, mass detection limits in terms of number of molecules injected for a single analysis were ca. 6.6×10^3, 6.6×10^3 and 7.8×10^3 molecules for arg, gly and asp respectively, comparable to values obtained with sheath-flow LIF detection, in which sheath-flow cuvette is used to perform off-column fluorescence detection to minimize laser scattering and luminescence from the fused silica capillary walls[150;220]. The observed improvement in sensitivity is due primarily to the lower fluorescence background provided through the use of CF.

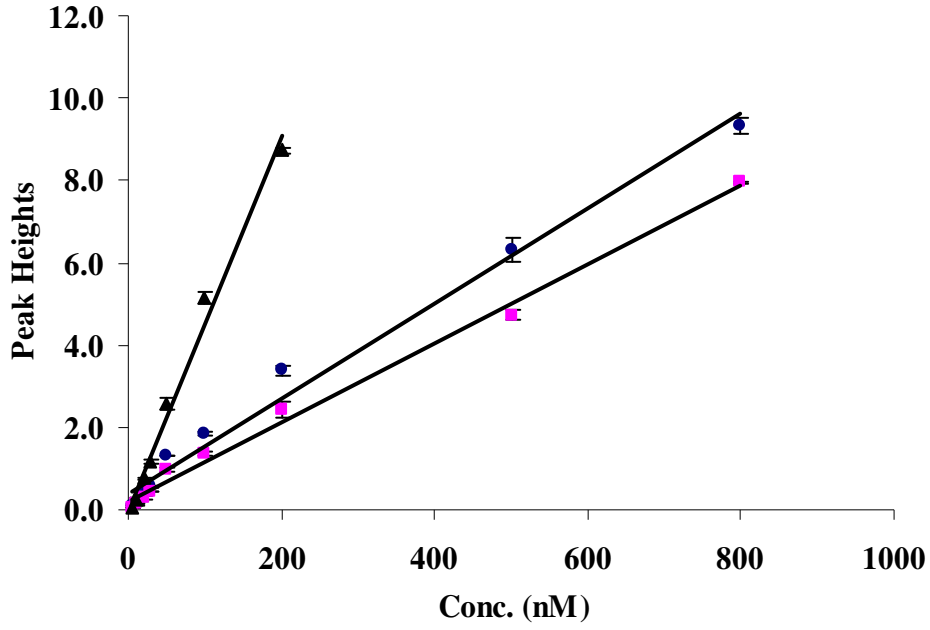

Figure 2.9. Instrument calibration for caged-fluorescein labeled amino acids. Calibration curves are constructed for glutamic acid (●), aspartic acid (■) and arginine (▲). R^2 values for glutamic acid, aspartic acid and arginine are 0.99, 0.99 and 0.99, respectively.

2.3.4 Temporal Measurements

Development and utilization of on-line, separation-based chemical sensors places extensive demands on the temporal resolution of the on-line separation. To evaluate the temporal response of POG-CZE, we first investigated the response time to step changes in CF concentration using the modified POG-CZE instrumentation described above. Briefly, the separation capillary was interfaced to the output capillary of a stream selecting valve using a Teflon connector. Sample solutions containing either 50 nM or 100 nM CF (samples A and B, respectively) were connected to the valve and constant pressure was applied to syringes using a syringe pump. When the valve was in position A, solution A was introduced to the separation capillary while sample B was sent to

waste. Switching to position B resulted in introduction of sample B to the separation capillary. POG-CZE sample injections were performed for 20 ms every 10 s throughout the time course of the experiment.

Figure 2.10A shows the peak height change associated with step changes in CF concentration from 50 nM to 100 nM to 50 nM. Based on our calculations of volumes and flow rates, the temporal response of the system are most likely limited by the volume of the connection capillary and dead volume in the capillary interface. Temporal effects of the connection capillary appear as increased lag (delay) times, as observed in the 30 s delay upon switching from 50 to 100 nM CF (Figure 2.10A and 10B) and can be readily adjusted by minimizing the length of the connector. The primary factors affecting the response (rise) time are the dead volume associated with the capillary interface and diffusion at the concentration interface in the connection capillary likely plays a role as well. Figure 2.10B illustrates the response curve constructed using individual peak areas,[221] calculated from the respective electropherograms in Figure 2.10A. Approximately two injections are needed to observe changes in concentration, thus resulting in a 20 s rise time. When faster injections were performed, the rise time was not significantly altered, further indicating the limitations of diffusion and dead volumes on rise time.

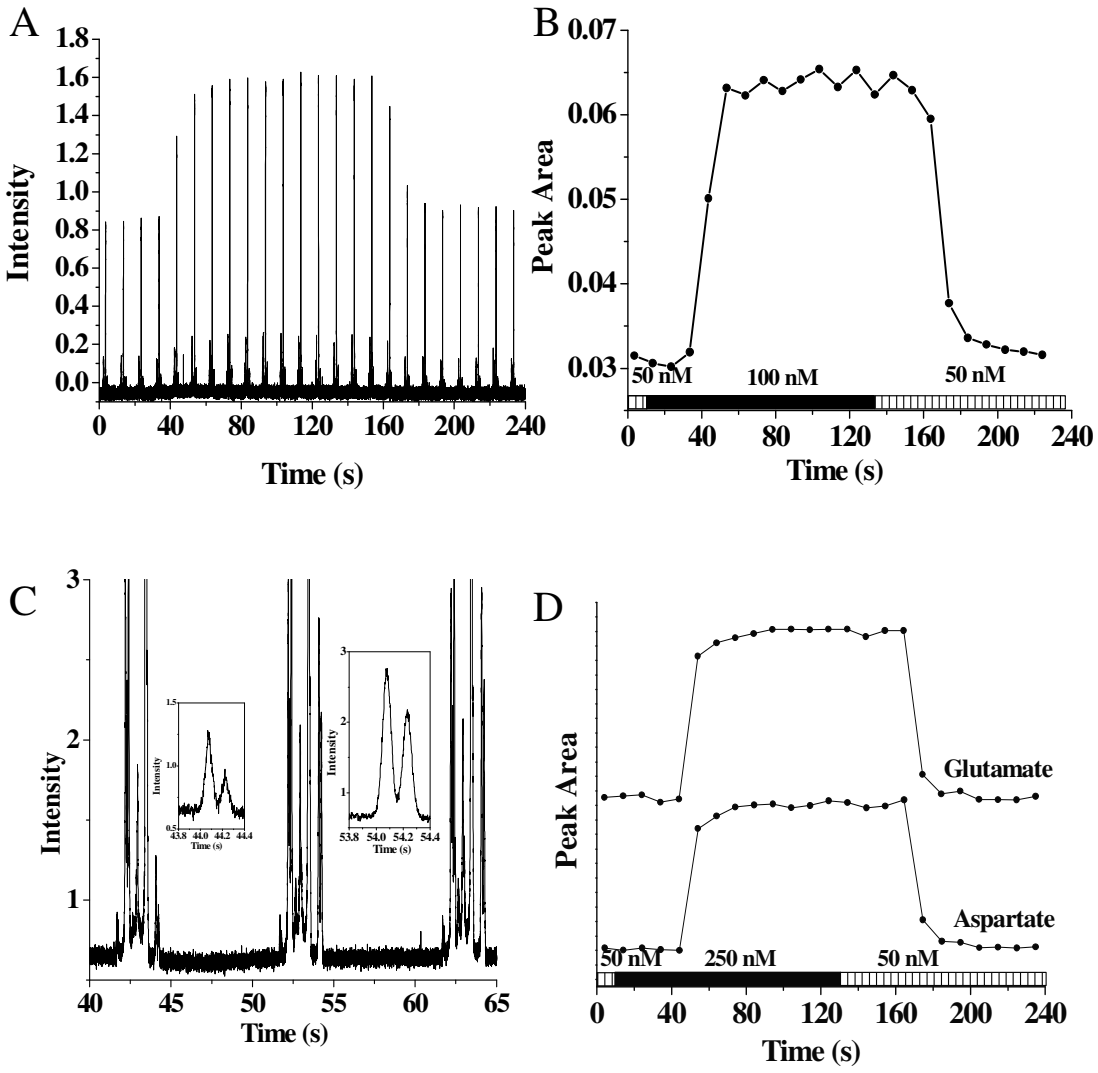

Figure 2.10. Dynamic chemical monitoring using POG-CZE. A) Plot of 24 consecutive electropherograms collected online during a step change in CF concentration. CF concentration was changed from 50 nM to 100 nM and back to 50 nM. B) Plot of peak area vs. time for data collected in A. C) Plot of 3 consecutive electropherograms (of 24) generated from a mixture of CF-labeled glu and asp. Concentration was changed from 50 nM to 250 nM as described in the text. Insets expand the glu and asp peaks for the injections at 40s and 50s. D) Plot of peak area vs. time for data collected in C. Each point represents the peak area from one individual separation in the series. Analyte concentration and time of solution switch are depicted by the bars at the bottom. E = 1.77 kV/cm, injection time = 20 ms.

Temporal responses measured with CF-labeled amino acids yield similar results. Figure 2.10C illustrates the temporal response upon step concentration changes in CF-labeled glut and asp. For clarity, only the electropherograms corresponding to the step change have been presented. The insets in Figure 2.10C show an expanded view of the glu and asp peaks corresponding to injections at 40 s and 50s. Figure 2.10D shows the temporal response curve generated by calculating the peak areas from 24 consecutive electropherograms (from Figure 2.10C) obtained at 10 s intervals. The rise time ($t_{10\text{-}90}$) and the delay time are 10 s and 30 s, respectively. The rise time and delay time measured in both cases are limited primarily by the current stream selection geometry and not by the speed of the separation, suggesting that with appropriate modifications, POG-CZE can be used for on-line, *in vivo* analysis, similar to other sampling interfaces.

2.3.5 Protein Analysis CZE with Photolytic Injection

While successful for a number of small molecules, separation and detection of proteins using on-line CZE methods has proven more difficult. A number of CZE-based immunoassays have been employed for protein analysis with a few extended to on-line monitoring of protein analytes, primarily through the use of flow-gated and flow-through interfaces.[112;189;191] The direct analysis of fluorescently labeled proteins has proven more problematic for on-line measurements due primarily to the low concentration of proteins in biological systems which imparts stringent sensitivity requirements. This problem is further exacerbated by the adsorption of proteins onto negatively charged capillary surfaces, resulting in band broadening and reduced sensitivity.[92] When the proteins interact with the capillary wall, speed of the separation is mainly dependent on the rate of

adsorption and desorption of the protein with the capillary surface. These limitations can be overcome with higher sensitivity on-line sampling schemes, which controls the amount of the sample injected into the capillary and/or coated capillaries. when the capillary is coated, protein-wall interactions is minimized rendering high efficient separations. In POG-CZE, cellulose acetate coated capillaries[92] were used.

Figure 2.11A shows three consecutive injection of CF-labeled streptavidin obtained at 5 s intervals. Close inspection of the electropherograms reveals three peaks, one from streptavidin and two smaller peaks due to unreacted CF in the sample. A calibration curve was also constructed for streptavidin (Figure 2.12) and showed excellent linearity ($R^2 \geq 0.99$). The calibration range for streptavidin labeled with caged-fluorescein was 5 nM to 20 nM as depicted in Figure 2.12. The CF-streptavidin sample was detected in less than 3 seconds with a 0.5 nM detection limit, comparable to the figures of merit obtained for small molecules (Table 2.1). Figures 2.11B and 2.11C illustrate the reproducibility of protein injections and detection, where 15 consecutive electropherograms were collected in 30 s at 2 s intervals with high injection and detection precision. Relative standard deviations were 0.8 %, 2.2 % and 1.8 % for migration time, peak height, and peak area, respectively. When non-coated capillaries were used, peak heights deteriorated rapidly, concurrent with increased peak broadening due to protein adsorption, until eventually no peaks were detected. Further optimization of the separation conditions allowed sub-second, on-line detection of proteins (Figure 2.11D). When the field strength was increased to 3.3 kV/cm, CF-streptavidin could be migrated under 500 milliseconds with high separation efficiency (5.6×10^5 plates/m). Thus, POG-

CZE provides a basis for high sensitivity, high speed, on-line injection of proteins, as well as small molecules, suggesting the utility of the method for on-line chemical monitoring.

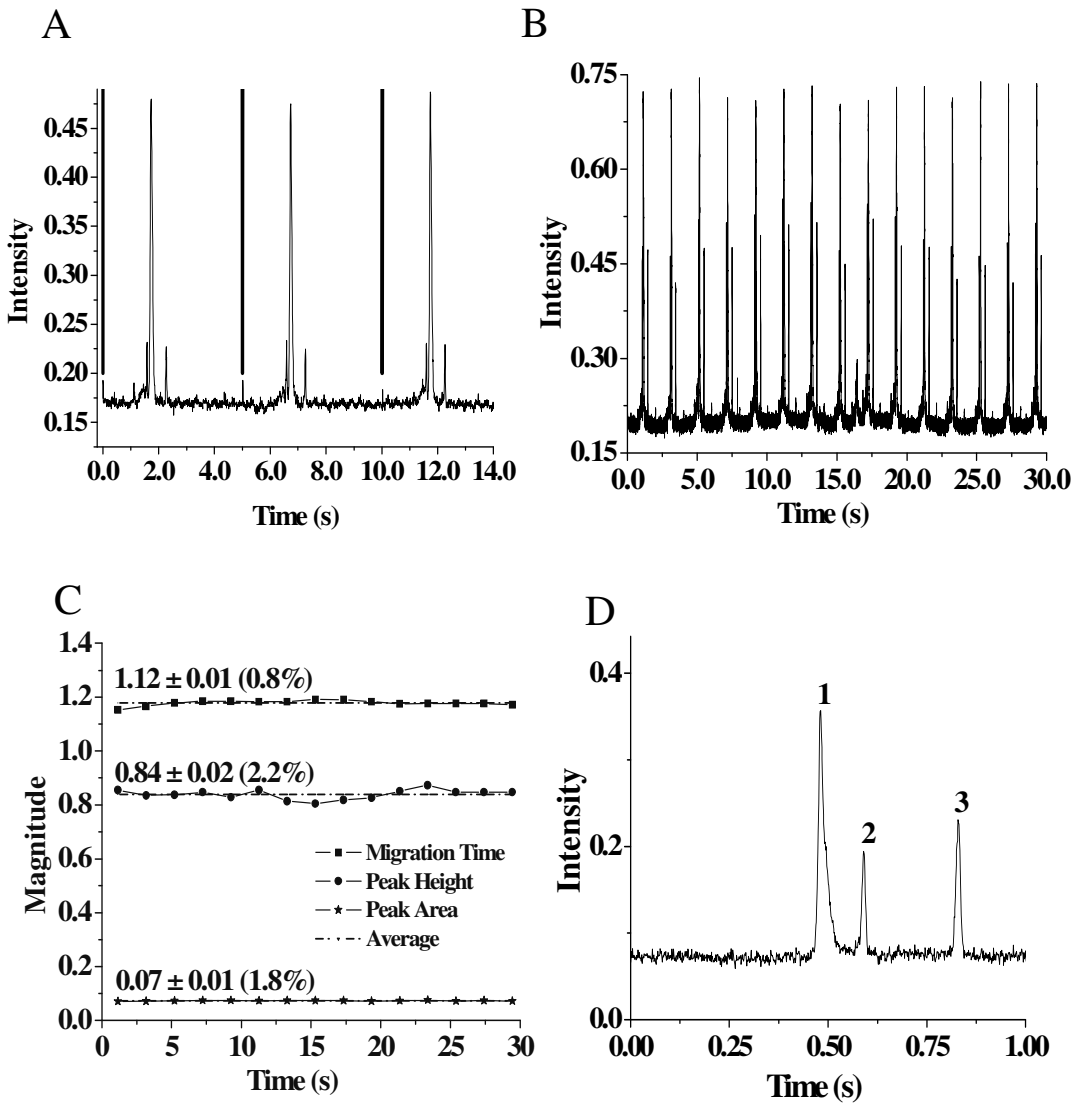

Figure 2.11. POG-CZE of CF-labeled protein. A) Three consecutive electropherograms obtained from the on-line injection and separation of 38 nM CF-labeled streptavidin. Lines in upper trace represent injection events. B) A series of 15 electropherograms obtained over 30 s to evaluate the reproducibility of protein injection and separation. C) Peak parameters calculated from data in B. D) Electropherogram obtained from separation of 38 nM CF-labeled streptavidin. Peak identities are: 1) streptavidin and 2 and 3) unreacted CF. E = A-C) 2.25 kV/cm and D) 3.3 kV/cm, injection time = A and D) 10 ms, B and C) 20 ms.

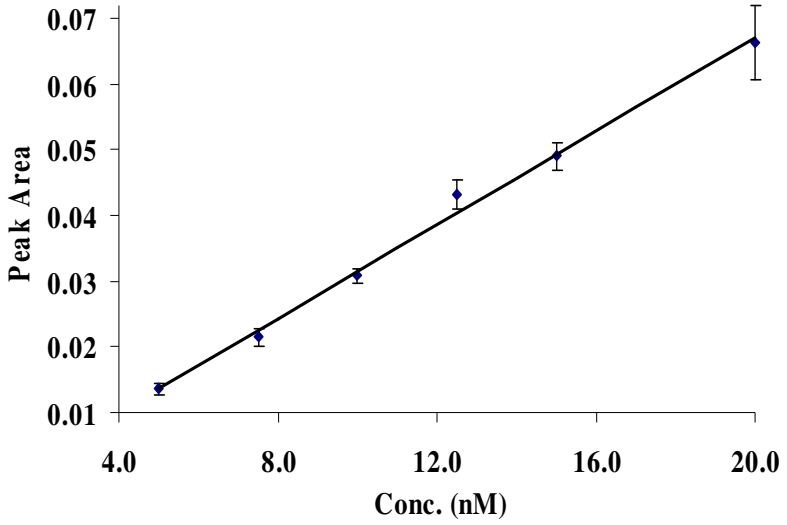

Figure 2.12. Instrument calibration for streptavidin. A calibration curve is constructed using peak area. R^2 value is 0.995.

2.4 Conclusions

We have developed a photolytic optical injection approach for CZE (POG-CZE) based on the photolysis of caged fluorescent labels. This approach provides an inherently low background and results in markedly improved sensitivity over other on-line capillary interfacing technologies. Separation times under 5 s for mixtures of small biologically important molecules and 500 ms for proteins were obtained with high separation efficiency. Thus, POG-CZE possesses the sensitivity, resolution and efficiency to be used for on-line monitoring of chemical and biological systems, as well as for interfacing multidimensional systems, multiplexed separation instruments and microchip separations.

CHAPTER 3. DESIGN, CHARACTERIZATION, AND UTILIZATION OF A FAST FLUORESCENCE DERIVATIZATION REACTION UTILIZING O-PHTHALDIALDEHYDE COUPLED WITH FLUORESCENT THIOLS

3.1 Introduction

Dynamic chemical monitoring using capillary electrophoresis (DCM-CE) has proven useful for time resolved chemical analysis of biological samples due to the unique combination of chemical information, sensitivity and temporal resolution that can be achieved [43;115;176;177]. Most commonly, DCM-CE has been used to investigate neurotransmitters, drug metabolites and hormone dynamics *in vivo* [41;42;44;115;118;176;190;191]. To achieve sufficiently fast sampling in DCM-CE, on-line sample collection, often coupled with fluorescence derivatization, is used, placing stringent demands on the sample injection and on the reaction kinetics for fluorescence derivatization reactions. Numerous fluorescent labeling reactions have been reported for use in CE, the most common of which involve either the fluorescent or fluorogenic derivatization of primary amines [168;222]. On-line DCM-CE most commonly utilizes fluorogenic reagents due primarily to the faster reaction kinetics provided by these reagents, e.g. OPA or naphthalene dicarboxaldehyde (NDA) [43;45;115;176;177].

OPA is used to derivatize primary amines in the presence of a thiol, e.g. β-mercaptoethanol (BME) [4;223], 3-mercapto-1-propanol [223], dithiothreitol [224], ethanethiol [225], or N-acetyl-L-cystein (NAC) [224;226]. The reaction of OPA with primary amines is intrinsically fast, making it the most commonly used fluorescent label for DCM-CE. The

primary limitation of the OPA/BME reaction is the UV excitation (ca. 335 nm) required for detection of the resulting isoindole products. As a result, UV lasers are used for detection, though these sources are generally more expensive and less stable than common visible lasers, and are not available with commercial CE instrumentation. Moreover, the quantum yield of the isoindole products varies depending on the analyte and thiol used in the reaction and varies between 0.33 and 0.47 [4], resulting in differing sensitivities, with relatively weak molar extinction coefficients (ca. 5700 M^{-1} at 334 nm [4]).

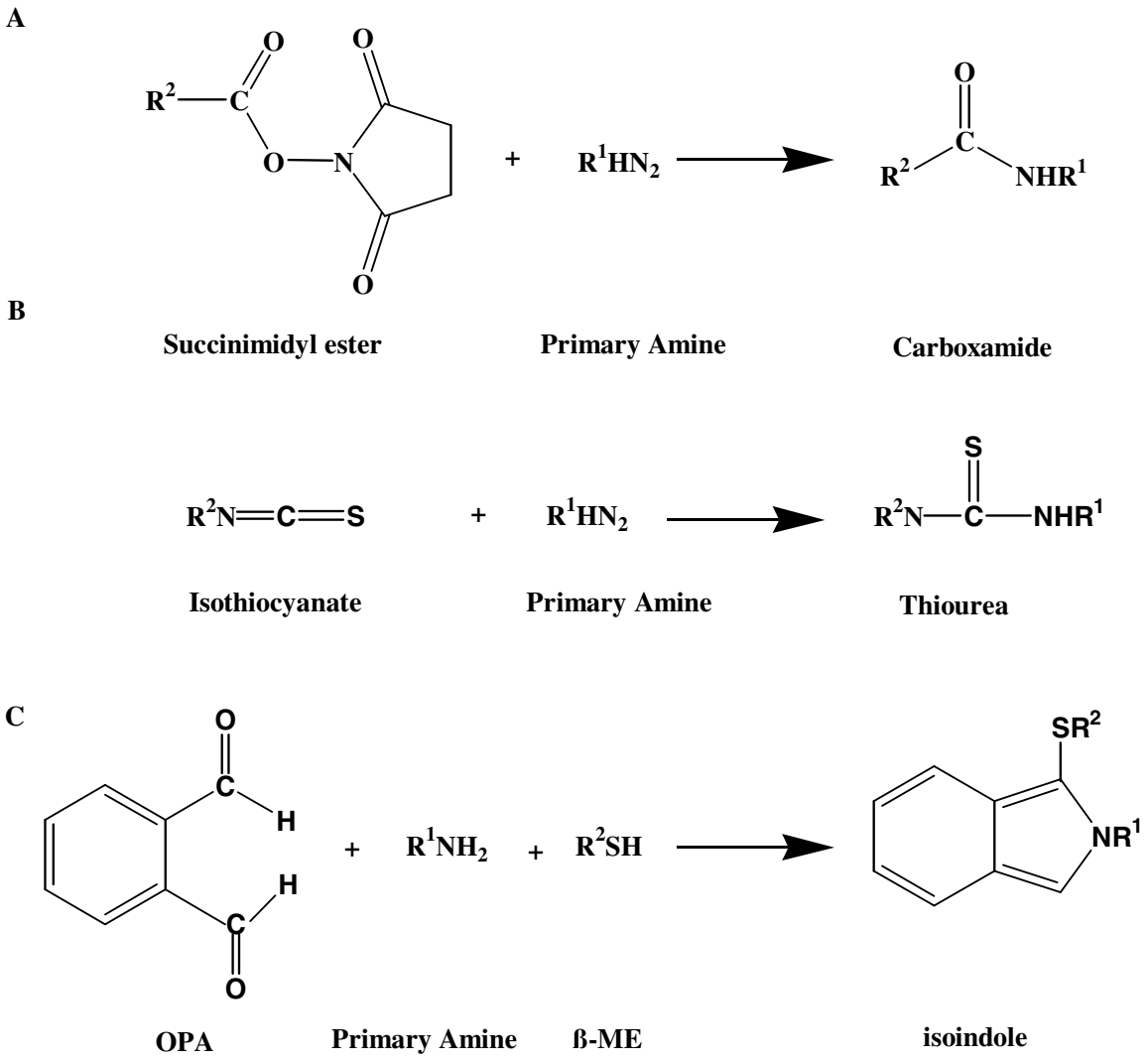

Figure 3.1. Derivatization schemes for primary amines with (A) a succinimidyl ester, (B) an isothiocyanate, and (C) OPA/β-ME.

In general, higher sensitivity is obtained in CE with highly absorbing, high quantum yield, fluorescence labels, e.g. fluorescein or rhodamine, that are excited with commonly available visible laser and laser diode lines [167;227]. Among these labeling reagents, isothiocyanate (ITC) and succinimidyl ester (SE) derivatives of fluorescein and rhodamine [150;168-171] are the most commonly used for CE (Figure 3.1). Though higher

sensitivity is attained, the slow reaction kinetics are not favorable for on-line derivatization required for DCM-CE and other situations where fast labeling reactions are desired. Recently, 5-(4,6-dichloro-s-triazin-2-ylamino) fluorescein (DTAF) [169;172-174] has emerged as an alternative to ITC and SE fluorescein derivatives as it reacts quickly with primary amines at high temperature (40-50 ^{0}C for less than 1 hr). Cao et al., have reported a new fluorescent label (6-oxy-(N-succinimidyl acetate)-9-(2-methoxycarbonyl)fluorescein (SAMF)), that can be used to label amino acids in 6 min at 30 ^{0}C [175]. While desirable for a number of applications, the reaction conditions and/or kinetics remain incompatible others, most notably with on-line labeling required in DCM-CE.

Label	(ε_{max})	(Φ)	λ_{ex} (nm)	λ_{em} (nm)
OPA	57 000	0.32 - 0.47	354	450
FITC	77 000	0.92	488	519
CFSE	78 000	0.92	488	520

Table 3.1. Optical properties of different derivatization reagents. Extinction coefficient (ε_{max}), fluorescence quantum yield (Φ),absorption maximum (λ_{ex}), and fluorescence maximum (λ_{em}). ε_{max} for FITC and CFSE was calculated at 490 nm[1] and ε_{max} for OPA was calculated at 334 nm[4]. Φ for FITC and CFSE reported here was calculated for fluorescein in 0.1 M NaOH solution.[5]

Label	k (min^{-1})
OPA	18
FITC	0.02
CFSE	0.40

Table 3.2 *P*seudo first order reaction rate constant (k) for different dyes. For fluorescein isothiocyanate (FITC) and carboxyfluorescein succinimidyl ester (CFSE), rate constants were calculated for the reaction between the dye and the Myoglobin at the conjugation ratio 5:1[1]. For o-phthalicdicarboxaldehyde (OPA), k was calculated for the conjugation with alanine[3].

An optimal derivatization reaction would incorporate the photophysical properties of visible, highly absorbing, high quantum yield dyes (Table 3.1) with the reaction kinetics (Table 3.2) of small molecule fluorogenic reagents, e.g. OPA. To achieve these goals, we have devised a reaction scheme whereby non-fluorescent thiol compounds utilized in the OPA reaction are replaced with a thiol-functionalized fluorescein, SAMSA-F (5-((2-(and-3)-S-(acetylmercapto)succinoyl) amino)fluorescein). Upon activation of SAMSA-F under basic conditions,[228] free thiol-functionalized fluorescein can be liberated and subsequently react with OPA in the presence of primary amines (Figure 3.2A). Reaction times of less than 10 s are obtained with sub-nM detection limits using the 488 nm laser line of a low power, air-cooled Ar^+ laser. Utilization of this reaction for DCM-CE, allows on-line monitoring of model amino acid and neurotransmitter mixtures with high sensitivity and high temporal resolution.

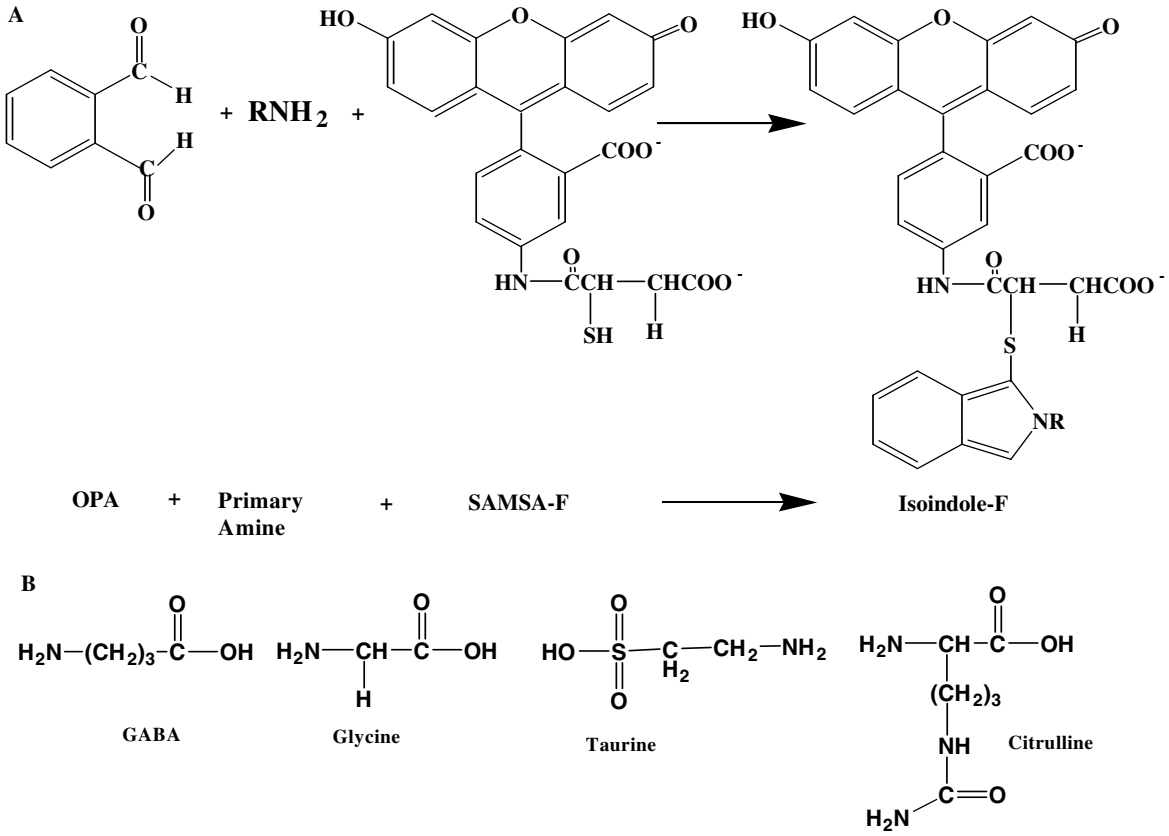

Figure 3.2. (A) Derivatization scheme for primary amines with OPA/SAMSA-F. Target analyte amines (RNH_2) are mixed with 15 and 3 fold excesses of OPA and SAMSA-F, respectively. (B) Chemical structures of primary amines used in the separation.

3.2 Experimental

3.2.1 Materials and Reagents

Amino acids were obtained from Sigma Chemical Co. (St. Louis, MO). OPA was obtained from Aldrich Chemical Co. (St. Louis, MO). SAMSA-F was obtained from Molecular Probes Inc. (Eugene, OR). All the other chemicals were from VWR and were used as received. Fused silica capillaries were from Polymicro Technologies (Phoenix, AZ). All solutions were prepared using 18 MΩ deionized water (Barnstead).

3.2.2 Capillary Electrophoresis Conditions

New capillaries were treated with 100 mM NaOH for 10 min followed by a 10 min wash with 10 mM phosphate buffer at pH 7.4 prior to use. Capillaries were reconditioned after a five runs via consecutive rinses with 10 mM HCl, DI water, 100 mM NaOH and running buffer, respectively.

3.2.3 CE-LIF Instrumentation

The LIF-CE detection system was built in-house and is shown in (Figure 3.3). The output of a multiline Ar^+ laser (Model 180-Series Laser Systems, Spectra-Physics, Mountain View, CA) operating at 20 mW total power was passed through a prism (Melles Griot, Irvine, CA) to separate the 488 nm line. The detection beam (488 nm) was focused into the center of the separation capillary using a plano-convex (f = 25 mm, Melles Griot, Irvine, CA) lens. Sample was injected into the separation capillary by siphoning. The fluorescence signal was collected using a microscope objective (10x, 0.25 N.A., Newport, Irvine, CA) before passage through a spatial filter and a band pass filter (D525/25 M, Chroma Technology, Rockingham, VT). The signal was then detected by a PMT (H957, Hamamatsu Photonics, Bridgewater, NJ), current, from which was amplified by a current amplifier (Model SR570, Stanford Research System, Sunnyvale, CA), and collected by an A/D converter (PCI-MIO-16E-4, National Instruments, Austin, TX) using in-house software written in LabView (National Instruments). Electric fields were applied using a 30 kV power supply (CZE-1000, Spellman High Voltage Corporation, Hauppauge, NY).

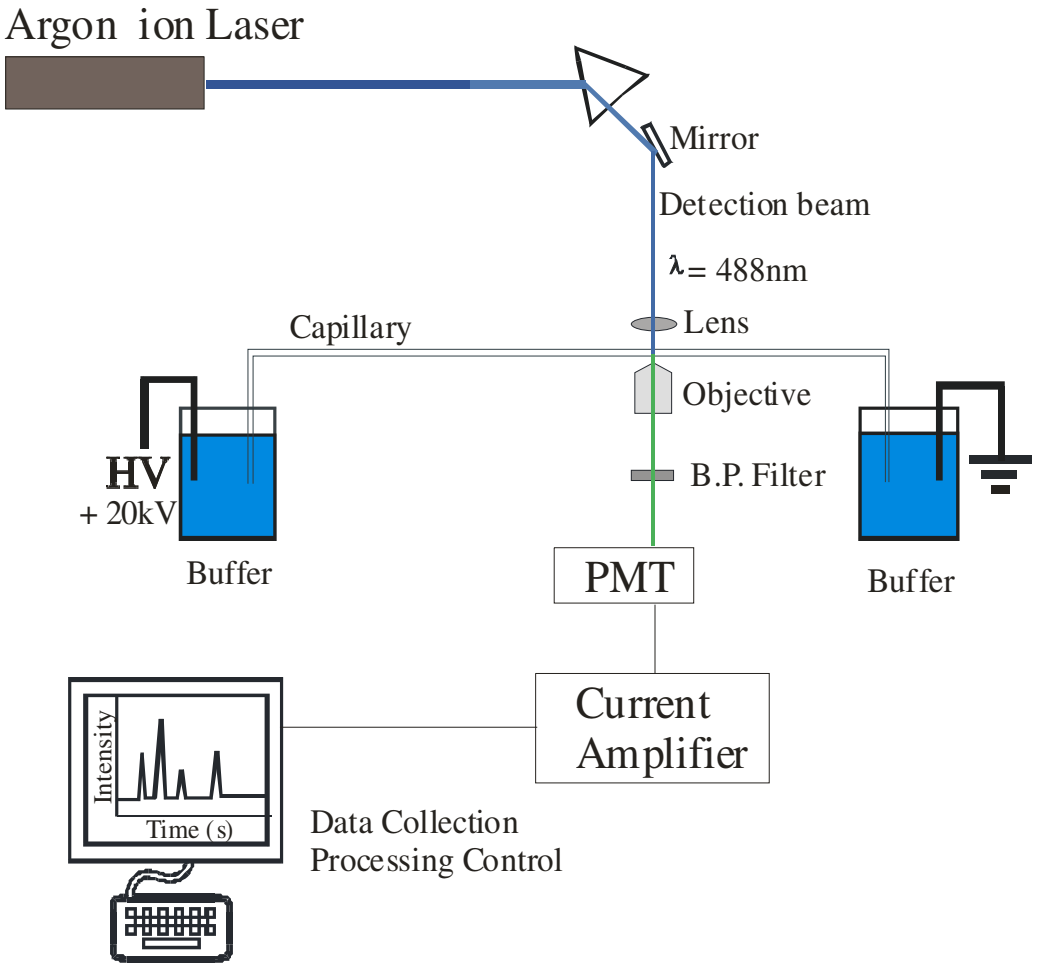

Figure 3.3. Schematic diagram of CZE instrumentation with the laser-induced fluorescence detection.

3.2.4 Off-line OPA/SAMSA Fluorescein Derivatization

Samples were derivatized off-line with OPA/SAMSA-F prior to analysis. Stock solutions of hydrolyzed SAMSA-F was prepared by dissolving SAMSA-F in 0.1 M NaOH [228]. After 30 minutes, the concentration of activated SAMSA-F was determined via absorbance spectroscopy. OPA stock solution (75 mM) was prepared by dissolving 10 mg of OPA in 100 µL methanol followed by dilution to 1000 µL with 10 mM borate buffer (pH 10.0). Amino acid stock solutions (Figure 3.2B) were prepared in 0.1 M

bicarbonate buffer (pH 9.0). For amino acid mixtures, derivatization was performed by adding 17.5 nmol aliquots of mixture components from the stock solution to 3 fold molar excess of SAMSA-F and 15 fold molar excess of OPA in borate buffer (pH 10.0). The mixture was allowed to react in the dark with constant stirring. The labeled sample was further diluted in running buffer prior to CE analysis.

3.2.5 Microdialysis Sampling and On-line Derivatization

Schematic diagram of the on-line derivatization system is given in Figure 3.4. Briefly, a loop-type microdialysis probe (0.5-mm o.d. x 2-mm length, 6 kDa cutoff, Harvard Apparatus, Holliston, MA) was conditioned in 70% ethanol overnight prior to use. The probe was perfused with borate buffer (pH 10.0) at a rate of 0.8 µL/min with a 1 mL air tight syringe (Hamilton, Reno, NE) controlled by a Harvard syringe pump (Harvard Apparatus). Dialysis was performed by inserting the probe into the sample vial. The dialysate was mixed on-line with OPA/SAMSA-F derivatization reagents (3 mM OPA and 300 µM SAMSA-F) pumped with a 1 mL syringe controlled by the same syringe pump at the same flow rate into a quartz tee (InnovaQuartz, Inc., Phoenix, AZ). After mixing the sample and the reagents, the output of the tee (150 µm i.d. capillary) was allowed to react in a 32 cm reaction capillary before collection at the end of the capillary. The collected sample was immediately diluted into the borate buffer followed by CE analysis.

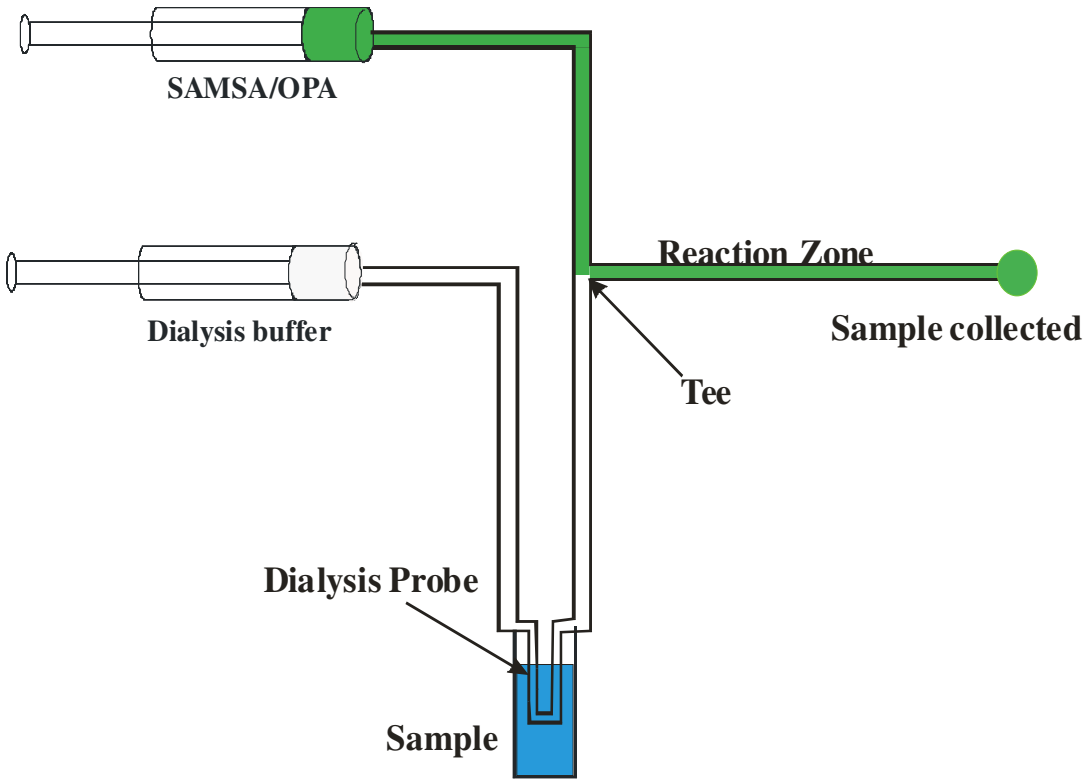

Figure 3.4. Schematic of diagram of on-line derivatization instrumentation. The microdialyzed sample was labeled using OPA/SAMSA-F.

3.3 Results and Discussion

Fluorescence detection of UV-excitable isoindoles, which result from the reaction of OPA with primary amines in the presence of BME is commonly used in CE and HPLC to detect biologically important small molecules.[229-231] Though the traditional OPA/BME reaction provides the high sensitivity and rapid reaction kinetics required for DCM-CE, UV-LIF detection typically requires the use of expensive and/or less stable UV lasers, e.g. the 350-360 nm lines of a water cooled Ar^+ laser or the 325 nm line of a HeCd laser for excitation. Here, we further explore OPA as a potential cross linking reagent for reaction with primary amines in the presence of a fluorescent thiol, SAMSA-F.

Detection is then based on excitation and emission of the incorporated fluorescein rather than the UV-excited isoindole (Figure 3.2), thereby eliminating the need for UV light sources.

3.3.1 UV/VIS Absorbance Study of OPA/SAMSA-F/Primary Amine Reaction

To investigate the validity of this approach for labeling primary amines we first monitored the formation of isoindole products upon reaction of OPA and SAMSA-F with primary amines, as an indicator for covalent attachment of the OPA/SAMSA-F/primary amine conjugate. The formation of isoindoles via the reaction of OPA with primary amines has been well documented for a variety of thiol containing compounds [4;223-226;232]. In the presence of a free thiol and primary amine, OPA forms an isoindole with a characteristic absorbance maximum ca. 335 nm [4;232], allowing formation of the isoindole product to be monitored spectroscopically. To monitor formation of isoindoles, UV-VIS absorbance spectroscopy was performed in the presence and absence of OPA or SAMSA-F, as well as upon addition of varying concentrations of amino acid (Figure 3.5). Figure 3.5A shows the absorbance spectra obtained when a primary amine (arginine (arg)) was added to 1) a 2 fold molar excess of SAMSA-F, and 2-5) to 15 and 2 fold molar excesses of OPA and SAMSA-F, with varying concentrations of arg. As seen in the spectra, OPA, SAMSA-F and a primary amine are required to generate the isoindole product. Additionally, the large absorbance associated with SAMSA-F (λ_{max} ~ 490 nm) is unaffected by the presence of OPA and the formation of the OPA/SAMSA-F/arg complex. Further, the absorbance at 336 nm increased linearly with respect to arg concentration, as seen when non-fluorescent thiols are used. This was further studied by

using different amines, in which calibration curves were constructed for glu, GABA, arg and gly using absorbance at 336 nm. The calibration range for all the analytes was 7.9 μM to 93.8 μM and excellent linear relationship was observed with R^2 values > 0.99 (Figure 3.5B). This indicates that proposed reaction also has reaction properties similar to OPA/BME reaction.

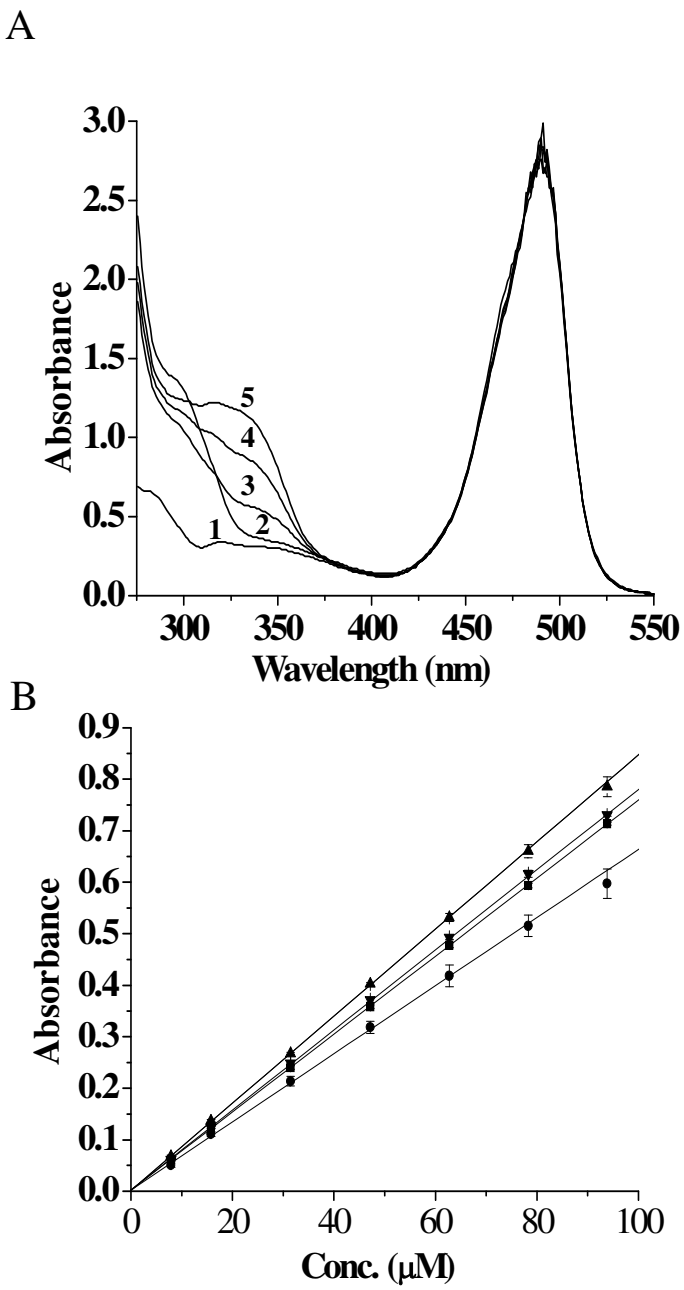

Figure 3.5. UV/VIS absorbance characterization of OPA/SAMSA-F/primary amine reaction. (A) Arg was reacted with an excess of 1) SAMSA–F and 2-5) an excess of OPA and SAMSA-F prior to collection of spectra. The OPA/SAMSA-F mixture was titrated with 2) 0 μM, 3) 64 μM, 4) 128 μM and 5) 190 μM arg. (B) Calibration curves prepared from UV/VIS absorbance measurements of OPA/SAMSA-F/arg. Absorbance was monitored at 336 nm. Absorbance versus concentration curves are shown for GABA (■), glu (●), arg (▲), and gly (♦). R^2 values exceed 0.999 for each plot.

3.3.2 CE-LIF Detection of OPA/SAMSA-F Derivatives

To determine the utility of the OPA/SAMSA-F reaction for detection of primary amines, mixtures of amino acids and neurotransmitters were fluorescently labeled and separated by CE. Figure 3.6 shows a series of electropherograms obtained for individual amines labeled with OPA/SAMSA-F. Migration time of each analyte was used subsequently to identify peaks in an electropherogram obtained for a mixture of amino acids. Figure 3.7A shows a series of electropherograms obtained upon reaction of amino acids with i) OPA alone, ii) SAMSA-F alone and iii) OPA/SAMSA-F mixture detected with 488 nm excitation. As seen in the electropherograms, both SAMSA-F and OPA are required to obtain detectable peaks that correspond to the migration of the four amino acids (iii). This result agrees well with that observed for ~ 350 nm excitation of OPA/BME labeled amino acids. In the absence of OPA, the only peaks observed correlated to the peaks observed from SAMSA-F alone (Figure 3.7A ii). The large number of peaks observed result from impurities in the commercial SAMSA-F sample and from the presence of two isomers of hydrolyzed SAMSA-F. Figure 3.7B shows the electropherograms obtained for the separation of a mixture of six amino acids and neurotransmitters labeled with excess OPA/SAMSA-F. Multiple peaks were observed for each amino acid, likely due to the presence of SAMSA-F isomers. The mixture was separated after labeling with OPA/SAMSA fluorescein and migration times for primary peaks were 170.3, 231.0, 251.9, 273.3, 372.6 and 385.2 for Arg, Citrulline, GABA, Gly, Glu and Asp, respectively. Calibration curves were constructed for selected amino acids, e.g. gly, glu, tau and GABA using the height of the primary peak for each derivative

(Figure 3.8) and showed excellent linearity ($R^2 \geq 0.99$). Limits of detection (S/N = 3) were measured to be 0.7, 0.5, 0.5 and 1.2 nM for GABA, tau, gly and glu, respectively, which are approximate one order of magnitude better than detection limits obtained with OPA/BME and NDA for these amino acids [167;177;222;227].

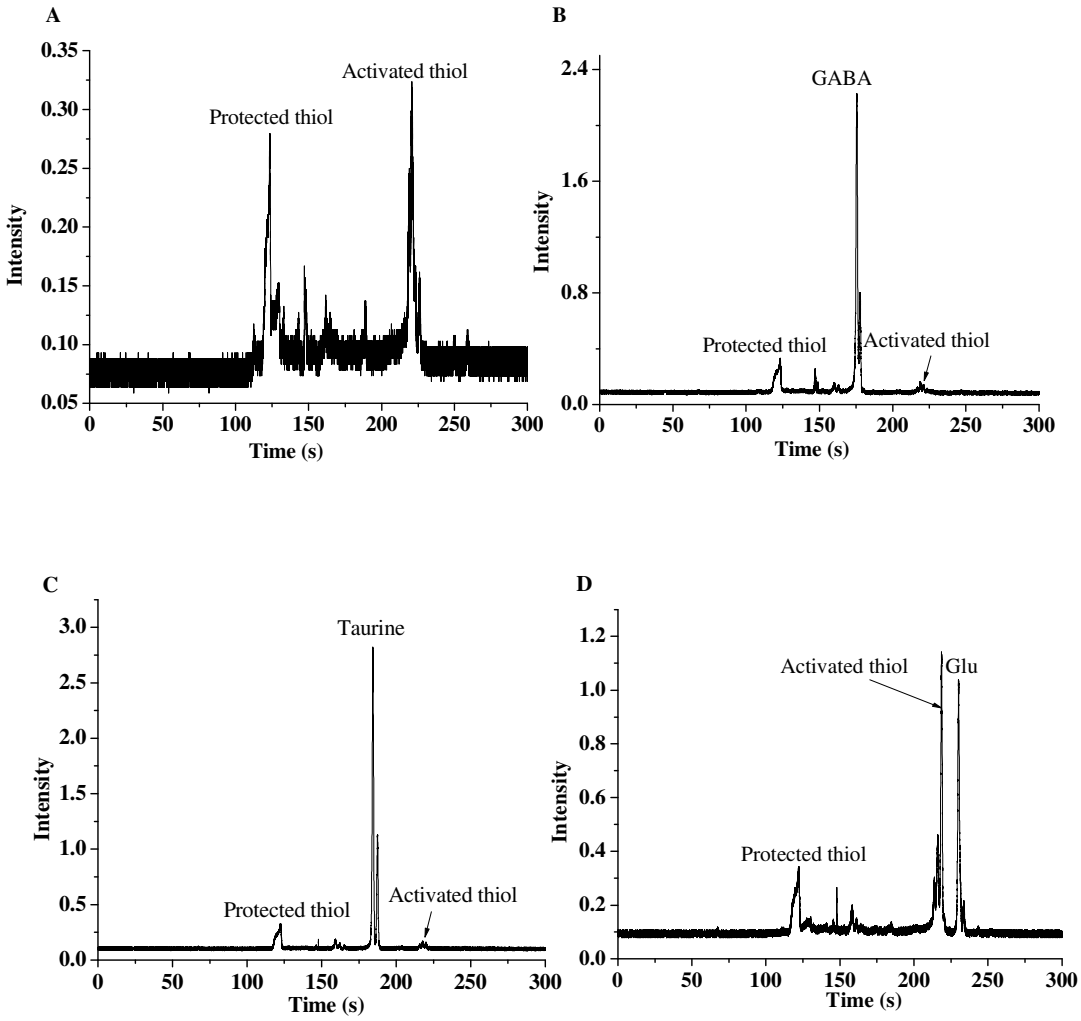

Figure 3.6. CE-LIF detection of OPA/SAMSA-F/primary amine derivatives. Electropherograms obtained for fluorescence detection of (A) SAMSA-F (B) OPA/SAMSA-F labeled GABA (C) OPA/SAMSA-F labeled Taurine, and (D) OPA/SAMSA-F labeled Glu. Separation conditions – E = 600 V/cm, 10 s injection, 10.0 mM phosphate, pH 7.4, capillary i.d. 25 μm, LD = 30 cm, filter frequency = 10 Hz, sampling rate = 100/s

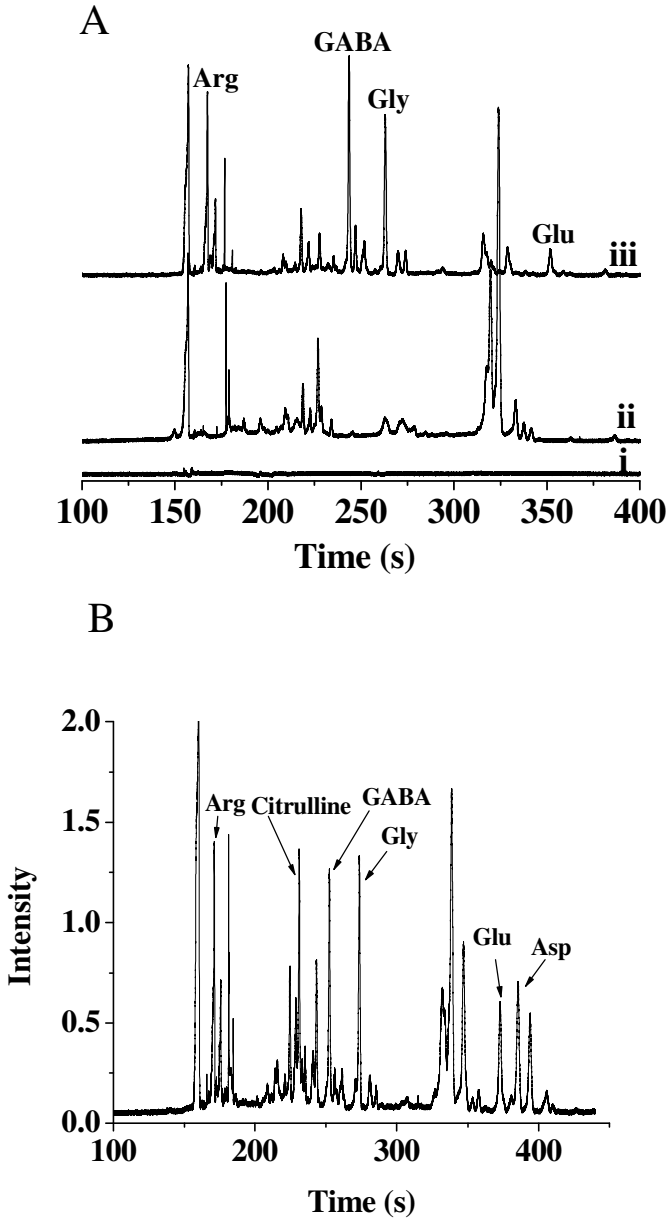

Figure 3.7. CE-LIF detection of OPA/SAMSA-F/primary amine derivatives. (A) Electropherograms obtained for fluorescence detection of 140 nM Arg, GABA, Gly, and Glu in the presence of excess i) OPA, ii) activated SAMSA-F, and iii) OPA and SAMSA-F. (B) Separation of a mixture of OPA/SAMSA-F labeled neurotransmitters and amino acids using CZE. The concentration of each analyte is 140 nM. Separation conditions: E = 600 V/cm, 5 s injection, 20 μm i.d., separation distance = 30 cm.

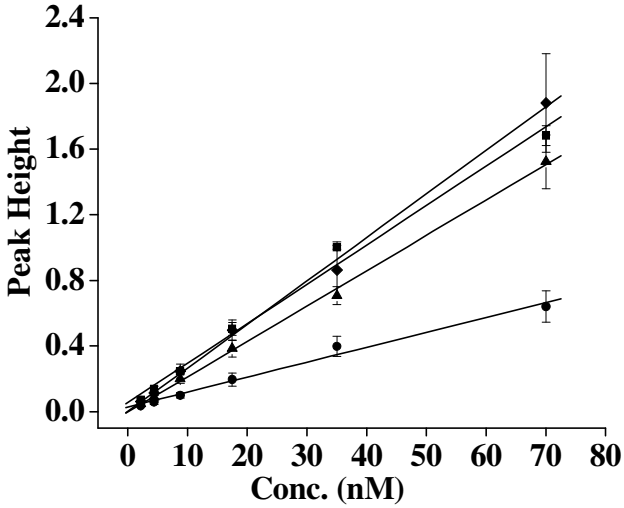

Figure 3.8. Calibration curves for OPA/SAMSA-F/primary amines analyzed by CE-LIF. Peak height versus concentration curves are shown for gly (■),glu (●), GABA (▲), and tau (♦). R^2 values exceeded 0.994 for each plot.

3.3.3 Study of Derivatization Conditions

After determining the feasibility for the OPA/SAMSA-F derivatization protocol, we examined the effects of derivatization conditions to optimize the reaction. Previous work has shown that both the concentrations and ratios of OPA and thiol are important in achieving fast, high efficiency reactions [4;223;232]. Figure 3.9A shows the effect of OPA concentration on the peak heights of derivatized glu and gly separated by CE. SAMSA-F was maintained at a 2 fold molar excess with respect to the analyte concentration, while the OPA concentration in the reaction mixture was titrated from 0 to 75 fold molar excess. As seen in Figure 3.9A, maximum peak heights for both amino acids were obtained at approximately 15-fold molar excess of OPA, though little statistical difference was observed once the molar ratio of OPA:analyte exceeded 5, in agreement

with previous reports to OPA/BME and other thiols [3;224;232;233]. Following the maximum at a molar ratio of 15 OPA:analyte, peak heights were observed to decrease at very high molar ratios, likely resulting from the instability of the isoindole product in the presence of excess OPA [115;223].

We next explored the effect of SAMSA-F concentration on the reaction mixture by varying the molar ratio of SAMSA-F with respect to the analyte while maintaining the OPA at 15 fold molar excess. Figure 3.9B shows the variation of peak intensities obtained following CE separation of derivatized glu, gly and GABA as a function of molar ratio SAMSA-F. For all three compounds, the peak intensities reached a maximum at a 2 fold molar excess of SAMSA-F, in good agreement with previous reports using OPA/BME [3]. The ability to use a low molar excess of SAMSA-F is advantageous in that unreacted SAMSA-F yields complex electropherograms (Figure 3.9A) that may result in interfering peaks when highly complex samples are analyzed.

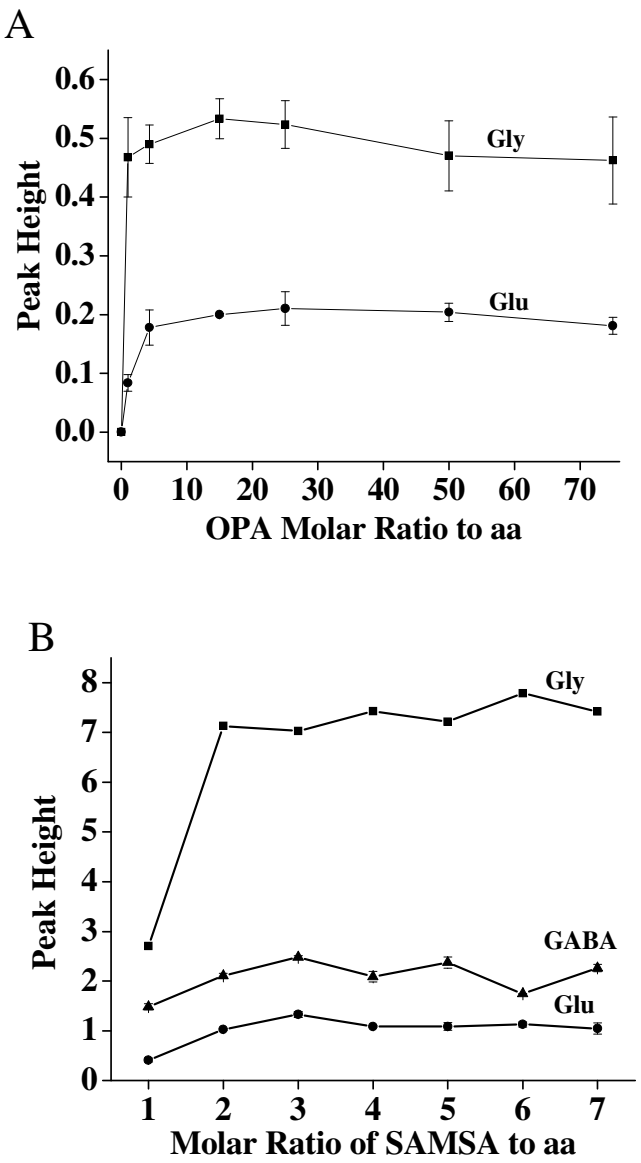

Figure 3.9. Effect of reaction conditions on derivatization of primary amines with OPA/SAMSA-F. (A) Effect of OPA concentration on derivative formation. Samples were derivatized in the presence of 0.28 mM SAMSA-F and 70 µM gly and glu for 180 s. The sample was diluted to 350 nM gly (■) and glu (●) and analyzed using CE. (B) Effect of SAMSA-F concentration on derivative formation. Samples were derivatized in the presence of 2.1 mM OPA and 70 µM gly and GABA for 180 s. The sample was diluted to 700 nM gly (●), GABA (▲) and glu (■) and analyzed using CE. Separation conditions: E = 600 V/cm, 5 s injection, 20 µm i.d., separation distance = 30 cm.

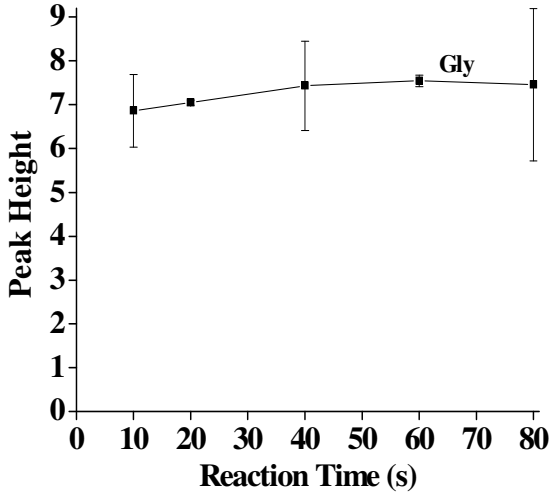

Figure 3.10. Effect of reaction time on the fluorescent signal of OPA/SAMSA-F reaction. 700 nM gly was reacted with a 15 fold and 3 fold molar excess of OPA and SAMSA-F, respectively for varying reaction times. In all cases, derivatives were separated by CE and the peak intensities measured. Separation conditions: E = 600 V/cm, 5 s injection, 20 μm i.d., separation distance = 30 cm.

For the OPA/SAMSA-F reaction to be useful for on-line labeling and thus DCM-CE, both the reaction kinetics of OPA must be maintained and the photophysical properties of fluorescein should be imparted onto the derivatized analyte. It is clear from Figure 3.7 that the excitation and emission wavelengths of fluorescein can be used for detection of the resulting derivatives. Hence, it is important to characterize the reaction dynamics of the OPA/SAMSA-F reaction to determine the validity of the approach for DCM-CE. The effect of reaction time on the peak heights of derivatized amino acids is summarized in Figure 3.10. Here, 15 fold and 3 fold molar excesses of OPA and SAMSA-F, respectively, were utilized. Reagents were mixed and reacted for a time period ranging from 10 s to 80 s, at which time the sample was immediately diluted into a buffer solution immersed in ice followed by immediate sample injection for CE

separations. The reaction was performed immediately adjacent to the CE instrument to minimize delay in the sample injection. Following CE separation, the mean peak intensity was measured. As seen in Figure 3.10, quantitative derivatization was complete within 10s of mixing, in agreement with the OPA/BME reaction, which has a 6s half-life [4].

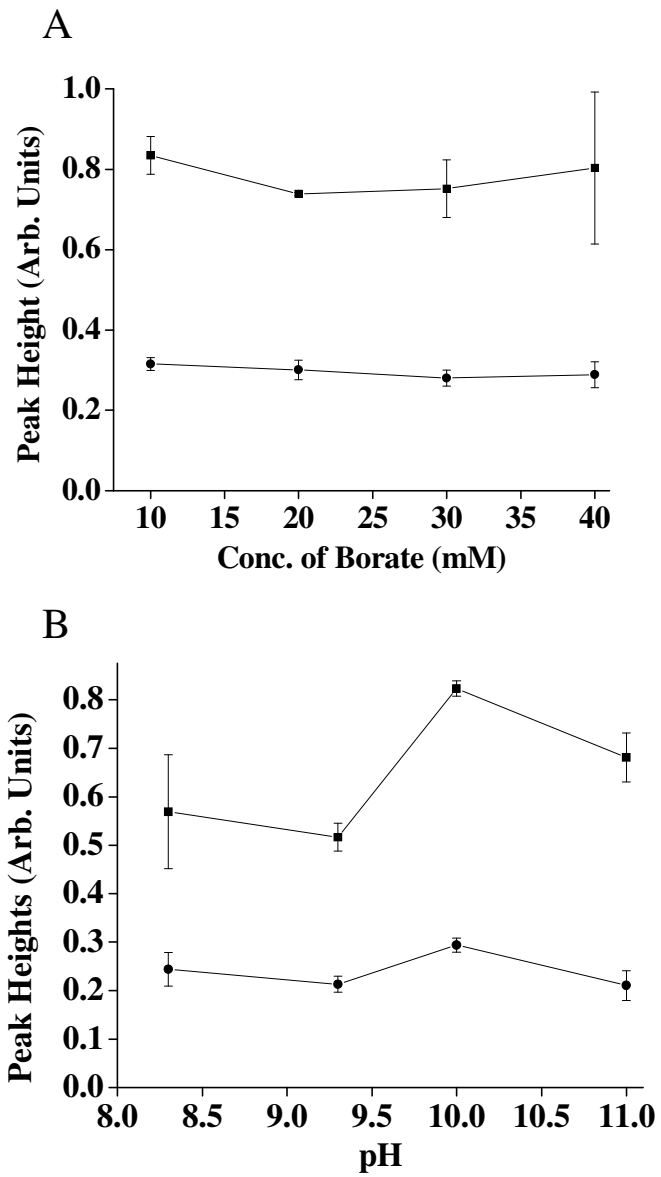

Figure 3.11. Effect of buffer concentration and pH on OPA/SAMSA fluorescein labeling reaction products separated by capillary electrophoresis. (A) Effect of borate buffer concentration on fluorescent signal of 350 nM glu (●) and 350 nM glycine (■). (B) Effect of pH on the peak heights of 350 nM glutamic acid (●) and 350 nM glycine (■). Total buffer concentration was maintained at 10 mM.

Among the other derivatization conditions examined were effect of pH and the ionic strength of the borate buffer on the reaction (Figure 3.11). Influence of the

concentration of buffer (Figure 3.11A) was not significant and this is in the agreement with OPA/NAC reaction with amines.[233] Effect of pH on OPA/SAMSA reaction was examined for the pH range of 8.3 to 11.0 (Figure 3.11B) and maximum derivatization was achieved at pH 10. Hence, derivatization was performed at pH 10 in the characterization experiments.

3.3.4 On-line Labeling of Amino Acids

DCM-CE is primarily performed using on-line sample collection, typically microdialysis, from a biological sample. Thus, on-line labeling and subsequent separation of collected samples are required. To realize maximal sensitivity and temporal resolution, rapid labeling using a highly sensitive dye is required. To validate the OPA/SAMSA-F reaction for DCM-CE, we performed on-line labeling reactions using a mixture of gly and GABA, followed by CE separation. Figure 3.12 shows series of electropherograms that were obtained for A) OPA/SAMSA-F, B-C) OPA/SAMSA-F reacted with microdialysate containing B) gly, C) gly and GABA and D) offline labeling of gly and GABA. Sample was collected on-line using a microdialysis probe immersed in a solution containing either A) buffer, B) 5 mM gly and C) 5 mM gly and 5 mM GABA. Following collection of analyte via the microdialysis probe, OPA and SAMSA-F were introduced to the microdialysate via a quartz tee coupler. As seen in Figure 3.12A, omission of primary amines results in an electropherograms comparable to that seen in Figure 3.6, where the only peaks observed are attributable to SAMSA-F. Upon inclusion of primary amine in the sample (Figure 3.12B-C), a series of peaks were observed that correspond to those obtained for offline labeling (Figure 3.12D) of gly and/or GABA, in

addition to peaks corresponding to SAMSA-F. Based on the dialysis buffer flow rate and the length of capillary, the reaction time was 3.5 min, comparable to previous demonstrations of DCM-CE using OPA/BME, [115;117] suggesting the feasibility of this approach for DCM-CE.

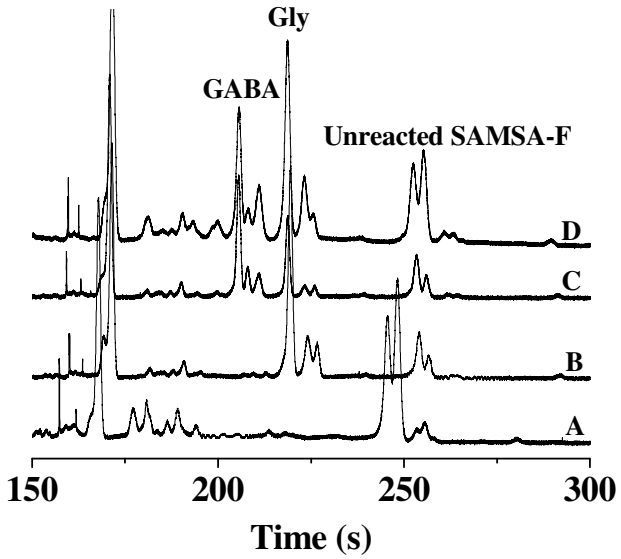

Figure 3.12. On-line derivatization of microdialyzed samples using OPA/SAMSA-F. (A) OPA/SAMSA-F, B-C) OPA/SAMSA-F reacted with microdialysate containing (B) gly or (C) gly and GABA and (D) offline labeling of gly and GABA. A mixture of GABA and gly were used to demonstrate on-line labeling capabilities of OPA/SAMSA-F. Labeled samples were collected and diluted immediately before the analysis. Separation conditions: E = 600 V/cm, 5 s injection, 20 µm i.d., separation distance = 30 cm.

3.4 Conclusions

The derivatization approach outlined here provides a rapid, high sensitivity derivatization method for primary amines that allows for sub-nM detection and a ≤ 10 s reaction time. The reaction kinetics are superior to traditional ITC and SE functionalized visible fluorophores, yet allow incorporation of highly desirable photophysical properties associated with high quantum yield visible fluorescent dyes and the utilization of visible

lasers. This approach should be easily extended to the incorporation of other visible excitation dyes, e.g. rhodamines, etc. The primary drawback of the derivatization scheme presented here is the presence of multiple peaks attributed to SAMSA-F isomers and the subsequent reaction products, though this phenomenon is seen with a number of commonly used fluorescent labels [170], and may potentially be overcome with the synthesis of modified fluorescent dye-thiol conjugates. While we have focused on the utility of the OPA/SAMSA-F reaction for DCM-CE, this approach should also prove useful as a derivatization strategy in additional CE and HPLC applications.

CHAPTER 4. CAPILLARY ELECTROPHORESIS WITH A UV LIGHT EMITTING DIODE SOURCE FOR CHEMICAL MONITORING OF NATIVE AND DERIVATIZED FLUORESCENT COMPOUNDS

4.1 Introduction

Capillary electrophoresis (CE) with laser induced fluorescence (LIF) detection is a powerful analytical tool routinely used to monitor analytes of biological[21;22] and environmental importance.[234] Sub-nM concentration and amol mass detection limits are routinely obtained using CE-LIF, with single molecule sensitivity possible.[21] While widely successful, LIF detection relies on the use of bulky and expensive laser sources for sufficient excitation of analyte fluorescence, particularly for UV-absorbing analytes [21]. The drive towards portable, miniaturized CE separation systems is limited by the size of the detection sources and optics as well as the power consumption of the laser. Hence, alternative light sources that are small, inexpensive, and possess the appropriate spectral characteristics are desirable.

Light emitting diodes (LED) are attractive as alternative light sources for CE due to the high stability, low cost, long life time, compact size, low power consumption and availability in a wide spectral range.[235] As LED technology has advanced, the emission intensity of these devices has increased considerably, enabling their use as light sources for applications such as UV/Vis absorption spectroscopy [157;160;236] and fluorescent spectrometric methods.[235] LEDs were first utilized for CE in 1994, with the introduction of LED-based absorbance, refractive index and fluorescent detectors [157]. A double beam

absorbance detector for CE using a red LED has been reported, with enhanced performance compared to a commercial CE instrument.[236] More recently, a series of fluorescence detectors have been developed using LED sources for excitation (LED-induced fluorescent detection, LED-IF). Using LED-IF, amino acids labeled with fluorescein isothiocyanate have been monitored using an integrated CE-liquid core waveguide device [237]. LEDs have been further coupled to microfluidic CE systems using optical fibers for the detection of fluorescently labeled analytes such as proteins and small molecules.[238] Utilization of LEDs in microchip platforms with confocal detection has allowed analysis of fluorescently-tagged oligosaccharides.[207] Additionally, indirect fluorescent detection of both anions and cations has also been achieved using a blue LED with the background electrolyte containing optically active complexation reagents [239;240].

The analysis of biogenic amines is commonly performed by CE-LIF, with the analyte often directly sampled from a biological specimen, followed by online labeling with fluorogenic dyes and CE separation. Naphthalene-2,3-dicarboaldehyde (NDA) is frequently used to label biologically important amines due to fast reaction kinetics for online labeling. Detection of NDA derivatives has commonly relied on HeCd (442 nm line)[45] or Ar^+ lasers (457.9 nm line)[241] with low nM detection limits for proteins and amino acids.[241] Recently, a blue LED was used to detect NDA-labeled amino acids in cerebrospinal fluids derivatized with NDA with low nM (10-30 nM) detection limits [242;243]. Xiao and co-workers also reported analysis of amino acids using LED-IF with low nM sensitivity [244].

Though LEDs have been used in a number of CE applications, the lack of suitable UV-LED sources has prevented their utilization for the detection of common UV absorbing chromophores. Recently, a deep UV-LED (280 nm) was used for native fluorescence detection of proteins[161] in CE suggesting the feasibility of the approach, though the wavelength range from 310-400 nm has remained largely unexplored with LED-based excitation sources. The recent introduction of a high power UV-LEDs in this spectral window may help to fill this void. Of particular interest for fluorescence detection in CE is a high power UV-LED with an emission maximum at 365 nm, an excitation wavelength that is potentially useful for fluorescence detection of common small molecule fluorogenic labels and environmental pollutants such as PAHs.

A very important and rapidly growing application of CE-LIF is on-line chemical monitoring of biological amines, e.g. neurotransmitters, using microdialysis sampling. Typically performed using *o*-phthalicdicarboxaldehyde (OPA) in the presence of thiol, e.g. β-mercaptoethanol (β-ME) [43;116;245], the resulting isoindole product can be readily excited at 365 nm, with emission detected at 450 nm (Figure 4.1).[232] CE-LIF of OPA/β-ME derivatives is typically performed using UV emission lines from HeCd (325 nm and 354 nm)[115] or Ar^+ lasers (351 nm)[43]. The emission of the UV-LED provides an ideal spectral match for this application and provides significant potential benefits compared to the laser sources, including size, cost and stability.

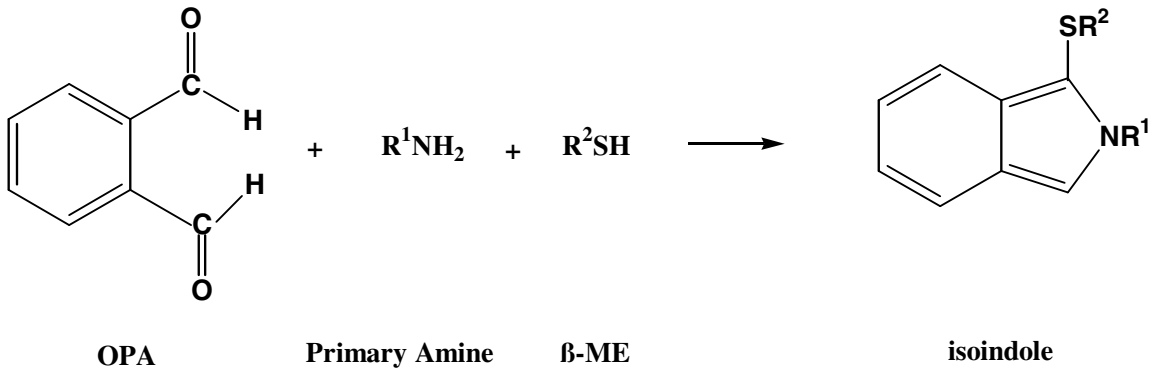

Figure 4.1. Derivatization scheme for primary amines with o-phthalaldehyde (OPA)/ β-mecaptoethanol (β-ME).

Here, we describe the use of a compact and inexpensive UV-LED light source for sensitive fluorescent detection of a range of biologically and environmentally important analytes, including PAHs, amino acids, peptide fragments and intact proteins. Sensitivities comparable to LIF detection were obtained for OPA-labeled amino acids and proteins. In addition, a flow-gated sample injection configuration was used to demonstrate the applicability of UV-LED-IF detection for real-time monitoring of biological analytes, providing significant cost and stability advantages of LIF detection. These experiments demonstrate the feasibility of CE-UV-LED-IF detection, which should be readily applicable to miniaturized CE instrumentation and microchip based separations.

4.2 Experimental

4.2.1 Material and Reagents

Amino acids and proteins were obtained from Sigma Chemical Co. (St. Louis, MO). o-phthalicdicarboxaldehyde (OPA) and β-mercaptoethanol (β-ME) were obtained from Aldrich Chemical Co. (St. Louis, MO). All other chemicals were obtained from

VWR and used as received. Capillaries were obtained from Polymicro Technologies (Phoenix, AZ). All solutions were prepared using 18 MΩ deionized water (Barnstead).

4.2.2 UV LED-IF-CE Instrumentation

The UV-LED-IF detection system built in-house is shown in Figure 4.2. The UV LED (Model NCCU033, Nichia America Corporation, Southfield, MI) was mounted on an aluminum cooling device (Nichia America Corporation, Southfield, MI). Emission from the LED (100 mW, λ_{max} = 365 nm, $\Delta\lambda$ = 8 nm) (Figure 4.3) was collimated with a fused silica plano-convex lens (f = 35 mm, ThorLabs, Newton, NJ) and then focused into the center of the separation capillary using a fused silica biconvex lens (f = 25 mm, Melles Griot, Irvine, CA). Fluorescence emission was collected at a 90^{o} angle to the excitation detection beam (12 mW) using a microscope objective (10x, 0.25 numerical aperture, Newport, Irvine, CA), passed through a spatial filter to remove scatter generated in the capillary walls and a band pass filter (450/30 nm, Omega Optical, Brattleboro, VT). The collected emission was detected using a PMT (H957, Hamamatsu Photonics, Bridgewater, NJ), the current from which was amplified using a current amplifier (Model SR570, Stanford Research System, Sunnyvale, CA), low pass filtered at 10 Hz and recorded using an A/D converter (PCI-MIO-16E-4, National Instruments, Austin, TX) with in-house software written in LabView (National Instruments, Austin, TX). Electric fields were applied using a 30 kV power supply (Spellman High Voltage Corporation, Hauppauge, NY).

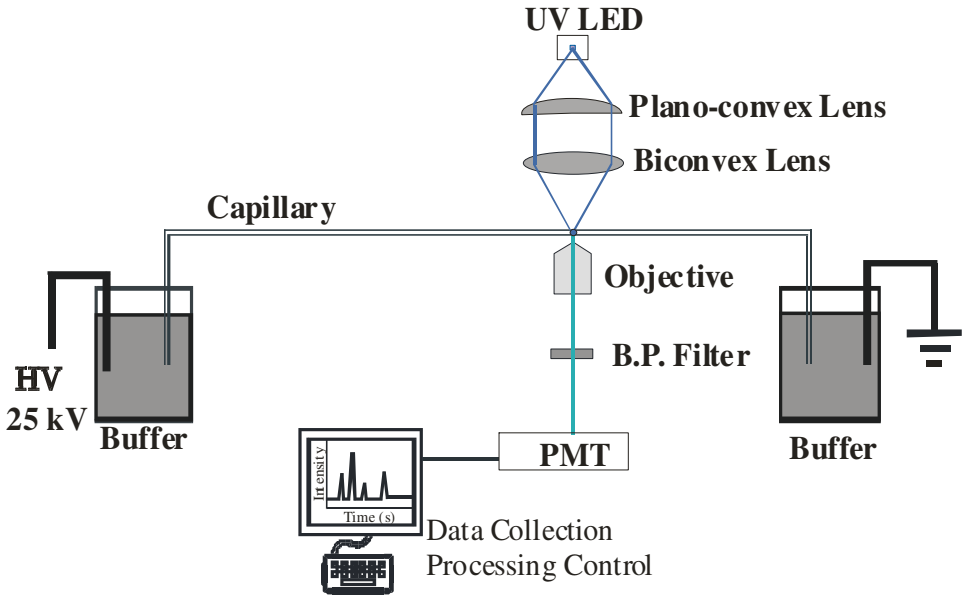

Figure 4.2. Schematic diagram of the UV light emitting diode induced-fluorescence detection system.

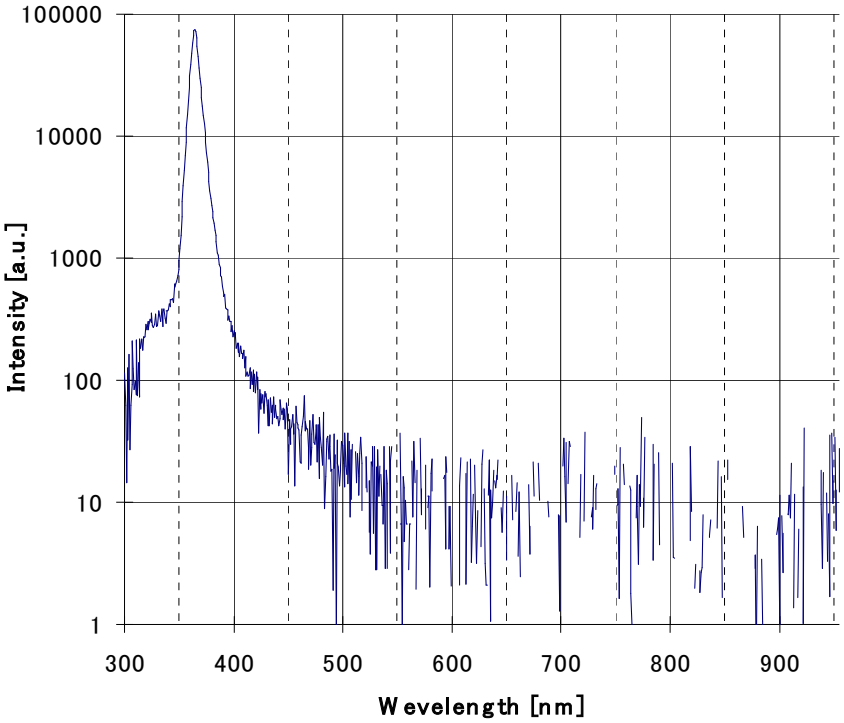

Figure 4.3. UV/Vis emission spectrum of UV LED (Courtesy of Nichia America Corporation, Southfield, MI).

4.2.3 Capillary Electrophoresis Conditions

The capillary was treated as follows: 100 mM NaOH for 5 min, deionized water for 10 min and 10 mM phosphate buffer at pH 7.4 for 10 min. For protein and tryptic digest experiments, separation was performed using micellar electrokinetic chromatography (MEKC). For MEKC, background electrolyte was prepared by dissolving 25 mM sodium dodecyl sulfate (SDS) in 10 mM borate buffer, pH 10. For PAH separation, MEKC was performed using 25 mM SDS in 10 mM phosphate at pH 7.4 containing 30% (v/v) acetone to modify the interaction between micelles and the PAHs thereby improving the resolution.[246]

4.2.4 Flow-gated Injection Interface

For online monitoring demonstrations, injections were performed using a flow-gated injection (Figure 1.6) interface similar to that described by Kennedy and coworkers [41]. Briefly, the outlet of the reaction capillary and the inlet of the separation capillary were aligned adjacent to one another, 30-75 μm apart, in a Plexiglas block. A cross-flow comprised of separation buffer was continuously applied across the gap at the rate of 1mL/min using a syringe pump (Sage M361 multi-rate pump, Orion Research, Beverly, MA) to prevent the analyte transfer between the two capillaries. Sample injection into the separation capillary is accomplished by temporary disruption of the cross-flow using a solenoid valve (Cole Palmer, Vernon Hills, IL), typically for 1 s. During the entire process, the separation capillary was maintained at constant high voltage, allowing electrokinetic injection of the sample when the cross-flow is stopped.

4.2.5 Temporal Measurements using CE-UV-LED-IF with a Flow-gated Interface

To characterize the feasibility of the CE-UV-LED-IF approach for monitoring temporal dynamics, we interfaced the instrument described above to an HPLC injection valve that served as a stream selector. Sample from one of two 1 mL syringes controlled by a Harvard syringe pump (Harvard Apparatus, Inc. Holliston, MA) was continuously introduced into the reaction/sample capillary at the rate of 5 µL/min. The syringes were connected to a six port injection valve (6UW, Valco Instruments, Houston, TX) through an 18 cm long, 50 µm i.d. capillary. The valve output (24 cm long, 100 µm i.d. capillary) was coupled to the separation capillary (25 µm i.d.) using the flow gated-interface. Samples were changed by switching the valve position where indicated.

4.2.6 Offline Derivatization of Amino Acids with OPA/β-ME

OPA/β-ME stock solution (75 mM) was prepared by dissolving 10.0 mg of OPA in 100 µL methanol and 10 µL β-ME followed by dilution to 1000 µL with 10 mM borate buffer (pH 10.0). Stock solutions of labeled amino acids were prepared by mixing 1.0 µL of 10 mM amino acid dissolved in 0.1 M bicarbonate buffer at pH 9.0 with 5 µL of OPA/β-ME stock followed by dilution to 1000 µL with borate buffer. The mixture was allowed to react in the dark for 10-30 min, with the mixture stirred. The original sample was diluted in running buffer prior to analysis. Preparation of amino acid mixtures was performed as described using 1.0 µL aliquots of the various amino acids and an excess of OPA/β-ME followed by dilution to 1000 µL with borate buffer.

4.2.7 On-line Derivatization of Amino Acids with OPA/β-ME

Online derivatization of amino acid mixtures was performed by introducing both sample and derivatization reagents (7.5 mM OPA/β-ME) into a mixing tee using a Harvard syringe pump (Harvard Apparatus, Holliston, MA) at a rate of 1.2 µL/min (Figure 4.4). The outlet of the reaction tee was connected to a 100 µm i.d. capillary, the length of which determines the reaction time. In this work the reaction capillary was 30 cm in length allowing 70 s for reaction. The reaction capillary was interfaced to the separation capillary via the flow-gating interface.

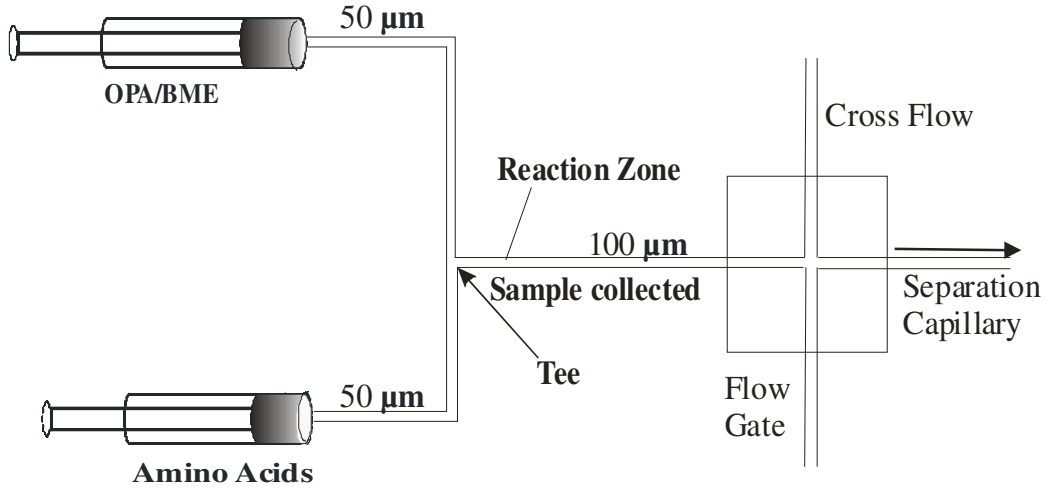

Figure 4.4. Schematic diagram of on-line derivatization coupled with flow-gated UV CE-LED-IF.

4.2.8 OPA/β-ME Derivatization of Proteins

Stock solutions of protein (BSA and myoglobin, 0.5 mM) were prepared in 10 mM borate buffer prior to derivatization and analysis. Labeling was accomplished by mixing 10 µM protein diluted in background electrolyte containing 25 mM SDS in 10 mM borate buffer , pH 10 (total volume = 975 µL) with 5 µL OPA/β-ME (75 mM) for 3 minutes.

4.2.9 Tryptic Digest

Stock solutions (10 mg/mL) of proteins were prepared in 0.1 M boric acid buffer, pH 8.4. Trypsin solution (1 mg/mL) was prepared in the same buffer. Prior to digestion, 1 mL of the protein sample was thermally denatured at 80 ^{0}C for 30 minutes in a water bath followed by addition of 200 µL trypsin solution. Digestion was performed at 37 ^{0}C for 24 hr with constant stirring. Following digestion, samples were diluted in borate buffer containing 25 mM SDS and derivatized with OPA/β-ME as described.

4.3 Results and Discussion

Fluorescence detection of UV-excited chromophores in CE allows high sensitivity analysis of a range of environmentally and biologically important compounds. CE-UV-LIF has proven useful for detecting natively fluorescent molecules, e.g. tryptophan derivatives,[165;247] PAH's,[77;248] etc. or analytes that have been derivatized with small molecule fluorescent labels,[166] e.g. OPA, fluorescamine, etc. Though this approach provides high sensitivity, UV-LIF detection typically requires the use of expensive UV lasers, limiting the widespread application of the technique. Further, the potential to miniaturize CE-based analyses of UV-excited analytes warrants the exploration of alternative excitation sources for CE-UV-LIF. Here, we demonstrate the utilization of a 365 nm UV-LED as an excitation source for fluorescence detection in CE-UV-LED-IF.

4.3.1 Native Fluorescence Detection of PAHs

PAHs are toxic components of fossil fuels that are introduced into the environment from various sources, including petroleum refineries, and underground storage tanks. The availability of sensitive, simple and low cost analytical

instrumentation for quantitative analysis of PAHs would be particularly useful for field analyses. PAHs possess intrinsic fluorescent properties that can be utilized for detection with a suitable excitation source. The UV-LED utilized here has a maximum emission wavelength at 365 nm that is spectrally matched with the absorbance of many PAHs, including anthracene, perylene, and their derivatives.[77;248] Though, the majority of PAHs possess no charge and therefore cannot be resolved using zonal CE separations, these compounds can be separated using MEKC when appropriate organic modifiers are utilized.[77;246;248]. Analysis of these compounds using MEKC without an organic modifier did not result in separation of analytes as shown in Figure 4.5. Both bromoanthracene and anthracene co-migrated. This is due to the strong interactions of neutral organic PAHs with micelles. Acetone in the background electrolyte alters the interaction of liphophilic compounds with micelles resulting the separation of neutral PAHs.[77;246;248] Here, we have coupled native fluorescence detection using an UV-LED source with MEKC to analyze a mixture of PAHs containing anthracene (AC), 9-bromoanthracene (9-BrAC) and diphenylanthracene (DPAC) (Figure 4.6).

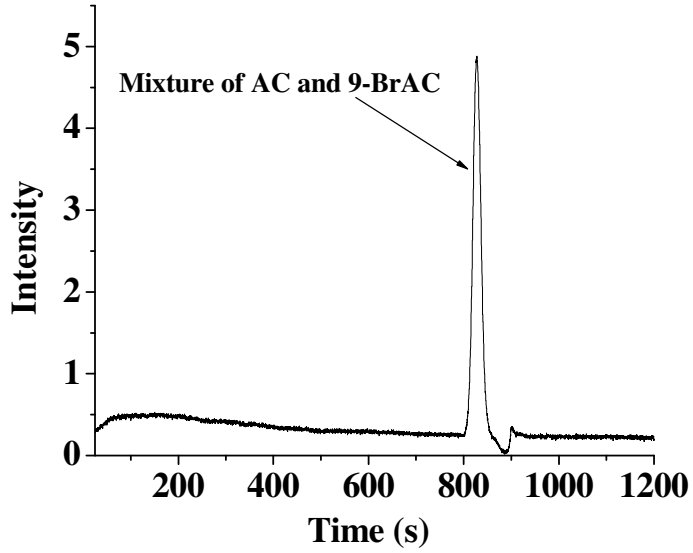

Figure 4.5. Analysis of a mixture of polyaromatic hydrocarbons using MEKC with UV-LED-IF detection. Electrokinetic injection was performed on a sample mixture containing 9-bromoanthracene (~10 μM) and anthracene (~10 μM). No separation was observed. Separation conditions – E = (-) 0.52 kV/cm, 10s injection with (-) 3 kV, 25 mM SDS in 10.0 mM phosphate at pH 7.4 , capillary i.d. 50 μm, L_D = 32 cm

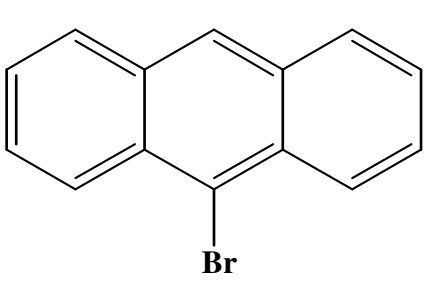

9-Bromoanthracene

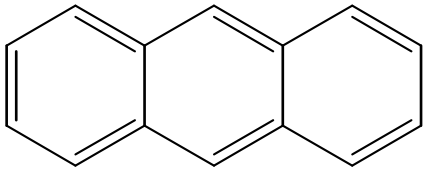

Anthracene

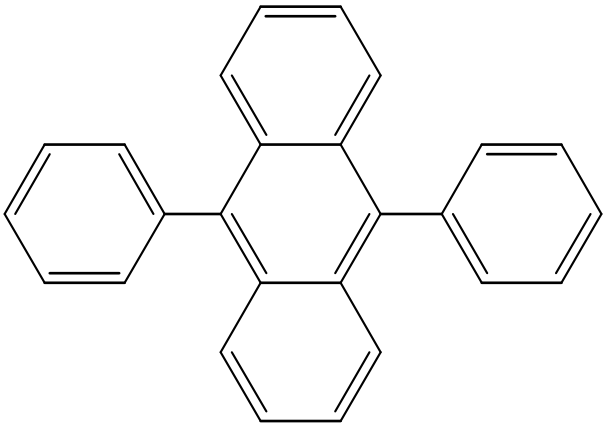

9,10-Diphenylanthracene

Figure 4.6. Chemical structures of PAHs used in the separation.

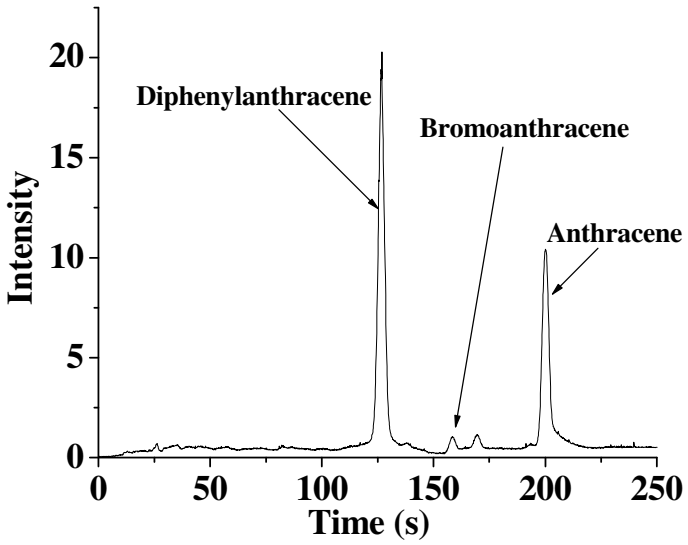

Figure 4.7. Separation of a mixture of polyaromatic hydrocarbons using MEKC with UV-LED-IF detection. Electrokinetic injection was performed on a sample mixture containing 9,10-diphenylanthracene (~1 μM), 9-bromoanthracene (~15 μM) and anthracene (~20 μM). Separation conditions – E = (-) 0.52 kV/cm, 10s injection with (-) 3 kV, 25 mM SDS in 10.0 mM phosphate at pH 7.4 containing 30% (v/v) acetone, capillary i.d. 50 μm, L_D = 32 cm

Figure 4.7 shows the resulting electropherograms obtained from a separation of a mixture containing 1 μM DPAC, 15 μM AC and 20 μM 9-BrAC (Figure 4.6). The unlabeled peak in Figure 4.7 results from impurities in the DPAC sample. Using MEKC-UV-LED-IF, the PAH mixture was separated in less than 4 minutes with high sensitivity. Limits of detection obtained using this approach were 0.17, 1.28 and 0.01 μM for AC , 9-BrAC and DPAC, respectively, with S/N = 3. Ishibashi and coworkers have developed methods based on cylodxtrin-modified MEKC to analyze anthracene derivatives, in which 7 nM LOD for 9,10-dimethylanthracene was reported using LIF detection using He-Cd laser (325 nm, 1 mW).[77] Detection limits obtained for anthracene derivative i.e. DPAC with UV-LED-IF was also in the same range even though direct comparison is not

possible since two compounds have different structures.[77] The variance in sensitivity of these compounds results from variations in the absorbance spectra and the quantum yield of the individual PAHs. Though LEDs are not collimated light sources compared to lasers, it is still possible to attain small spot sizes using the optical arrangements described above (Figure 4.2) allowing detection in capillaries with > 25 μm i.d.

4.3.2 Detection of Fluorescently Labeled Biomolecules

Among the most common applications of CE-UV-LIF is the analysis of small molecules, e.g. neurotransmitters and related compounds. Generation of fluorescent species is generally accomplished via reaction with small molecule fluorescent probes. The use of small molecule probes, e.g. OPA, fluorescamine, etc. improves separation of the labeled compounds, allows pre- and post-column derivatization and exerts less of an affect on the electrophoretic mobility of the derivative compared to larger, visible excitation dyes. Detection of UV-chromophore labeled compounds is typically performed using a HeCd laser, [41;115] limited by laser lifetime and stability or the UV lines of an Ar^+ laser, [43] limited by cost and power consumption. Due to the fast reaction kinetics of OPA, CE-UV-LIF has been utilized extensively for online monitoring of neurotransmitter dynamics in a number of systems [43;115]. To overcome the cost, complexity and limitations associated with UV-lasers, we have utilized a UV-LED source to detect OPA/β-ME labeled biogenic amines.

Figure 4.8 illustrates a typical electropherogram obtained from the online injection and separation of OPA/β-ME labeled inhibitory neurotransmitters, glutamic acid (glu) and aspartic acid (asp) using a flow-gated injection interface with a 365 nm

LED excitation source. The separation was completed in 21 s in an 8 cm separation distance with separation efficiencies of 4.1 x 10^5 theoretical plates (5.1 x 10^6 N/m) for glu and 3.7 x 10^5 (4.7 x 10^6 N/m) for asp, respectively, with near baseline resolution (Table 4.1). Calibration curves were constructed for glu and asp using the peak heights (Figure 4.9) and showed linearity ($R^2 \geq 0.99$) in the concentration range 50 nM to 500 nM for both glu and asp. The sensitivity of the CE-UV-LED-IF approach was 11 and 10 nM for glu and asp, respectively, comparable to OPA/β-ME derivatization performed with on-capillary detection using a He-Cd laser[115], or an Ar^+ laser.[106] These data demonstrate the applicability of CE-UV-LED-IF for detection of fluorescently-labeled compounds biogenic amines. With continued instrumental improvement, particularly improved optical design and the use of smaller i.d. capillaries, it should be possible to further increase the sensitivity of the UV-LED-IF detection, though sensitivity for online monitoring is typically limited by the derivatization chemistry to ~ 10^{-8} M.[161] Thus with the UV-LED it is possible to obtain comparable sensitivity with a 300-700 fold reduction in the cost of the excitation source. This low cost, simple optical arrangement should be amenable to a large number of CE-UV-LIF applications, particularly for analysis of biological compounds.

Online monitoring of neurotransmitters and biogenic amines requires online sample collection, delivery, derivatization and injection into the separation capillary. Sampling is typically performed using a microdialysis probe or other continuous flow sampling device. Delivery and derivatization is performed simply using pressure driven flow through flow channels of defined length and diameter, followed by online injection

most commonly employing flow-gated interfaces. In this system, the excitation source (laser) is typically the most expensive component. To evaluate the potential for on-line monitoring of temporal dynamics using a UV-LED, the CE-UV-LED-IF system was further developed and characterized to incorporate each of these core components.

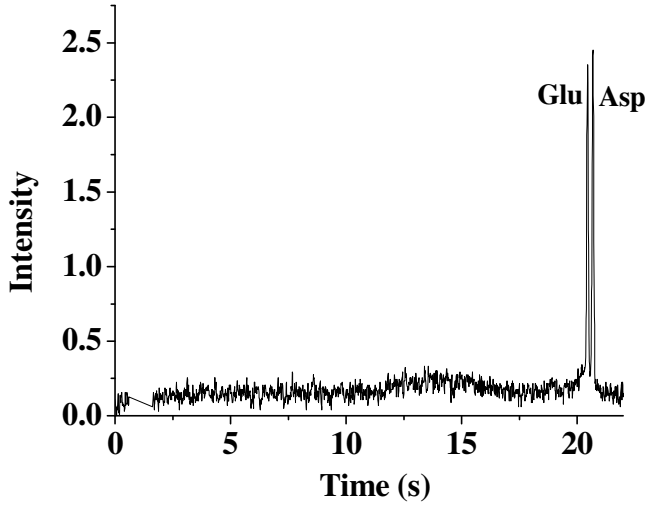

Figure 4.8. Typical electropherogram of a binary amino acid mixture labeled with OPA/β-ME. A 0.5 μM glutamate and aspartate mixture was injected into the separation capillary using a flow-gated interface. Separation conditions: E = 1.13 kV/cm, 1 s injection, cross flow 1 mL/min (10.0 mM phosphate, pH 7.40), capillary is 25 μm i.d., L_D = 8 cm.

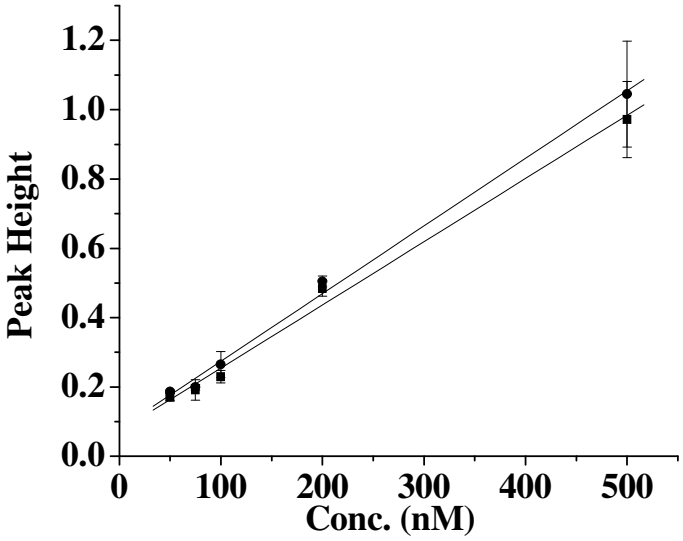

Figure 4.9. Instrument calibration for OPA/β-ME labeled amino acids. Calibration curves are constructed for glu (■) and asp (●). R^2 values for glu, asp are 0.996 and 0.998, respectively.

Peak	Migration Time (s)	LOD /nM	Plates
Glu	20.4	11	410,000 5,100,000/m
Asp	20.7	10	370,000 4,700,000/m

Table 4.1. Summary of experimentally measured values for amino acids analysis with UV LED-IF-CE

Figure 4.10 shows a series of electropherograms obtained upon continuous introduction and separation of a sample mixture containing 5 μM glu and asp with on-

line chemical reaction and flow-gated injection. The reaction time for the OPA/β-ME reaction was maintained at 70 s by controlling the flow rate of derivatization reagents and the reaction capillary i.d.. The sample and derivatization reagents were directly pumped into the reaction tee at 1.2 μL/min. Efficient mixing of the sample and the reagents was obtained in the reaction tee followed by transfer through the 30 cm long, 100 μm i.d. reaction capillary to the injection interface. The average peak heights obtained were 7.8 ± 0.25 (3.2 % RSD) for glu and 7.9 ± 0.25 (3.2 % RSD) for asp. LODs for online labeling were 46.9 and 46.5 nM for glu and asp, respectively, comparable to those obtained using CE-LIF with HeCd excitation source.[115] These limits are well-below the basal levels of glu (5.0 ± 0.4 μM) and asp (1.2 ± 0.1 μM) in the caudate nucleus of rats previously measured using CE-UV-LIF and are comparable to LODs obtained using HeCd lasers for excitation.[115] Though it is possible to increase the sensitivity for online labeling by increasing the reaction time or improving the optical arrangement, this appears unnecessary as LODs are below the concentration ranges expected for this application. Thus, CE-UV-LED-IF should prove useful for monitoring temporal dynamics of neurotransmitters and other biogenic amines.

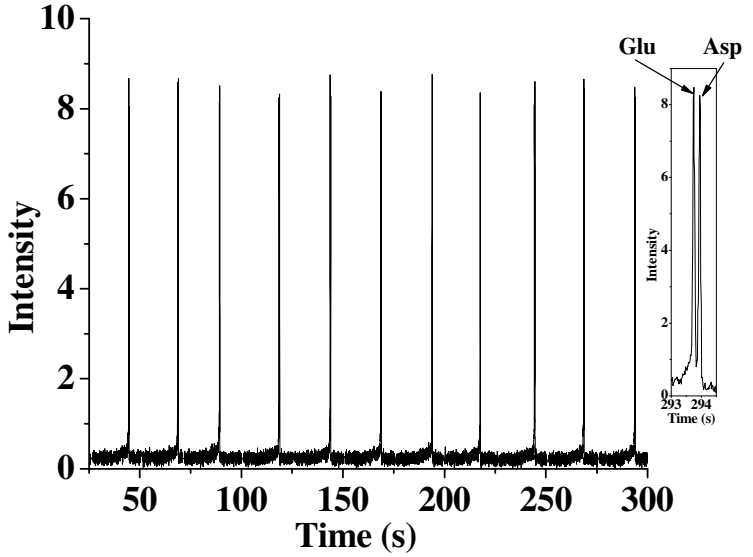

Figure 4.10. Online derivatization of a mixture of amino acids. A mixture of 5 μM glutamate and aspartate was labeled online with OPA/β-ME for 70 s before injection into the separation capillary using a flow-gated interface. Consecutive online injections were performed every 25 s for 300 s. Separation conditions - E = 1.04 kV/cm, 1 s injection, cross flow 1 mL/min (10.0 mM phosphate, pH 7.40), capillary is 25 μm i.d., L_D = 8 cm.

To further evaluate the potential of the UV-LED-based system for on-line chemical monitoring, we applied mixtures of OPA/β-ME labeled amino acids with step changes in concentration. The separation capillary was interfaced to the output capillary of a stream selecting valve using a flow-gated interface. Sample solutions containing either 0.50 μM or 2.0 μM glu and asp were connected to the valve and a constant pressure was applied to both solutions using a syringe pump. Samples were injected for 1s every 25 s into the separation capillary using the flow-gating interface. Figure 4.11A shows the peak height change associated with step changes in amino acids concentration from 0.50 μM to 2.0 μM to 0.50 μM. Temporal effects of the connection capillary appear as increased lag (delay) times, as observed in the 30 s delay upon switching from

0.50 µM to 2.0 µM (Figure 4.11A and 4.11B) and can be readily adjusted by minimizing distances between valve to the flow-gate. The primary factor affecting the response (rise) time is the ~ 50 nL dead volume associated with the valve with a lesser contribution due to linear diffusion in the reaction capillary.[42;115] Figure 4.11B illustrates the response curve constructed using individual peak heights, calculated from the respective electropherograms in Figure 4.11A. Approximately two separations are needed to observe changes in concentration, thus resulting in a 50 s rise time that can be reduced by using improved components for sample delivery. These data suggest the feasibility of using CE-UV-LED-IF for detection of dynamic chemical events in biological systems.

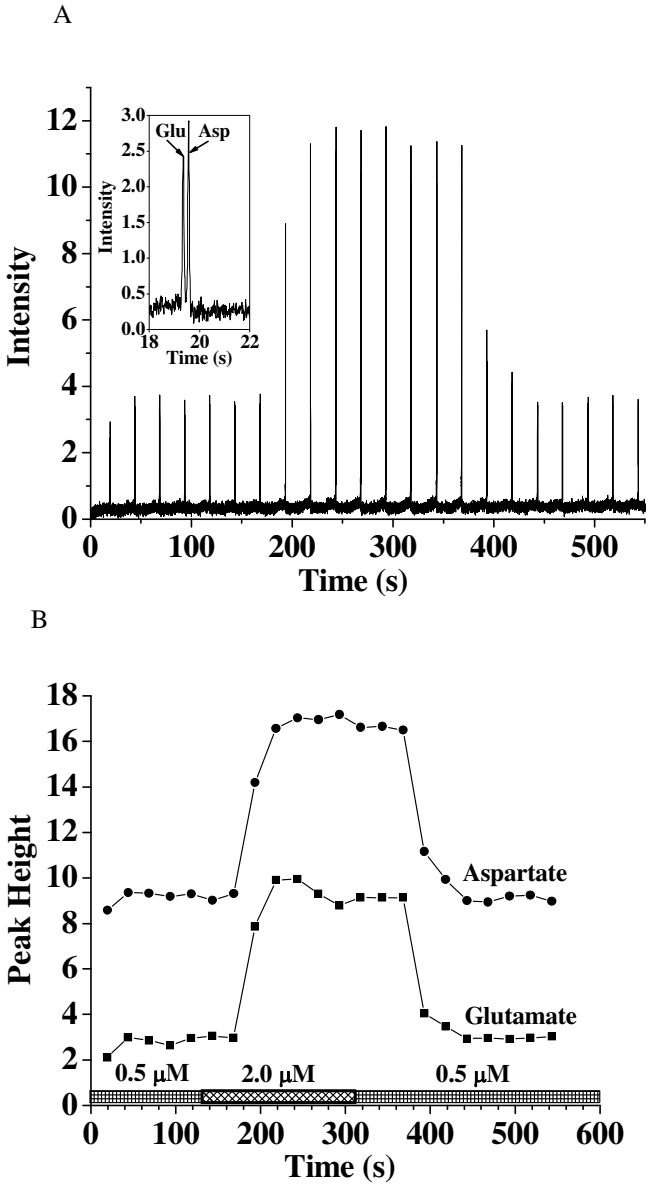

Figure 4.11. Response of the flow-gated LED-IF system to dynamic chemical changes in a mixture of glutamate and aspartate. A) Plot of 22 consecutive electropherograms collected online during a step change in glutamate and aspartate concentration. Amino acid concentration was changed from 0.5 µM to 2 µM and back to 0.5 µM. B) Plot of peak height vs. time for data collected in A. Analyte concentration and time of solution switch are depicted by the bars at the bottom. E = 1.17 kV/cm, injection time = 1s.

4.3.3 Analysis of Proteins and Peptides using CE-UV-LED-IF

While successful for amino acid detection, separation and detection of proteins using LIF detection of OPA labels has proven to be more difficult. Separation and detection of proteins using precolumn labeling with OPA has not been reported for solutions containing more than one protein, although post-column labeling has been reported.[249] Hence, OPA labeling of proteins has not been explored as frequently as other dyes, e.g. FITC and FQ, which possess much slower reaction kinetics.[21] Additionally, CE separations of proteins are problematic due to adsorption of protein onto the negatively charged capillary surface, resulting in increased band broadening and reduced sensitivity. Based on these factors, we have explored the use of the MEKC-UV-LED-IF described above to separate and detect OPA labeled proteins.

Figure 4.12 shows a separation of a binary mixture of 1 μM bovine serum albumin (BSA) and 10 μM myoglobin (Myo) labeled with OPA/β-ME. Derivatization of proteins was performed in borate buffer containing 25 mM SDS, to denature proteins resulting in the exposure of all potential labeling sites. Proteins were separated in less than 4 minutes with 28 nM and 47 nM LOD's for BSA and Myo, respectively. The higher sensitivity obtained for BSA compared to Myo likely results from increased labeling of the BSA which contains 60 lysine residues.[241] With labeling times 2 orders of magnitude shorter than those obtained for FITC, TRITC and other common protein labels, OPA/β-ME derivatization offers the opportunity for markedly enhanced throughput, while simultaneously reducing cost per analysis.

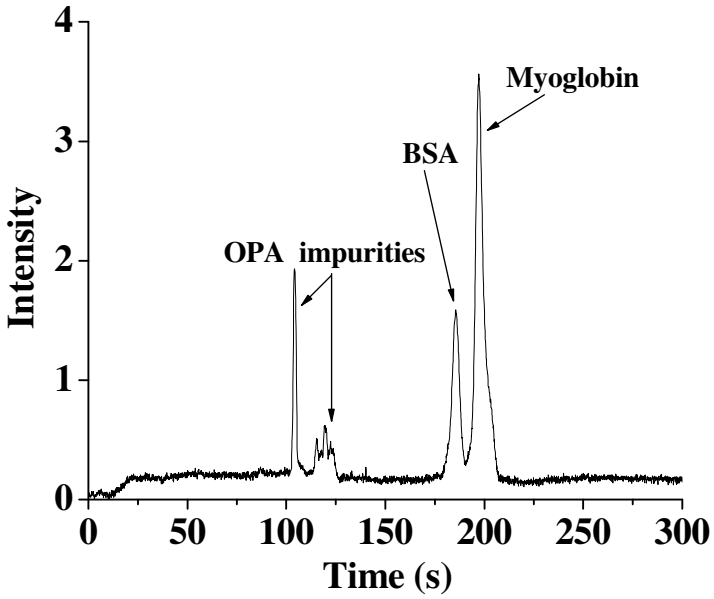

Figure 4.12 Separation of a mixture of proteins using MEKC with UV-LED-IF detection. Separation of OPA/β-ME labeled myoglobin (10 μM) and BSA (1 μM) Separation conditions – E = (+) 0.43 kV/cm, 5s injection with 4kV, 25 mM SDS in 10.0 mM borate at pH 10.0, capillary i.d. 50 μm, LD = 30 cm.

In addition to protein separations, CE has evolved into an important tool for peptide mapping and protein sequencing,[199] via the separation of peptide fragments. The low prevalence of native fluorescent residues (tyrosine and tryptophan) in the resulting peptide mixtures requires the introduction of fluorescent labels, typically FITC and other slow reagents. Though enzyme kinetics have been the primary limitation in throughput for peptide mapping applications, recent advances in CE-based tryptic digests have shifted the limitation to fluorescence labeling reactions. Combined, these results suggest that the utilization of OPA/β-ME labeling may allow markedly increased sample throughput.

To explore the potential of using UV-LED-IF for peptide analysis, a tryptic digest of BSA was prepared and the resulting peptides were labeled with OPA/β-ME prior to analysis. A representative electropherogram for the separation of a BSA peptide mixture obtained from 10 μM BSA labeled with OPA/β-ME using MEKC-UV-LED-IF is shown in Figure 4.13A. As shown in Figure 4.12A, not all of the peaks are baseline resolved, and some of the peaks in the electropherogram are from OPA impurities. A tryptic digest of BSA protein is expected to produce 74 peptide fragments according to the amino acid sequence but fewer than 20 fragments were observed in this analysis. However, the resulting electropherogram is similar to those previously reported.[250] One of the main reasons is the low peak capacity with this method, unlike 2D separations where most of the peptide fragments were separated and identified [250]. The reduced number of peaks may also be due to the fact that labeled fragments carry identical charge to volume ratios, resulting in co-migration of peptides and a reduced number of peaks. The analysis of three individual digests resulted in identical electropherograms (Figure 4.13B), emphasizing the unique protein digestion of the sample and potentially allowing protein fingerprinting. These results show the capability of MEKC-UV-LED-IF for the rapid, high throughput analysis of peptides.

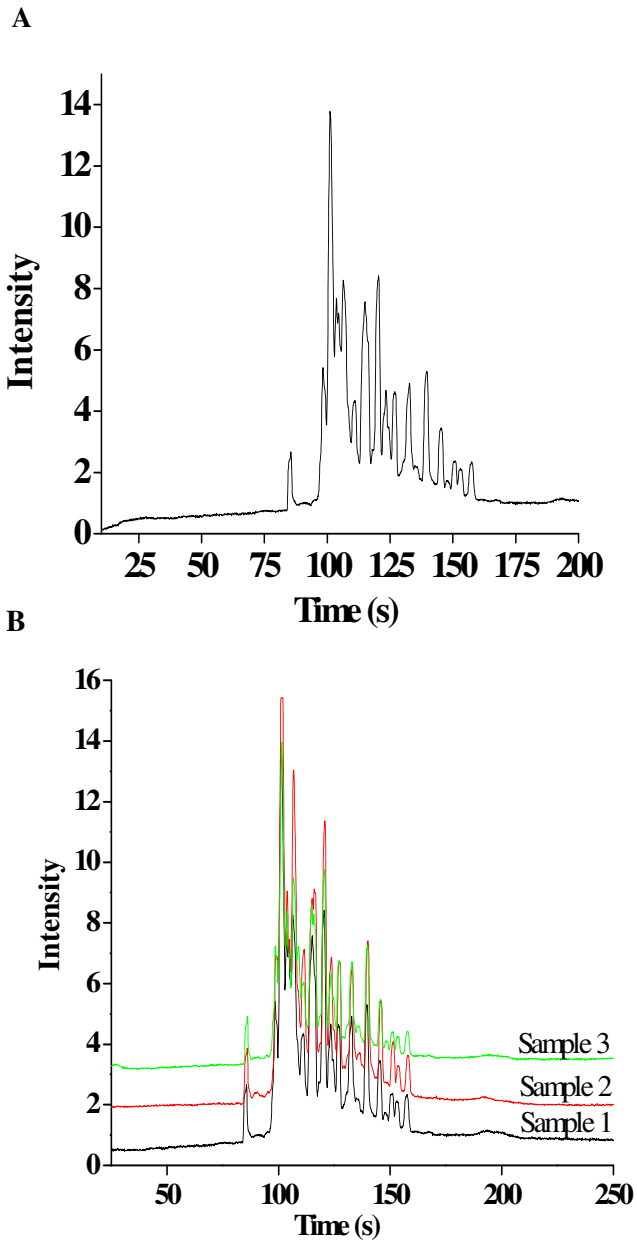

Figure 4.13. Separation of a mixture peptides using MEKC with UV-LED-IF detection. Separation of tryptic digest of BSA (10 µM). (A) Single analysis and (B) multiple samples analysis are given. Separation conditions – E = (+) 0.43 kV/cm, 5s injection with 4kV, 25 mM SDS in 10.0 mM borate at pH 10.0, capillary i.d. 50 µm, L_D = 30 cm.

4.4 Conclusions

We have integrated an UV-LED to a capillary electrophoresis system for induced fluorescence detection of environmentally and biologically important compounds possess intrinsic native fluorescence or have been derivatized to yield fluorescent moieties. Utilization of inexpensive, compact UV LED light sources for sensitive fluorescent detection provides an alternative to the use of expensive, bulky lasers without a substantial loss of sensitivity. Separation of mixtures of amino acids, protein, peptides and PAHs was performed by CE-UV-LED-IF detection with comparable detection limits with LIF detection. These devices show a great potential to replace expensive light sources in miniaturized microfluidic devices for online chemical monitoring applications, as well as for the construction of low-cost CE systems for routine laboratory use.

CHAPTER 5. MONITORING TAT MEDIATED PROTEIN DELIVERY IN SINGLE CELLS BY CAPILLARY ELECTROPHORESIS WITH POST COLUMN FLUORESCENCE DETECTION

5.1 Introduction

Capillary electrophoresis (CE) combined with high sensitivity detection has become a viable analytical tool for cellular analysis.[20;164;251-257] CE-LIF provides sub-attomole detection limits and a large dynamic range making CE-LIF potentially attractive for such studies.[184;252;258] Cellular studies can be performed using a large number of cells or using a single cell.[259] Bulk analysis usually involves examination of cellular extracts, and masks the effects and observation of cellular heterogeneity. However, investigation of single cells provides the potential to elucidate chemical information regarding cellular heterogeneity.

Analysis of single cells provides the possibility to construct molecular libraries and to directly correlate molecular events with cellular function. Techniques utilized for single cell analysis must present high sensitivity, high specificity, high temporal resolution and high spatial resolution. Detection of intracellular signaling events is made difficult by the chemically complex intracellular environment and the lack of suitable fluorescent or electrochemical indicator chemistries for the majority of interesting pathways.[181] One potential approach for analyzing intracellular signaling events is the creation of genetically encoded "molecular reagents" that possess intrinsic biological activity or that serve as targets for native biological signaling cascades.[260] One specific example is the analysis of protein kinases within the cell.[185-187] Kinases are vital

components of almost all intracellular signaling cascades and serve to phosphorylate specific peptide sequences.[260]

A number of groups have synthesized peptide substrates that are kinase specific, introduced these substrates to the inside of single cells and then activated the kinases in cell to study enzyme activity.[185;186] Following activation, substrates are removed and the phosphorylated version is separated from the non-phosphorylated version by capillary electrophoresis.[186;261] The primary drawback to this approach is the need to penetrate or disrupt the cell membrane in order to introduce the substrate and the low throughput obtained for introduction. Additionally, synthetic peptides have to be homogenously labeled with fluorescent indicator which may limit the utility.[186;261] To combat this problem, a green fluorescent protein has been fused to the peptide substrate, thereby ensuring homogenous labeling, though again, cellular introduction is a problem.[262;263] Though viral vectors can be used to transfect tumor cell lines, it is desirable to use primary culture cells for a number of studies as tumor cell lines typically possess metabolic defects.[262] Thus the need exists for peptide substrate reagents that can be efficiently and directly loaded into single primary cells without the need for physical perturbation of the cell membrane.

Cell membranes act as barriers for flux of molecules trying to penetrate the cell, making the delivery of chemical reagents into cells more challenging. Cell penetrating molecules have been utilized to transport reagents or analytes across the cell membrane without damaging it. In this regard, cell penetrating peptides (CPP) known as protein transduction domains (PTD) have extensively been explored over the last decade to

internalize cell impermeable reagents.[264;265] One such peptide is HIV TAT (Transactivator of Transcription) protein transduction domain, which is widely used for cellular delivery of a range of biomarkers, via fusion of the PTD to the target molecule or marker.[253;266-268] It has been shown that internalization using TAT sequence provides an effective method to deliver chemical reagents. Although the utilization of TAT peptide is becoming a common practice in cellular analysis, the process, which TAT penetrates the cell membrane is not fully documented.[266;269] Some studies have shown that cellular uptake does not depend on a specific receptor. Further, studies have shown that TAT is not specific for a given cell. Hence, it can be used to deliver a wide variety of cargos to a wide range of cells.[264;268]

By taking all the requirements for reagents to analyze cellular chemistry, we have prepared a series of reagents that possess the general structure: 6xHis-TAT-peptide substrate-EGFP. The key components of this peptide geometry are as follows: a) the 6xHis tag allows high yield purification; b) the TAT protein, of HIV origin, serves to translocate proteins across the cell membrane; c) the peptide substrate serves as the phosphorylation site; and d) EGFP serves as the fluorescent label. To date we have constructed 6xHis-TAT-EGFP and loaded it into HeLa cells with high efficiency simply through addition of the protein to the cellular medium, thus avoiding physical disruption of the membrane. Loaded cells were analyzed by flow cytometry, confocal microscopy and CE-LIF. In CE-LIF detection, TAT-EGFP loaded single cell was lysed in the separation capillary followed by electrophoretic separation to analyze intracellular TAT-EGFP. These experiments demonstrate the feasibility of CE-LIF detection of loaded

TAT-EGFP, which should be extended to different substrates genetically attached to TAT-EGFP. In addition, we were able to estimate intracellular TAT-EGFP content using CE-LIF with post column sheath flow detector.

5.2 Experimental

5.2.1 Material and Reagents

Sigmacoat was obtained from Sigma-Aldrich Chemical Co. (St. Louis, MO). Sodium dodecyl sulfate was obtained from EM Science (Gibbstown,, NJ). All other chemicals were obtained from VWR and used as received. Capillaries were obtained from InnovaQuartz (Phoenix, AZ). All solutions were prepared using 18 MΩ deionized water (Barnstead).

5.2.2 TAT-EGFP Expression and Purification

TAT-EGFP was expressed in and purified from BL-21 cells, as follows. A single colony from a freshly streaked plate was inoculated in 5 mL of culture [LB broth plus 50µg/ml kanamycin]. The culture was incubated overnight at 37 ^{0}C (250 rpm) for 12 hours and then was used to inoculate a 400 mL culture [LB broth plus 50µg/mL kanamycin]. The 400 mL culture was grown for 6 h at 37^{0}C (250 rpm) until it reached an OD_{600} of 1.0. The culture was induced with 1mM IPTG and was grown overnight at 24 ^{0}C (250 rpm). The cells were harvested by centrifugation [Eppendorf 5804 R, 5000 rpm, 4 ^{0}C, 20 min]. The cell pellets were washed with 15 mL of 50 mM Tris- succinate (pH 7.8) buffer and repelleted. The cells were lysed via sonication using fifteen 10 s bursts. The cell lysate was collected by centrifugation [eppendorf 5804 R, 5000 rpm, 4^{0}C, 20 min]. The clear lysate was applied onto a Ni^{2+}-NTA (Qiagen) column which was pre-

equilibrated with lysis buffer [50 mM Tris-succinate pH 7.8]. The column was washed three times with lysis buffer, followed by an imidazole step gradient (10, 50, 100, 250, and 500 mM imidazole in 50 mM Tris-succinate pH 7.8). The pure fraction of the protein was stored at 4^0C in the presence of protease inhibitor and 3 mM DTT.

5.2.3 Cell Culture

The HeLa cells were used for loading experiments. Cells were grown in Dulbecco's 1 modified eagle medium (DMEM) supplemented with 10% fetal bovine serum and 1% L-glutamine at 37 ^{0}C, 5% CO_2 in an incubator. Cells were grown on plastic culture dishes at least 24 hours prior to use.

5.2.4 Loading Cells with TAT-EGFP

After removing the extracellular media, HeLa cells were washed with KRB buffer supplemented with 10 mM glucose. A solution of TAT-EGFP (6 μM) was prepared freshly in KRB buffer and it was transferred into the cell plate. Cells were maintained in the incubator for 30 min at 37 ^{0}C. Cells were then washed three times with PBS buffer after removing the loading solution from the cell plate. The cells were washed with Pucks-EDTA, followed by trypsin digest for 10 min to harvest them. Harvested cells were pelleted by centrifugation at 1,300 x g for 2 min and supernatant was removed. PBS buffer (1 mL) was added to the pelleted cells to remove TAT-EGFP in the extracellular medium. The process was carried out 6 times before the cells were resuspended in the PBS buffer (400 μL). The cell suspension was kept on ice until CE analysis. The cells were further diluted in borate buffer (10 mM, pH 9.2) prior to injection. All the washing solutions were eventually analyzed by CE-LIF.

5.2.5 Confocal Microscopy

HeLa cells grown on glass cover slips with O-rings were used to monitor cellular loading via confocal microscopy. The cells were incubated with both TAT-EGFP (7 μM) and His-EGFP (7 μM) in OPTI-MEM 1 reduced serum free media (Invitrogen) and kept for 30 min at 37^0C and 5% CO_2 in the incubator. After the incubation, the cells were washed three times with KRB buffer to remove excess loading solutions prior to imaging. The confocal fluorescence images were acquired using a MRC-1024 Laser Scanning Confocal Imaging System (Bio-Rad Laboratories, Hercules, CA). The 488 nm line of an Ar^+ laser was used as the excitation source and the emission was collected at 525 nm.

5.2.6 Flow Cytometry

HeLa cells incubated with TAT-EGFP recombinant proteins were analyzed by a FACScan Flow Cytometer (Becton Dickinson, BD Bioscience, San Jose, CA) using the 488 nm line of an Ar^+ laser. Fluorescence emission was monitored at 520 nm via passage through a bandpass filter (530/30 nm). Two parallel controls, in which cells without TAT-EGFP and cells incubated with EGFP lacking TAT peptide, were also analyzed under the same conditions for the monitoring of loaded EGFP in cells.

5.2.7 CE and Cell Injection

An electric field was applied using a 30 kV power supply (Spellman High Voltage Corporation, Hauppauge, NY) for the separation. A 50 cm long, 25 μm i.d., 150 μm o.d. fused-silica capillary was used for the separation. Capillary separation was performed using 10 mM borate buffer at pH 9.2 as the running buffer. The injection end of the capillary was kept at a high positive voltage (20 kV) and the detection end was

held at ground. Polyimide coating at the injection end of the capillary was removed to improve the light transmittance through capillary walls, which improved focusing of the cell during injection. The injection end was positioned inside a single-cell injector block, which was controlled by three dimensional translational stage assembled in house. To inject a cell, 50 μL of diluted cell solution was placed on a cell plate coated with Sigmacoat according to the manufactures instructions. The cell plates were coated to prevent cells from sticking to the bottom.[270] Using an inverted microscope, the injection end of the capillary was positioned near the single cell. Once the cell was focused, a partial suction (-11 kPa) was applied from the detection end of the capillary using water tube connected via three way solenoid valve (Cole Palmer, Vernon Hills, IL) until the cell is injected into the capillary (~ 1-2 s). Before the cell injection, a plug of SDS (5 mM) in borate buffer was injected into the capillary for 1 s. Following cell injection, a second SDS plug was injected. Upon completion of the cell injection, the capillary was placed in the running buffer followed by applying a high voltage (20 kV) for 5 s in order to mix the detergent (SDS) with the cell and initiate lysis. After 90 s, a high voltage was again applied for the separation.[262;271] TAT-EGFP loaded into the cell was separated and detected using CE-LIF. All washing solutions were analyzed by injecting the same volume onto the capillary to confirm that no detectable amount of TAT-EGFP was in the extracellular buffer. The capillary was reconditioned between each run by consecutive pressure washing with 100 mM NaOH, water and running buffer for 2 min in order to remove cellular debris adsorbed on the capillary wall.

5.2.8 Post Column LIF Detection

Post column CE-LIF detection comprised of a sheath flow cuvette was used to analyze single cells (Figure 5.1). The injection end of the capillary was connected to a multipurpose single cell injector block[252] while the detection end of the capillary, which was ground to a tip was inserted into a quartz cuvette (Mindrum Precision,Inc., Rancho Cucamonga, CA) with 200 µm x 200 µm inner bore, 2 mm thickness and 3 cm long. The cuvette was placed in a PEEK holder, which was mounted on a 3-D translational stage assembled in house. The sheath buffer, which was similar to the running buffer (10 mM borate buffer) was gravimetrically pumped through the cuvette at the rate of 1 mL/hr. A constant flow rate was maintained by keeping the height of the sheath flow buffer to the waste collector constant (15 cm). For the detection, the 488 nm line from an Ar^+ laser (Innova 70C series, Coherent, Inc., Santa Clara, CA) operating at 118 mW total power was reflected off several mirrors, through an iris then focused into the sample stream just below the tip of the capillary using a planoconvex lens (f = 20 mm, Melles Griot). The fluorescent signal was collected using a long working distance microscope objective with N.A. (40x, 0.65 N.A., Fisher Scientific) and passed through a band pass filter (D525/25 M, Chroma Technology, Rockingham, VT) and a spatial filter. The signal was detected by a PMT (H957, Hamamatsu Photonics, Bridgewater, NJ), the current from which was amplified (Model 428, Keithley Instruments, Cleveland, OH), low pass filtered (950, Frequency Devices, Haverhill, MA) and collected with an A/D converter (PCI-MIO-16E-4, National Instruments, Austin, TX) using in-house software written in LabView (National Instruments).

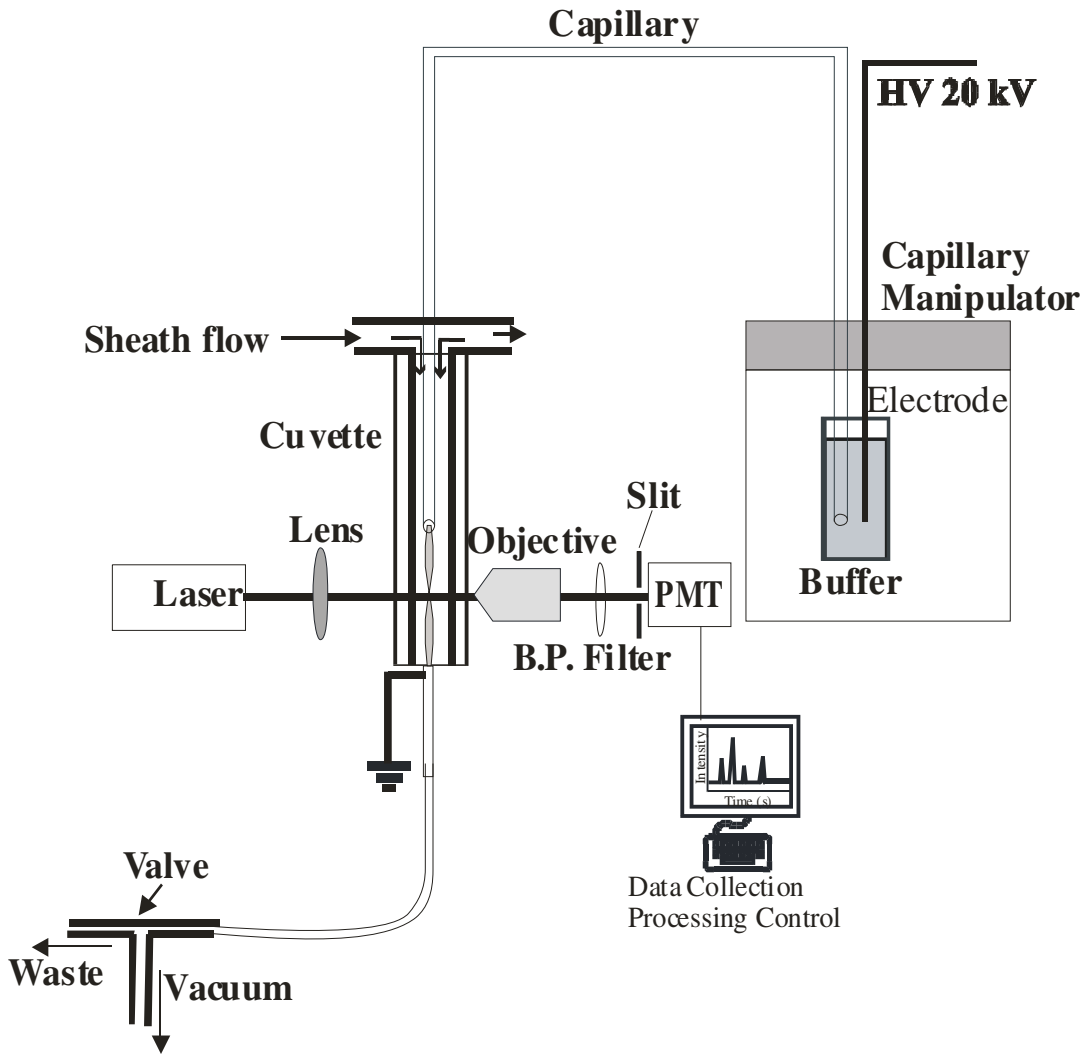

Figure 5.1. Schematic diagram of CE-LIF with sheath flow cuvette.

5.2.9 Estimation of the Intracellular TAT-EGFP Concentration

To estimate the mass of TAT-EGFP loaded into individual HeLa cells, a calibration curve was constructed by injecting know concentration of TAT-EGFP. Standards were injected electrokinetically into the separation capillary (48 cm x 25 µm i.d., total volume of the capillary 235.6 nL) by applying 42 V/cm potential for 2 s and

injection volume of standards are ca 192 pL. Peak heights were used to construct the calibration curve and it was used to estimate the number of moles of TAT-EGFP loaded into a single cell. The intracellular TAT-EGFP concentration in loaded cells was calculated by taking the HeLa cell volume as 2 pL[272].

5.3 Results and Discussion

To evaluate the effective delivery of TAT-EGFP-based molecular reagents, we expressed and purified 6xHis-TAT-EGFP recombinant protein. The 6xHis tag in the construct was used for purification purposes and TAT was introduced into the construct to deliver EGFP across the cell membranes. The purified recombinant protein was used in further studies, in which cellular translocation of TAT-EGFP was monitored by flow cytometry, microscopy and CE-LIF. Various literature reports suggest that TAT and other arginine-rich peptides are capable of penetrating the cell membrane in a receptor-independent manner and these peptides facilitate transporting of a cargo attached to them.[264;265;273]

5.3.1 Fluorescence Analysis of TAT-EGFP Loaded Cells

To evaluate the TAT mediated EGFP delivery into cells, modified EGFP with a TAT sequence was incubated with HeLa cells for 30 min. After the incubation, loaded cells were washed repeatedly with PBS buffer before the cells were imaged. Figure 5.2A shows a typical image from confocal laser scanning microscopy of HeLa cells. According to Figure 5.2A, TAT-EGFP has accumulated into cells after 30 minutes of incubation with HeLa cells, generating the fluorescence. This data suggests that TAT can effectively facilitate the translocation EGFP into HeLa cells. In control experiments, where EGFP

without TAT was incubated with HeLa cells, no detectable fluorescence was observed (image not shown), a similar observation to that made by Tremblay and coworkers[267]. In a second control experiment, cells were imaged without incubation of TAT-EGFP and no fluorescence was detected. Hence, the microscopic study indicates that fluorescence from the cells resulted from the internalization of TAT-EGFP. Although some studies have suggested that organelle localization is common with TAT mediated delivery, Figure 5.2 did not clearly indicate such localization.[273] These results were further confirmed by flow cytometric analysis of loaded HeLa cells. Flow cytometry was used to analyze cells incubated with TAT-EGFP and analysis was performed for different incubation times. A summary of flow cytometry data was given in Figure 5.2B, in which flow cytometry profiles of three samples are depicted. Fluorescence of cells was measured at different loading times as given in Figure 5.2B. The mean fluorescence intensity for the sample incubated for 30 minutes was different from that of the sample incubated for 20 hr. However, no significant difference in the average fluorescence intensity was observed for the sample loaded for 3 hr vs 30 min, in which similar profiles were obtained,(not shown) suggesting that internalization of TAT-EGFP gradually increases with the time. Control cells, which were not exposed to TAT-EGFP did not show fluorescence (Figure 5.2B).

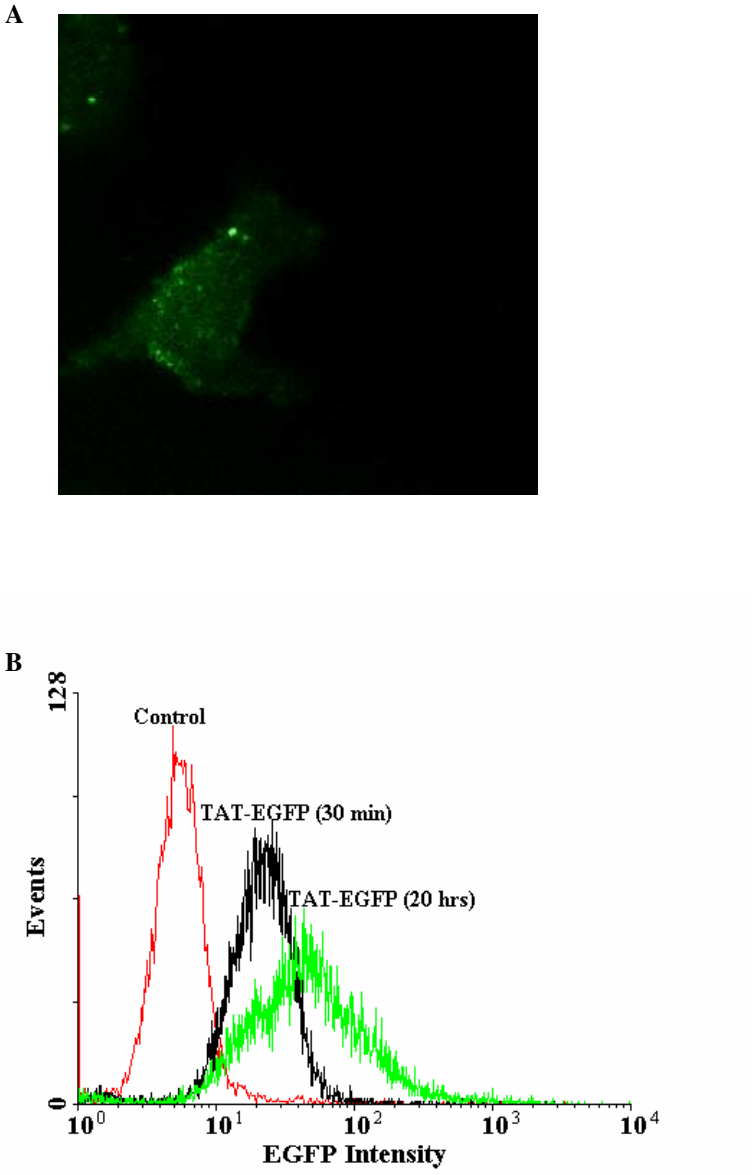

Figure 5.2. Fluorescence analysis of extracellular TAT internalization of EGFP. TAT-EGFP recombinant proteins were incubated with HeLa cells and extensively washed before the analysis. Loaded cells were analyzed by (A) laser scanning confocal microscopy and (B) flow cytometry. For flow cytometry, cells were treated with TAT-EGFP for different times as shown in Figure before they were harvested from cell plates for analysis. Control cells were not incubated with recombinant TAT-EGFP.

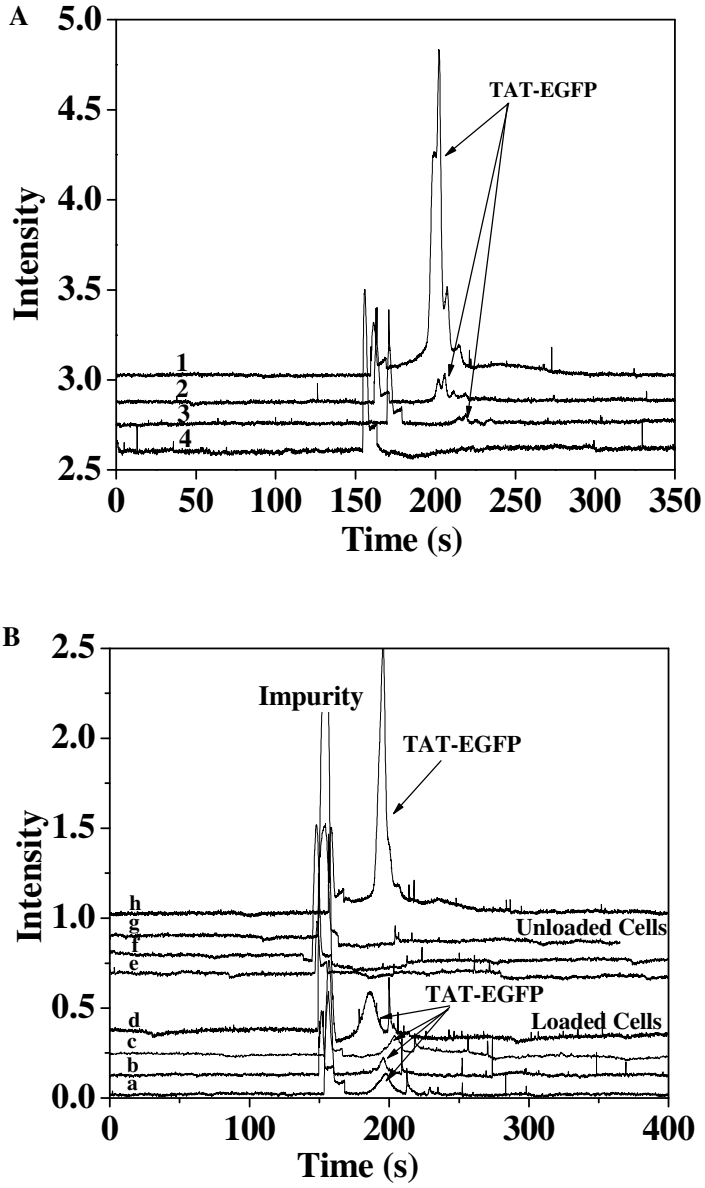

Figure 5.3. Analysis of single HeLa cells loaded with TAT-EGFP by CE-LIF. Washing solutions were analyzed to monitor the efficiency of protein removal from the solution. (A) Electropherograms obtained for individual washing solution. (B) Electropherograms obtained for individual HeLa cells, with TAT-EGFP loading (Trace a-d) and without loading TAT-EGFP (Trace e-g). Trace c is standard sample of TAT-EGFP in PBS buffer.

5.3.2 CE-LIF Analysis of Single HeLa Cells Loaded with TAT-EGFP

Next, CE-LIF was utilized to analyze TAT mediated cellular uptake of EGFP in HeLa cells. The cells were incubated with TAT-based reagents and loaded cells were washed six times with PBS buffer after harvesting the cells. Washing solutions were saved for further analysis. The cells were kept in an ice bath until analysis via CE-LIF.

Figure 5.3A shows the electropherograms obtained for washing solutions and traces were offset for clarity. In the first washing solution, there were two peaks: one at 158 s and other at 196 s, which result from impurities in the PBS buffer and TAT-EGFP in the solution, respectively. The electropherogram for washing solution two (trace 2) also contained some residual TAT-EGFP. Electropherogram for the washing solution four did not contain detectable amounts of TAT-EGFP although the impurity peak at 155 s was still present. According to Figure 5.3A, no detectable quantities of TAT-EGFP were left in the extracellular solution after the fourth washing cycle. Thus the cells were subsequently washed two times more before analysis. These experiments ensure that results from the TAT-EGFP loaded cell experiments by CE-LIF are from the internalized TAT-EGFP compounds.

For single cell analysis, a fraction of cells was diluted in borate buffer prior to the injection to lower the cell density. A single cell was identified under an inverted microscope and injected into the capillary. To lyse the cell inside the capillary, the cell was injected such that it is sandwiched between two plugs of 5 mM SDS in run buffer.[262;271] Subsequently, cellular components were detected by LIF with post column sheath flow detector. Figure 5.3B summarizes the data obtained for the single cell

analysis. A series of representative electropherograms a-d) four TAT-EGFP incubated HeLa cells, e-g) three control HeLa cells (without TAT-EGFP incubation), and h) standard solution of TAT-EGFP in PBS buffer are shown in Figure 5.3B. Two main peaks were observed in the single cell electropherograms (a-d) with average migration times of 155 ± 3.1 s and 196 ± 7.5 s (n = 4). The peak at 155 s results from impurities in PBS buffer, which was used to wash the cells and the peak at 196 s arises from intracellular TAT-EGFP. As shown in Figure 5.3B, the cells loaded with the protein had detectable amounts of TAT-EGFP while unloaded cells (e-g) did not generate a peak corresponding to TAT-EGFP. Separation of a standard TAT-EGFP in trace h reveals a migration time for TAT-EGFP of 195 s in close agreement with that from TAT-EGFP loaded cells. The peak for TAT-EGFP in single cell experiments was broad, due to band broadening, likely resulting from interaction of highly positive TAT peptide with the capillary wall or protein diffusion during the 90 s cell lysis period. Single cell analysis for the cells incubated with EGFP without TAT peptide resulted a similar electropherogram similar to traces (e-g) (data not shown). By using a calibration curve constructed by analyzing TAT-EGFP standards, intracellular TAT-EGFP concentration was estimated. A total of 5 cells were considered in the calculation and intracellular concentration was calculated by assuming a cell volume as 2 pL [272]. The average amount of TAT-EGFP was 5.1×10^{-19} moles per cell. The average TAT-EGFP cellular concentration was estimated to be ~0.3 μM. For this analysis, a calibration curve was constructed using peak heights of respected TAT-EGFP standard solutions (n = 3). A calibration range was 2.5 nM to 20 nM and the detection limit for TAT-EGFP was measured to be 0.3 nM, for S/N = 3

(3σ). In another word, calibration range was 0.5 attomole to 3.8 attomole and the detection limit was 0.05 attomole (5 x 10^{-20} mole). As shown in Figure 5.3B, the peak height fluctuated for the peak at 196 s and this was due to variation of the cell injection time.

5.4 Conclusions

We have demonstrated TAT mediated delivery of EGFP protein into HeLa cells. Loaded cells are subsequently lyzed and analyzed by CE-LIF to monitor intracellular EGFP content. Potential use of this technique is the intercellular delivery of EGFP attached to an enzyme substrate, which can be used to measure the enzyme activity in cells. This approach is particularly interesting because substrate is not required to undergo optical changes in order for detection because EGFP can be used as the fluorescence tag. Hence, this method can be useful for the measurement of activation of a range of enzymes including kinases, phosphatases and proteases. Moreover, TAT-EGFP can be modified to create an array of molecular reagents with enzyme substrates to probe enzyme activation in single cell levels. On the other hand, this could be an alternative way of delivering substrates attached to a fluorescent molecule over microinjection methods, which eliminate both labor intensive labeling of the substrate and highly invasive microinjection.

CHAPTER 6. CAPILLARY ELECTROPHORESIS WITH LASER-INDUCED FLUORESCENCE DETECTION FOR THE DETERMINATION OF BIOGENIC AMINE LEVELS IN THE ANTENNAL LOBES OF THE *MANDUCA SEXTA*

6.1 Introduction

The regulated secretion of neurotransmitters and hormones serves as a cornerstone for normal physiological function in higher organisms. Upon release from the cell, hormones and neurotransmitters bind to receptors on target cells thereby initiating a biophysical and/or biochemical response in the target cell. The ability to monitor release dynamics of these important classes of chemicals with high-sensitivity and high-temporal resolution markedly increases the understanding of physiological functions of these cellular systems. Moreover, explicitly understanding the temporal dynamics of hormone and transmitter release, transport and reuptake will improve the diagnostic and prognostic capabilities in a number of important disease states such as addiction, and depression, as well as some forms of cancer. The primary limitation to date has been the lack of sufficient methods that allow minimally invasive monitoring of these processes with sufficient temporal and spatial resolution as well as sufficient sensitivity to monitor pM to nM concentrations of these classes of compounds that are encountered in the *in vivo* environment. Hence, chemical monitoring using capillary electrophoresis (CM-CE) has proven useful for such studies due to the unique combination of chemical information, sensitivity and temporal resolution that can be achieved.[20] Most commonly, CM-CE has been used to investigate neurotransmitters, drug

metabolites and hormone dynamics both in *in vivo* and *in vitro* environments.[20] To achieve high sensitivity, CE with laser induced fluorescence detection (LIF) is used since it provides routine sub-attomole detection limits in nL to pL volumes.[152] CE-LIF has been accepted recently as a tool to study neurologically important systems, which are present in limited sample volumes. However, the analysis of biogenic amines using CE-LIF requires the labeling of analytes with fluorescent reagents due to the weak optical characteristics of these analytes. Otherwise, CE coupled with electrochemical detection has also been reported for such studies.[144;145]

Biogenic amines play a major role in the central nervous system (CNS) of insects and other animals. Such molecules can function as neurotransmitters, neuromodulators, neurotransmitter inhibitors, and neurohormones.[274;275] It is important to map the biogenic amine levels in such systems to understand their physiological importance and also to devise relationships between the dynamic changes of biogenic amines in the system with respect to cellular activities. Moreover, quantitative measurements provide valuable information in understanding signal transduction mechanisms and their contribution to the cellular function. *Manduca sexta* has been extensively studied to understand the neurochemistry in insects since it is a good model, which can provide information to understand neuronal processes of other more advanced neurochemical systems such as mammalian. A wealth of information on this system that has been published in the literature during the past two decades is a clear indication of the importance of such a system.[276] The antennal lobes (ALs) in the brain of *Manduca sexta* have been identified as the primary olfactory centers, which play a role in information processing and

recognizing odor and other stimuli.[277]. ALs have been the center of studies investigating insect neurotransmission. Further, it is reported that certain biogenic amines are synthesized and stored in ALs, which are subsequently used for cellular signaling.[278]

Since Otsuka and coworkers reported that GABA is an inhibitory neurotransmitter found in Crustacea at their neuromuscular junctions[279], various studies showed that GABA plays a significant role as a major inhibitory neurotransmitter in the CNS of various animals, including mammals and insects. Hildebrand and coworkers have extensively studied *Manduca sexta* to understand the neurochemistry associated with insects. They have reported that GABA is produced and subsequently stored in both AL and the CNS in *Manduca sexta*.[280;281] Furthermore, several studies published by the same group [278] pointed out that there are other biogenic amines, such as histamine, tyramine, and acetylcholine, in AL lobes at various concentrations. GABA is evidently produced from glutamate by glutamic acid decarboxylase, which in fact suggests a substantial amount of glutamate present in these systems.[280] There is other evidence that suggests that glutamine and proline may also play a considerable role in the synthesis of GABA.[280]

HPLC has predominantly been used in the quantitative analysis of such compounds in ALs, where both electrochemical and fluorescence detection has been reported.[275;280;282] Hildebrand and coworkers have determined certain biogenic amines including acetylcholine, GABA, serotonin and dopamine in certain structures in the CNS including ALs, optical lobe and prothoracic ganglion using radiochemical neurotransmitter screening.[278] Although HPLC based methods have been successfully used to analyze extracts of ALs, some of the potential drawbacks of such an approach are

high sample volume requirement and tedious sample preparation steps in fluorescence detection. On the other hand, not all biogenic amines are electroactive, thereby limiting the number of analytes that can be detected using electrochemical methods.[282] In practice, multiple AL lobes are used to prepare samples for analysis and this specially a concern in the case of fluorescence detection, where analytes are labeled. Thus heterogeneity among individual lobes cannot be distinguished with such an approach. Additionally, HPLC is not useful for chemical monitoring applications since it cannot be easily coupled to the tissue sample, and is not amenable to low volume sampling.

Here, we introduce for the first time, the application of CE-LIF for the analysis of biogenic amines in the homogenate of individual ALs and releasate of *Manduca sexta.* Samples were labeled with fluorogenic dye (FQ) and then separated using CZE. Biogenic amines in the homogenate were identified by co-elution with FQ-labeled standards. In particular, this study focused on determination of GABA levels in antennal lobes as the first step toward using CE for the analysis of neurochemically important analytes in *Manduca sexta*. We report the versatility of CE-LIF for the analysis of chemical content of individual ALs.

6.2 Experimental

6.2.1 Materials and Reagents

Amino acid standards were obtained from Sigma Chemical Co. (St. Louis, MO). ATTO-TAG FQ (3-(2-furoyl)quinoline-2-carboxaldehyde) (FQ) was obtained from Molecular Probes Inc. (Eugene, OR). Boric acid was obtained from Spectrum Chemicals & Laboratory Products (New Brunswick, NJ). All the other chemicals were from VWR

and were used as received. Fused silica capillaries were from InnovaQuartz (Phoenix, AZ). All solutions were prepared using 18 MΩ deionized water (Barnstead).

6.2.2 *Manduca sexta*

Manduca sexta was raised in the laboratory at the Division of Neurobiology, (University of Arizona, Tucson) according to the protocol describe by Sanes & Hildebrand (1976).[283] Briefly, once pupae reached stage 18, animals were fed with artificial diet and they were maintained under light and dark cycles of 14 hr of light and 10 hr of dark at 25^0C.[284] Male adult moths (age > 4 day) were used for the isolation of AL lobes.

6.2.3 Tissue Isolation

Adult moths were selected for the isolation of ALs during the dark cycle, at which time biogenic amines are reported to be in high concentration.[285] Moths were decapitated immediately prior to isolation of tissue and the heads were kept on ice. The antennal lobes were manually removed with a sharp scalpel. Each dissected antennal lobe was transferred into a centrifuge tube and frozen under liquid nitrogen. The lobes were stored at -80^0C until further use. On the day of analysis, the tissue sample was thawed prior to the digestion.

6.2.4 CZE-LIF

The CE-LIF instrument was described in Chapter 3. Briefly, 488 nm laser line from a multiline Ar^+ laser (Model 180-Series Laser Systems, Spectra-Physics, Mountain View, CA) operating at 20 mW total power was selected to excite the FQ-labeled amines. Sample was injected into the separation capillary (42 cm x 25 µm i.d x 360 µm o.d.) by

siphoning before the analysis. The fluorescence signal collected using a microscope objective (10x, 0.25 N.A., Newport, Irvine, CA) was filtered by a long pass filter (LP 600, Chroma Technology, Rockingham, VT). The signal was then detected by a PMT (H957, Hamamatsu Photonics, Bridgewater, NJ), current, from which was amplified by a current amplifier (Model SR570, Stanford Research System, Sunnyvale, CA), and collected by an A/D converter (PCI-MIO-16E-4, National Instruments, Austin, TX) using in-house software written in LabView (National Instruments). Electric fields were applied using a 30 kV power supply (CZE-1000, Spellman High Voltage Corporation, Hauppauge, NY).

6.2.5 Tissue Homogenization

An antenna lobe placed in a centrifuge tube was mixed with 2 μL of 0.1 M perchloric acid. The sample was homogenized manually using a glass rod to break the tissue. Then, 2 μL of 0.2 M NaOH was added to the homogenate to elevate the pH of the solution (pH > 10). The sample was diluted with 10 μL of borate buffer at pH 10 (20 mM) and was subsequently transferred into a Nanosep centrifugal device with a 3 kDa molecular weight cutoff (Pall Life Sciences, Ann Arbor, MI). The homogenate was centrifuged for 10 min at 10 000 rpm (VWR International, Bristol, CT) to remove tissue debris and proteins in the solution. Filtrate was collected and derivatized using FQ prior to the CE analysis (Figure 6.1).

6.2.6 Derivatization Procedure for Standards

A standard mixture was derivatized off-line with FQ prior to the analysis. FQ stock solution (10 mM) was prepared by dissolving 10 mg of FQ in 4.0 mL methanol

followed by dividing into 20 µL aliquots that were stored at -20^{0}C until further use. FQ was dried to remove methanol using Ar gas prior to the derivatization reaction. KCN stock solution (200 mM) was prepared in water and diluted to 25 mM in 20 mM borate buffer at pH 10. Amino acid stock solutions (10 mM) were prepared in 0.1 M bicarbonate buffer at pH 9.0. For a standard amino acid mixture, derivatization was performed by adding 2 µL aliquots of mixture components, 200 nmol dry FQ and 4 µL of 25 mM KCN. The mixture was allowed to react for 16 min in a 65^{0}C water bath in the dark. The labeled sample was further diluted in the running buffer prior to the CE analysis. The labeling reaction is shown in Figure 6.1.

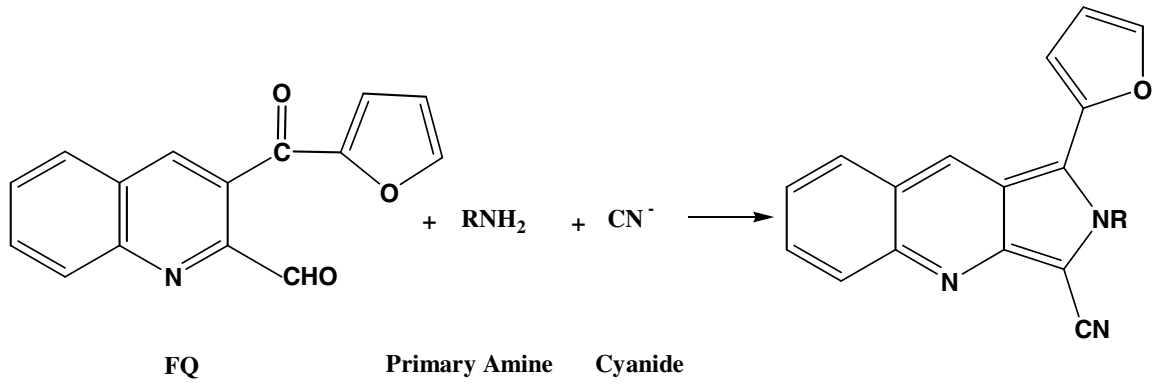

Figure 6.1. Amine derivatization reaction using FQ.

6.2.7 Derivatization Procedure for AL Homogenate

A 10 µL aliquot of the digested antennal lobe and 2 µL of 25 mM KCN in borate buffer were mixed with 200 nmol dried FQ. The mixture was allowed to react for 16 min in a water bath at 65^{0}C in the dark. Sample was diluted in borate buffer at pH 10 before the analysis. For the control experiment, 2 µL of 0.1 M perchloric acid was mixed with 2 µL of 0.2 M NaOH. Mixture was diluted with 10 µL of borate buffer and mixed with 200

nmol dried FQ and 2 μL of 25 mM KCN. Then, the mixture was reacted as described above.

6.2.8 Capillary Zone Electrophoresis

New capillaries were treated with 100 mM NaOH for 10 min followed by 10 min wash with 20 mM borate buffer at pH 10 prior to use. Borate buffer (20 mM) at pH 10.0 was used as the running buffer. All the samples were injected into the separation capillary by siphoning for 4 s. Separation was carried out using 470 V/cm. Capillaries were reconditioned after a five runs via consecutive rinses with 10 mM HCl, DI water, 100 mM NaOH and running buffer, respectively. Analyte peaks were identified by comparing migration times of standards to that of sample peaks and also homogenate was spiked with FQ-labeled standards to further verify the identity of analytes. Peak parameters i.e. peak height and migration time in standards and homogenate were calculated using the Cutter program.[221]

6.3 Results and Discussion

A primary goal of this work is to demonstrate the utility of CE-LIF as a tool to quantify biogenic amines in the ALs of *Manduca sexta*. A key aspect of this approach is selection of a suitable derivatization agent one that quickly reacts with analytes and introduces minimum dilution to the volume limited sample. FQ, which is routinely used to label microdialysis samples obtained from rat brains with high sensitivity, as reported by Dovichi and coworkers, was selected for derivatization of homogenate.[179] Some advantages of FQ are the fast reactivity and fluorogenic nature, thus excess dye in the solution, required to obtain quantitative labeling does not generate interfering peaks in

the electropherograms. Additionally, no dilution from the derivatization reagent results since the labeling reagent was dried before use. FQ is particularly interesting since it has a large stokes shift thus helping to avoid autofluorescence from contaminants in the sample e.g. cellular material. In this work, as for the first step toward characterizing CE as a tool for the determination of biogenic amines in AL of moths, we have focused on identifying and quantifying GABA and gly in AL samples. Thus FQ was chosen as a derivatizing reagent to allow identification and quantification of primary amines in the sample.

6.3.1 Instrument Performance

Initially, the sensitivity of the CE-LIF instrument toward FQ labeled biogenic amines was evaluated. The instrument was calibrated using FQ-labeled standards to determine LODs for the respective biogenic amines. FQ reacts with primary amine groups and derivatized amines can be excited at λ = 488 nm, from an Ar^+ laser. Emission is observed with a maximum of λ = 630 nm. In particular, gamma-aminobutyric acid (GABA) was selected as the one of the standards since GABA is present in ALs in large quantities since GABA functions as an inhibitory neurotransmitter in ALs.[281] Figure 6.2 illustrates a typical electropherogram for an FQ-labeled standard amino acid mixture containing GABA and glycine (gly). The average migration times (n = 3) were 128.2 ± 1.6 s and 132.0 ± 1.3 s for GABA and gly, respectively. The separation distance was 30 cm and separation efficiencies of 3.6 x 10^5 (1.2 x 10^6 N/m) and 3.2 x 10^5 (1.1 x 10^6 N/m) theoretical plates were obtained for GABA and gly, respectively. Calibration curves were constructed for GABA and gly using the peak heights of labeled standards (Figure 6.3)

and showed linearity in the concentration range of 6.8 nM to 250 nM for both GABA and gly with $R^2 > 0.99$. The LODs for standard amino acid mixture were 1 and 2 nM for GABA and gly, respectively, for S/N = 3. These slight differences in sensitivity may result from the different reaction rates between FQ and varying amino acids.[286].

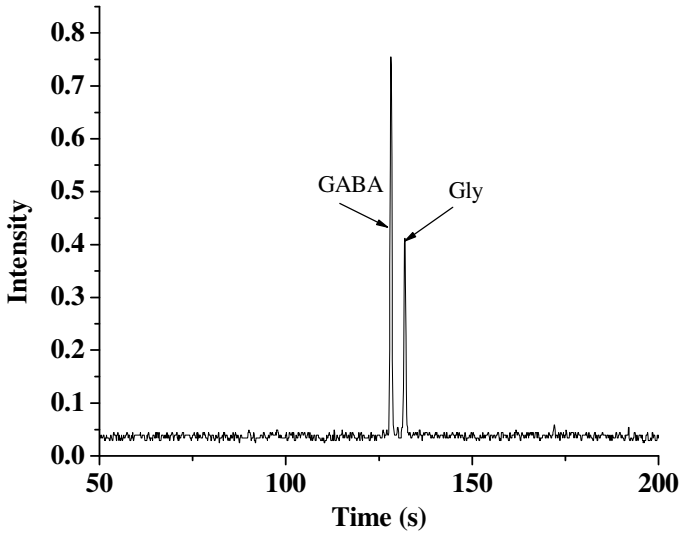

Figure 6.2. CE-LIF detection of standard amino acids. Typical electropherogram obtained for a sample mixture containing 50 nM FQ-labeled GABA and gly. Separation conditions: E = 470 V/cm, 4 s injection, 25 μm i.d., separation distance = 30 cm.

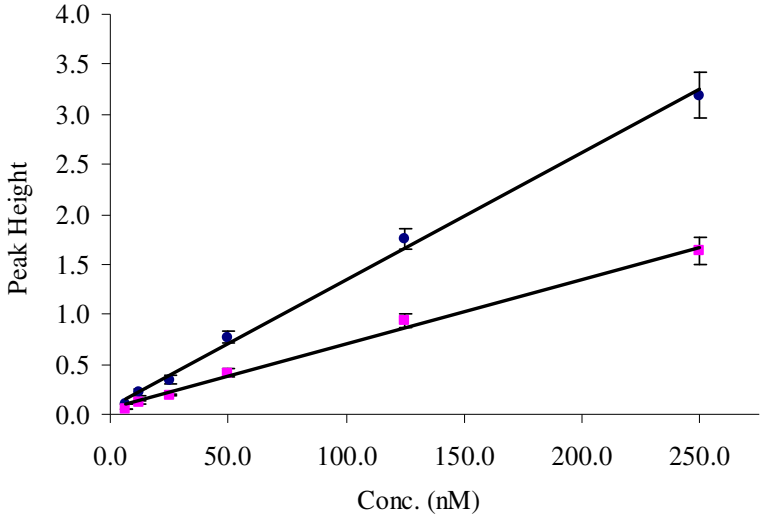

Figure 6.3. Instrument calibration for FQ labeled amines. Calibration curves were constructed for GABA (●) and Gly (■). R^2 values for GABA and Gly were 0.997 and 0.994, respectively.

6.3.2 CE-LIF Analysis of AL Homogenate

Since sensitivity is good enough CE-LIF detection can be used to identify compounds in the homogenate of ALs and these studies will eventually help to understand their physiological importance and compare the results obtained using other techniques, such as HPLC and immunoassays. To study the feasibility of the method, the antennal lobe was digested followed by labeling the homogenate prior to CE analysis. The homogenate was filtered using a membrane filter to remove proteins and tissue debris in the sample prior to derivatization to remove large MW $–NH_2$ sources and thereby to ensure that only small molecules remain in the sample, which is a key step in realizing efficient derivatization and clean electropherograms. In addition to serving as NH_2 sources, proteins degrade the analysis due to migration time irreproducibility. Figure 6.4 gives a single lobe analysis of the homogenate and sample was only diluted 2 fold

prior to the analysis and electropherogram demonstrates that the sample contains a large number of analytes. Three lobes from moths were analyzed in parallel and the results are shown in Figure 6.5. Samples were diluted 100 fold before the analysis due to high concentrations of some biogenic amines in the homogenate. More than 15 peaks were observed in individual antennal lobe samples. Similar profiles were obtained for all the samples suggesting the highly reproducible nature of the analysis. Figure 6.4 shows that the amine composition in individual lobes is similar. Each lobe contains roughly the same number of peaks but peak intensities vary, which suggests that relative abundance of biogenic amines in each lobe varies slightly. This may be due to the heterogeneity in ALs.

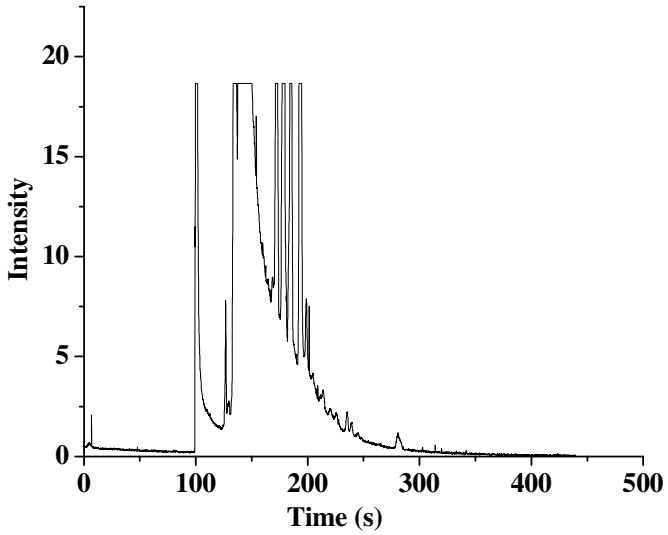

Figure 6.4. Electropherograms of antennal lobe homogenates from *Manduca sexta*. Sample was diluted 2 fold before the analysis. Separation conditions: E = 470 V/cm, 4 s injection, 25 µm i.d., separation distance = 30 cm.

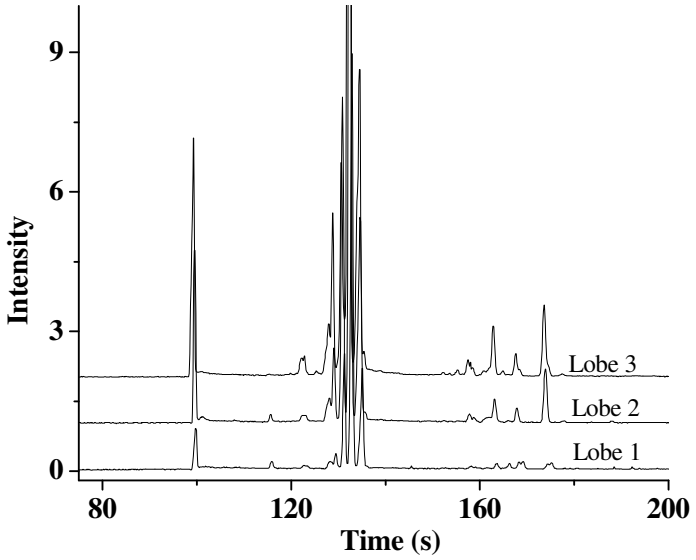

Figure 6.5. Off set electropherograms of antennal lobe homogenates from *Manduca sexta*. Three electropherograms were obtained for three different lobes. The samples were diluted 100 fold before analysis. Separation conditions: E = 470 V/cm, 4 s injection, 25 µm i.d., separation distance = 30 cm.

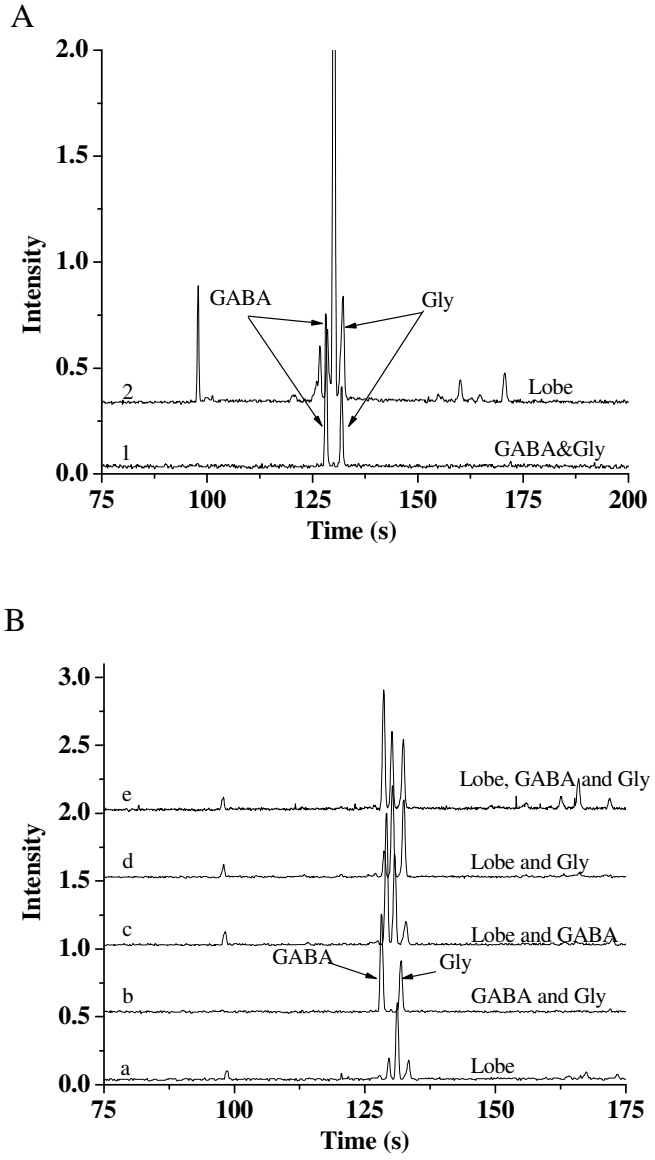

Figure 6.6. Electropherograms used for peak identification. (A) Overlaid electropherograms of (1) CE-LIF analysis of standards and (2) homogenate of AL. (B) a series of electropherograms obtained for CE-LIF detection of (a) homogenate of an antennal lobe of *Manduca sexta,* (b) 50 nM GABA and gly, (c) homogenate spiked with 50 nM GABA, (d) homogenate spiked with 50 nM gly (e) homogenate spiked with 50 nM GABA and gly. Separation conditions: E = 470 V/cm, 4 s injection, 25 µm i.d., separation distance = 30 cm.

As shown in Figure 6.4 and Figure 6.5, there is a large number of peaks, which may be from both biogenic amines and peptides that have molecular weight of 3 kD or less. Peak identification was accomplished using two methods, i.e. co-migrating standards with analytes and analyzing the homogenate spiked with standards, i.e. GABA and gly in this particular experiment. Figure 6.6 summarizes the peak identification experiments. As shown in Figure 6.6, two peaks corresponding to GABA and gly were identified. Figure 6.6 (A) gives overlaid electropherograms of a mixture of standards (GABA and gly) and AL homogenate. When comparing the migration times of standards and the sample, there are two peaks in the sample that have similar migration times as GABA and gly. This was further confirmed by a series of experiments performed by analyzing the FQ-labeled homogenate spiked with known amounts of standards as shown in Figure 6.6 (B), in which a series of electropherograms are shown for analysis of (a) digested samples of antennal lobes of *Manduca sexta,* (b) 50 nM GABA and gly, (c) homogenate spiked with 50 nM GABA, (d) homogenate spiked with 50 nM gly, and (e) homogenate spiked with 50 nM GABA and 50 nM gly. When the samples are spiked with standards, peak heights of respected analytes i.e. GABA and gly peaks were changed confirming the presence of GABA and gly in the sample.

The quantification of biogenic amines, which were identified, was done using the calibration curves (Figure 6.3) constructed for GABA and gly on the same day to ensure that all the parameters associated with the analysis were the same since an internal standard was not used in the analysis. Average peak heights were used to estimate the amounts of GABA and gly per antennal lobe. The average molar content of GABA in

the homogenate were calculated using three homogenates prepared separately and the average was 195 pmoles per structure, which is comparable to the data published by other methods.[278;280] Gly levels were also calculated in the same way and the average gly was 412 pmoles per structure. There was a considerable variation in both GABA and gly levels among individual homogenates as indicated in Table 6.1. It is necessary to analyze more samples in order to look at the heterogeneity.

Amine	pmol/structure	SD (n = 3)
Gly	412	272
GABA	195	136

Table 6.1. Levels of GABA and Gly in ALs. Contents were calculated using average peak heights for three different (n = 3) AL analysis. Some assumptions were made in this calculation i.e. all the ALs were completely digested during the homogenization and no sample lost during the preparation.

6.4 Conclusions

Here, we presented a new approach for analysis of biogenic amines in ALs of *Manduca sexta*. CE-LIF was an ideal tool for such an application due to its inherent sensitivity and low volume requirements. The analysis of a single lobe was possible unlike HPLC methods in which multiple lobes (≥ 1) were used to prepare samples for the analysis. GABA and gly levels in AL lobes were determined in a short time. As shown in the electropherograms obtained for the homogenates, there were a large number of other biogenic amines in the AL homogenate. Hence, more studies are necessary to identify and to quantify other compounds to understand their physiological importance in

Manduca sexta. It will be important to explore the possibility of coupling CE to live ALs using online sampling technique such as push-pull to study temporal dynamics.

CHAPTER 7. SUMMARY AND FUTURE DIRECTIONS

7.1 Summary

Since Lukacs and Jorgenson introduced high efficiency electrophoretic separations in narrow bore capillaries, utilization of CE has expanded exponentially into a wide range of scientific areas including biochemistry, clinical chemistry, environmental chemistry, and biotechnology.[20] This growth has been fueled by the contribution of researchers from various backgrounds who have explored aspects of CE methodology and instrumentation including novel detection strategies, injection methods and new applications.[14-24] CE has become the method of choice for low volume separations, in particular for biological analysis due to inherently high separation efficiency and mass sensitivity. The utilization of narrow bore capillary columns in CE facilitates separations using high voltages while maintaining effective heat dissipation from the capillary walls to minimize excessive band broadening.

Recently, much of the attention has focused on developing CE-based methods for the analysis of cellular chemistry as CE is amenable to low volume biological samples. The regulated secretion of neurotransmitters and hormones serves as a cornerstone for normal physiological function in higher organisms. Upon release from the cell, hormones and neurotransmitters bind to receptors on target cells thereby initiating a biophysical and/or biochemical response in the target cell. The ability to monitor release dynamics of these important classes of chemicals with high-sensitivity and high-temporal resolution will markedly increase the understanding of physiological functions of these cellular systems. The primary limitation to date has been the lack of sufficient methods

that allow minimally invasive monitoring of these processes with sufficient temporal and spatial resolution as well as sufficient sensitivity to monitor pM to nM concentrations that are encountered in the *in vivo* environment. Hence, CE-LIF methods have been attractive for such studies and with fast separations, sufficient temporal resolution may be obtained to map the chemical dynamics within the sample, thus providing an information rich, separation-based sensor.[18;41;44;177] Separation-based chemical monitoring has primarily utilized capillary zone electrophoresis (CZE) due to the rapid separation capabilities, high resolution and high mass sensitivity.

Goals of this research included the development of sensitive instrumentation and eventual utilization of those methods to analyze biologically important species both in *in vivo* and *in vitro* environments. In particular, development of (1) a novel injection scheme, (2) a new labeling reaction for primary amines, (3) a new fluorescence detector for CE using a UV-LED, (4) CE-LIF analysis of single cells, and (5) the analysis of biogenic amines in ALs of *Manduca sexta* were the main areas of focus. Thus an interdisciplinary approach based on instrument design, chemical synthesis, and novel method development was taken to realize such goals, which were described in the previous Chapters.

Several advances in CE, e.g. optical gating [51;106;125], flow gating [42;47;53;115] and micro-fabricated chips have paved the way to sub-second to second separations of biologically important molecules in real time without disturbing the chemical functions of these systems. These interfaces provide the key advance to interface CE to *in vivo* biological systems. CE systems utilizing online injection schemes have been widely used

for applications such as reaction kinetic studies, multi-dimensional separations, online chemical monitoring, *in vivo* chemical monitoring, rapid screening combinatorial compounds and high throughput assays.[41;46;48;49;200] The primary limitation of these methods has been a lack of sensitivity for monitoring hormones and neurotransmitters that are present at < 50 nM concentration.

In this work, we developed a novel injection method that improved the speed and sensitivity of CE by introducing a new chemical labeling technique and development of a novel sample injection interface based on photophysical activation of fluorogenic labels. Caged fluorescein, a fluorogenic probe that can be used to label compounds with free amino groups, which are present in a range of neuropeptides, neurotransmitters and hormones, was used. Fast separations of biologically important molecules were achieved allowing analysis of neurotransmitters and proteins with high sensitivity (ca. 1 nM), high resolution (>1,000,000 plates/m) and high speed (ms-s) temporal resolution. Moreover, we demonstrated that POG-CE possesses the required sensitivity and temporal resolution for monitoring hormones and neurotransmitters in the *in vivo* environment [126]. Combination of this instrumentation with a mathematical multiplexing method has allowed us to further increase our sensitivity (<10 pM) while only sacrificing temporal resolution by a factor of two[218]. Thus we have developed an instrument that presents significant advances in sensitivity and temporal resolution (Chapter 2) for on-line chemical monitoring.

A primary drawback of POG-CE is the lack of available caged-dye analogs with sufficiently fast reaction kinetics for online derivatization. To overcome this limitation,

we have developed a rapid high sensitivity derivatization scheme combining the fast reaction kinetics of o-phthaldialdehyde (OPA)[4] and the photoactivation properties of caged-fluorescent labels by utilizing thiol derivatives of the caged-dye in the reaction. To demonstrate the feasibility of this approach, we used an OPA/fluorescent thiol (SAMSA fluorescein) reaction to monitor neurotransmitter mixtures and proteins[287] (Chapter 3). The resulting chemical reaction provides high efficiency labeling with fast reaction rates. Further, characterization of the reaction showed that reaction properties were similar to the conventional OPA/β-ME reaction. Using this approach, biomolecules including amino acids, neurotransmitters, peptides and proteins were labeled efficiently in a short time allowing high sensitivity detection in CE-LIF. While we have focused on the utility of the OPA/SAMSA-F reaction for DCM-CE, this approach should also prove useful as a derivatization strategy in additional CE and HPLC applications.

Another area of study focused on developing a novel detector for CE using a UV-LED. Fluorescence detection of UV-excited chromophores in CE allows high sensitivity analysis of a range of environmentally and biologically important compounds. CE-UV-LIF has proven useful for detecting natively fluorescent molecules, e.g. tryptophan derivatives,[165;247] PAH's,[77;248] etc. or analytes that have been derivatized with small molecule fluorescent labels[166], e.g. OPA, fluorescamine, etc. Though this approach provides high sensitivity, UV-LIF detection typically requires the use of expensive UV lasers, limiting the widespread application of the technique. Further, the potential to miniaturize CE-based analyses of UV-excited analytes warrants the exploration of alternative excitation sources for CE-UV-LIF. Here, we demonstrated the utilization of a

high power 365 nm UV-LED as an excitation source for fluorescence detection in CE. CE-UV-LED-IF allows analysis of a range of environmentally and biologically important compounds, including polyaromatic hydrocarbons (PAHs) and biogenic amines, including neurotransmitters, amino acids, proteins and peptides, that have been derivatized with UV-excited fluorogenic labels, OPA/β-ME. UV-LED-IF was used with both zonal CE separations and MEKC to analyze such compounds. These devices show great potential to replace expensive light sources in miniaturized microfluidic devices for online chemical monitoring applications, as well as for the construction of low-cost CE systems for routine laboratory use.

To understand cellular chemistry, it is imperative that single cells be studied. Single cell analysis using CE-LIF is becoming popular since it can be used to understand single cell chemistry. In particular, this work was focused on developing a CE based method to characterize the cellular uptake of novel cellular reagents based on cell penetrating peptide, i.e. TAT. In our lab, we have demonstrated TAT mediated delivery of EGFP protein into HeLa cells. Cells loaded with TAT-EGFP were analyzed by CE-LIF to determine the intracellular EGFP content. This approach is particularly attractive since substrate is not required to undergo optical changes in order for the detection and EGFP is used as the fluorescence molecule, which can be produced by molecular biology techniques while TAT protein serves to translocate reagents across the cell membrane. Hence, such an approach can be useful for measuring activation of a range of enzymes including kinases, phosphatases and proteases. Here, we have demonstrated an alternative

method for cellular delivery of chemical reagents over highly invasive microinjections and also utilization of CE-LIF to monitor cells loaded with such reagents.

Prior to this work, the determination of biogenic amines in ALs of moths was mainly accomplished by HPLC, which requires a large mass of tissue and tedious sample preparations. Here, CE-LIF was explored for the determination of biogenic amines in insects' ALs as an alternative method to monitor neurochemically active species in such samples. CE-LIF is attractive for such studies due to the inherent advantages such as sensitivity, low volume requirements, separation speed and capability to multiplex. We demonstrated that single antennal lobes can be analyzed to determine the biogenic amine content using CE-LIF. With this method, samples were analyzed in a short time with high sensitivity. The levels of GABA and gly in an AL were calculated. Another potential advantage of CE-LIF system is that it can be coupled to ALs directly using low volume perfusion systems such as push-pull and direct sampling probes.

7.2 Future Directions

Improving Sensitivity of POG-CE-LIF Instrument

Sensitivity of POG-CE depends on several factors such as efficient photolysis, derivatization and the optical configuration in the instrument. One possible way to improve the sensitivity is to replace some of the optical components in the instrument. For separations, capillaries of 10 μm i.d. or smaller were used. For the work mentioned in Chapter 2, a low N.A. objective was used. By replacing the existing objective in the POG-CE instrument with a microscope objective with high N.A., or an oil immersion

microscope objective, the emission collection efficiency might be significantly improved making the system more sensitive.

Further, reduction of the band broadening due to injection can be achieved by utilizing sub-pL injection volumes, which can be achieved by reducing the injection time, typically below 10 ms, reducing velocity or using smaller i.d. capillaries. This puts a great demand on the shutter, which manipulates the photolytic beam during the injection. The mechanical shutter that is currently used in the lab does not provide accurate or precise gating times below 5 ms. Hence, shutters that provide accurate open and closing times < 5 ms are needed to achieve a reliable short injection time.

Fast and efficient separation is achieved by applying high field strengths for the separation. However, high voltage can cause dielectric breakdown of the capillary due to the radial field generated at such high electric fields.[288;289] An alternative way of increasing the separation speed, i.e. decreasing the separation time, is to shorten the separation distance, which is defined by the distance between the gating beam and the detection beam, if we are willing to sacrifice efficiency. With optical gating, the separation distance can be easily changed by moving the beams closer to each other. Although shorter migration times may be achieved with this approach, shortening the separation distance may have an adverse effect on the resolution as well. Hence, separation distance should be chosen such that the optimum resolution is achieved. For such a short separation distance e.g. 1-2 mm, migration time will be in ms time scale and would require extremely short injection times (≤ 1 ms) to minimize band broadening for injection[51].

New Labeling Reagents for DCM using POG-CE

The lack of highly reactive caged dyes for labeling of non-fluorescence biological analytes hinders us from utilizing the photolytic optical injection for on-line chemical monitoring applications. Most of the caged-dyes do not have high reactivity toward primary amines. Hence, the need for the caged-dyes with fast reaction kinetics is high in order to use POG injection for online chemical monitoring applications. As described in Chapter 3, the coupling of OPA to fluorescein thiol was one approach to overcome slow reactivity associated with fluorescein based reagents. However, a caged-dye (Figure 7.1) attached to a thiol group is not commercially available, which makes this task more difficult. We are currently working on a synthesis, which is targeted for a caged-fluorescein thiol compound. Caged-fluorescein thiol/OPA reaction should also have the reaction properties similar to that of SAMSA-F/OPA. This reaction should have the potential to be coupled to the POG-CE for online chemical monitoring applications.

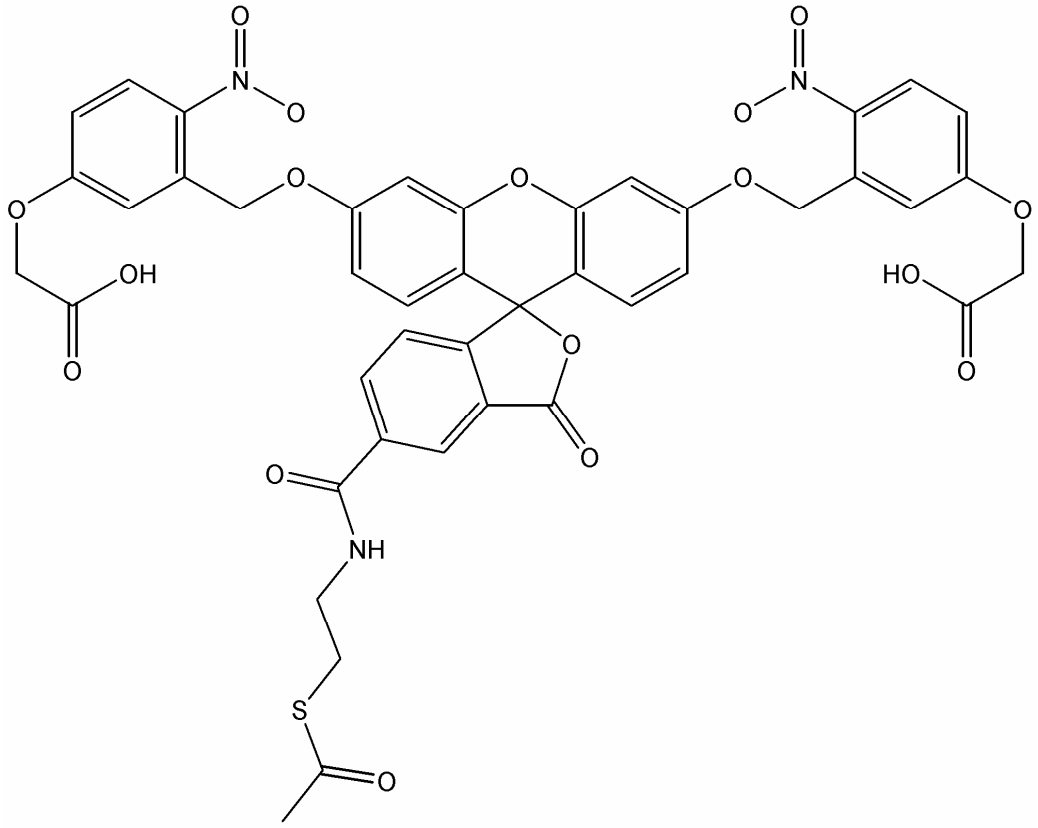

Figure 7.1. Proposed caged-fluorescein thiol for POG-CE

Immunoassay using POG-CE

Capillary electrophoresis based immunoassays present a fast, highly selective platform for the analysis of a number of proteins and peptides in complex chemical environments. One of the main advantages of POG-CE is its applicability in biologically-relevant assays. Online chemical monitoring of a particular analyte can be performed by an immunoassay. In particular, the competitive form of immunoassay (IA) is predominantly used for small peptides and proteins, in which prelabeled antigen is competitively reacted with an antibody that is specific for the analyte. Hence, on-line labeling of the analyte is not required in competitive IA. Such assays provide high

throughput compared to the traditional immunoassays, which require long analysis time. The coupling of the high sensitivity and high speed obtained from POG-CE with the exquisite sensitivity of immunoassays should provide improved sensitivity in POG-CE-IA. POG-CE-IA should provide the temporal resolution to monitor hormone secretion e.g. parathyroid hormone secretion from the parathyroid gland. This can eventually be useful in understanding the dynamics of hormone secretion in response to physiological and pharmacological stimuli. Further, as shown in the Aspinwall lab, the combination of POG-CE-IA with Hadamard transformation techniques can further improve the detection limits of such assay. This can be further improved by using an antibody with a very low dissociation constant in the assay.

POG-CE for Multi-dimensional Systems

POG-CE provides an inherently low background during the separation and results in markedly improved sensitivity over other on-line capillary interfacing technologies such as photobleching based optical gating, which has been used in multi-dimensional separation instruments. Separation times under 5 s for mixtures of small biologically important molecules and 500 ms for proteins were obtained with high separation efficiency. Thus, POG-CZE possesses the sensitivity, resolution and efficiency to be used as a second dimension in a multidimensional system. POG injection should be useful in coupling the two dimensions.

POG-CE for Micro-fabricated Devices

Utilization of photolytic optical injection on microfluidic chips allows rapid sequential sample injection into the separation channels with a high reproducibility. This

arrangement provides the ability to change the separation distance by varying beam positions without changing chip geometry. Sample introduction on chips was traditionally accomplished by T-type channels geometry, and is limited by the time required to toggle the potential between buffer reservoirs to obtain a reproducible sample injection. However, injections on chips can be achieved with just one channel using optical gate interfaces rather than using the cross injection interfaces. Further, integration of POG injection to microchips would help to utilize the chip space more efficiently to perform parallel separations by reducing the chip space occupied by the extra buffer reservoirs (Appendix B).

UV-LED for POG-CE

As shown in this work, UV-LED was used for fluorescence detection of molecules, which absorb around 365 nm. POG-CE, photolysis is achieved by using UV laser lines from Ar^+ laser. These sources are generally more expensive. Hence, it is advantageous to look for alternative light sources to accomplish photolytic injection. It has been shown that UV-LED can be used for flash photolysis of caged-fluorescein[290]. However, in that application, caged-fluorescein was exposed to UV-LED light for a long period of time ($\geq$ 100 ms) due to the low power at the focal point. In the future, the UV-LED should be tested for POG injection. In order to use UU LED for CE injection, high power is necessary. This could be achieved by using a high power UV LED module (LEDMOD365.100, Omicron Laserage, Rodgau, Germany) that has been introduced to the market very recently by Omicron Laserage. One advantage of this source over the UV

LED in our lab was that output of the source is connected to a 250 µm plastic optical fiber, which can be coupled to the separation capillary easily.

UV-LED for DCM using Microfluidic Devices

UV-LED-IF can be used for miniaturizing purposes given the size and the price of the device. Microfabricated devices are also used for fast CE separations. These devices are produced using lithographic techniques in which a network of channels is formed on a substrate, which can be utilized for separation and sample manipulation. One of the limitations of miniaturization of these devices is that lack of small light sources that can be coupled to such systems to make compact separation devices. Coupling the LED to microfluidic devices can potentially create a total analysis system to monitor amino acids from the biological sample, which can be labeled with OPA/BME. These devices can also be useful in making portable CE devices for field applications.

Single Cell Kinase Study using CE-LIF with Sheath Flow Post Column Detection

This approach can be used to study enzyme activity, in which enzyme substrates can be genetically mutated to contain TAT-EGFP, serving two purposes: EGFP provides the tag for the detection and TAT mediates effective cellular uptake. We have already expressed and purified TAT-EGFP with the protein kinase A (PKA) substrate, which can potentially bind to protein kinase A. It is important to further characterize this recombinant protein *in vitro* before being used in the single cell study to understand the activation of kinase A. Once the *in vitro* study is completed, it will be very interesting to perform assay in single cells, in which TAT-EGFP-PKA can be incubated with the cells following CE-LIF detection. It has been shown that TAT can localize the cargo inside

cells after the delivery[253]. Hence, having molecular reagents with TAT attached with a labile bond, TAT will be detached from the substrate once internalization is completed. Further, it is important to study the effects of TAT and EGFP on the binding of the substrate to the enzyme to make sure that TAT does not interfere with the binding. Having a large tag near the substrate, binding affinity may be altered.

Dynamic Chemical Monitoring of *Manduca sexta*

To determine temporal dynamics in ALs of *Manduca sexta*, online chemical monitoring is necessary. Successful coupling of sampling techniques e.g. microdialysis and push-pull with CE via injection interface i.e. flow-gated interface or optical-gated interface is required to obtain time resolved measurements. Although microdialysis is frequently used for biological sampling, the size of the probe can sometimes be a disadvantage, which can limits the spatial resolution and damage the tissue around the sample. Size of an AL is in range of 100-200 µm hence, microdialysis probes cannot be implanted into a lobe due to size constrains. However, push-pull probes[291] or direct sampling probes[106;292] should be small enough to be inserted into an antennal lobe. Hence, coupling online sampling probes with online derivatization reagents e.g. FQ[179] or OPA[43] should provide means to obtain *in vivo* analysis of biogenic amines and peptides. Such a system will provide capabilities to study relationships between neurotransmitters release and their dynamics with respect to chemical changes in the system. On the other hand, push-pull probes can be used for delivery of reagents e.g. drug to ALs to study the pharmacological aspects.

CZE-LIF was used in the preliminary work, but resolving small molecules which have similar charge to mass ratios was not easily achieved just by using zonal electrophoresis as shown by this work. MEKC may provide better resolution for the homogenate. There are reports of neuropeptides in ALs and the current instrument may not provide adequate sensitivity to detect such analytes due to their low abundance. CE-LIF system based on off-column sheath flow detection should provide low mass sensitivity to such analytes in the homogenate. Besides, it has been reported that acetylcholine is a major biogenic amine in ALs but FQ does not react with such compound since acetylcholine does not have a primary amine group. Electrochemical detection coupled with CE[145] will be a good tool to study such analytes since they are electrochemically active.

Fluorescence Resonance Energy Transfer (FRET) Probe Based on OPA/SAMSA-F Reaction

Formation of isoindoles via the reaction of OPA/SAMSA-F with primary amines has been discussed in Chapter 3. In the presence of a free thiol and primary amine, OPA forms an isoindole with a characteristic absorbance maximum ca. 335 nm [4;232], and fluorescence emission maximum ca. 450 nm.(Figure 7.2) SAMSA-F can be excited at λ = 488 nm and emission is observed with maximum ca. 525 nm. Therefore, emission spectra of the isoindole and absorbance spectra of SAMSA-F can possibly be overlapped as shown in Figure 7.2 and it is one of the requirements for FRET. If we are to use FRET in CE-LIF detection, only labeled amines will be detected and side peaks from excess SAMSA-F will not be detected. This will improve the quality of the separation since

SAMSA-F contributes to a lot of side peaks in the electropherogram as shown in Figure 3.6.

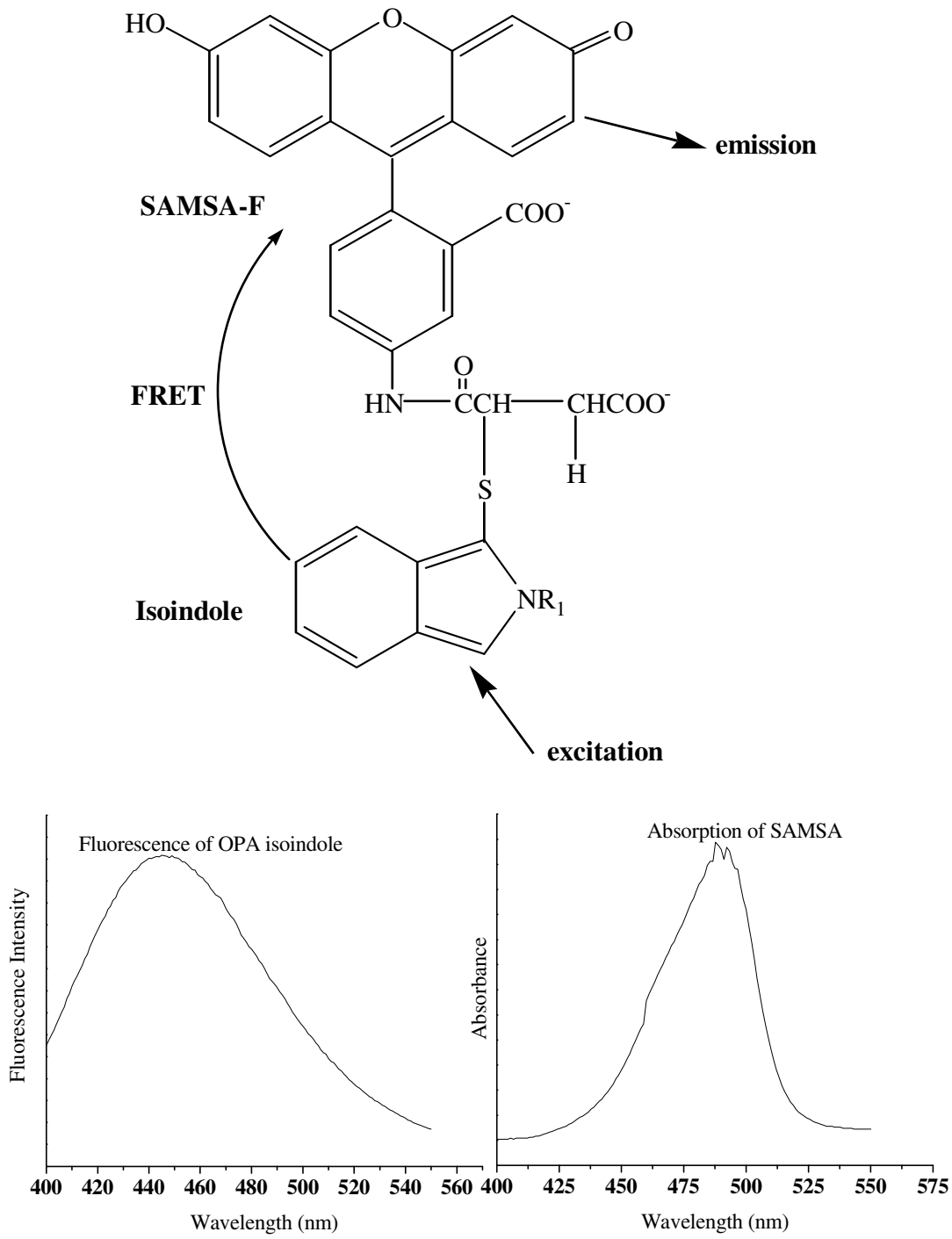

Figure 7.2. Proposed FRET probe based on OPA/SAMSA-F reaction.

APPENDIX A. OPTICAL FIBER COUPLED UV LED-IF DETECTOR FOR CE

Though LEDs are not collimated light sources compared to lasers, it is still possible to attain small spot sizes using the optical arrangements described in Chapter 4 allowing detection in capillaries with > 25 µm i.d. However, it is important to look for possible optical arrangements that may provide better beam profiles at the focal point. This is particularly important if small capillaries < 25 µm i.d. are used. Hence, we tested a new optical arrangement with a goal of improving beam quality. Figure A-1 summarizes the optical arrangement, which includes multi-mode optical fiber and a collimator. Briefly, the UV LED (Model NCCU033, Nichia America Corporation, Southfield, MI) was mounted on an aluminum cooling device (Nichia America Corporation, Southfield, MI). Emission from the LED (100 mW, λ_{max} = 365 nm, $\Delta\lambda$ = 8 nm) was collected and focused into a multi-mode optical fiber (Cat. No. FT200UMT, 200 µm core diameter, 225 µm clad diameter, 0.39 NA, High OH, ThorLabs, Newton, NJ) with a fused silica biconvex lens (*f* = 35 mm, ThorLabs, Newton, NJ). Light was passed through a collimator (Cat. No. F220SMA-A, ThorLabs) connected to the fiber at the other end and then was focused into the center of the separation capillary using a fused silica plano-convex lens (*f* = 25 mm, Melles Griot, Irvine, CA). Fluorescence emission was collected at a 90^{o} angle to the excitation detection beam (12 mW) using a microscope objective (10x, 0.25 numerical aperture, Newport, Irvine, CA), passed through a spatial filter to remove scatter generated in the capillary walls and a band pass filter (450/30 nm, Omega Optical, Brattleboro, VT). The collected emission was detected using a PMT

(H957, Hamamatsu Photonics, Bridgewater, NJ). Even though, beam quality was improved with this optical arrangement, the intensity at the focal point was 0.2 mW. Less than 1 mW was measured, which was inadequate for fluorescence detection. The primary reason for the poor throughput with an optical fiber was that the light collected by the fiber was not sufficient. In this optical arrangement, optical fiber with 225 μm core diameter was used. However, optical fibers with higher core diameter should also be tested for this application since more light can be focused into the fiber in such instances. Another way to alleviate problems associated with spot size is to utilize epi-illumination, in which a high quality microscope objective (fused silica) can be used to focus and collect light. Having fused silica microscope objective for focusing, high throughput of UV LED light can be obtained.

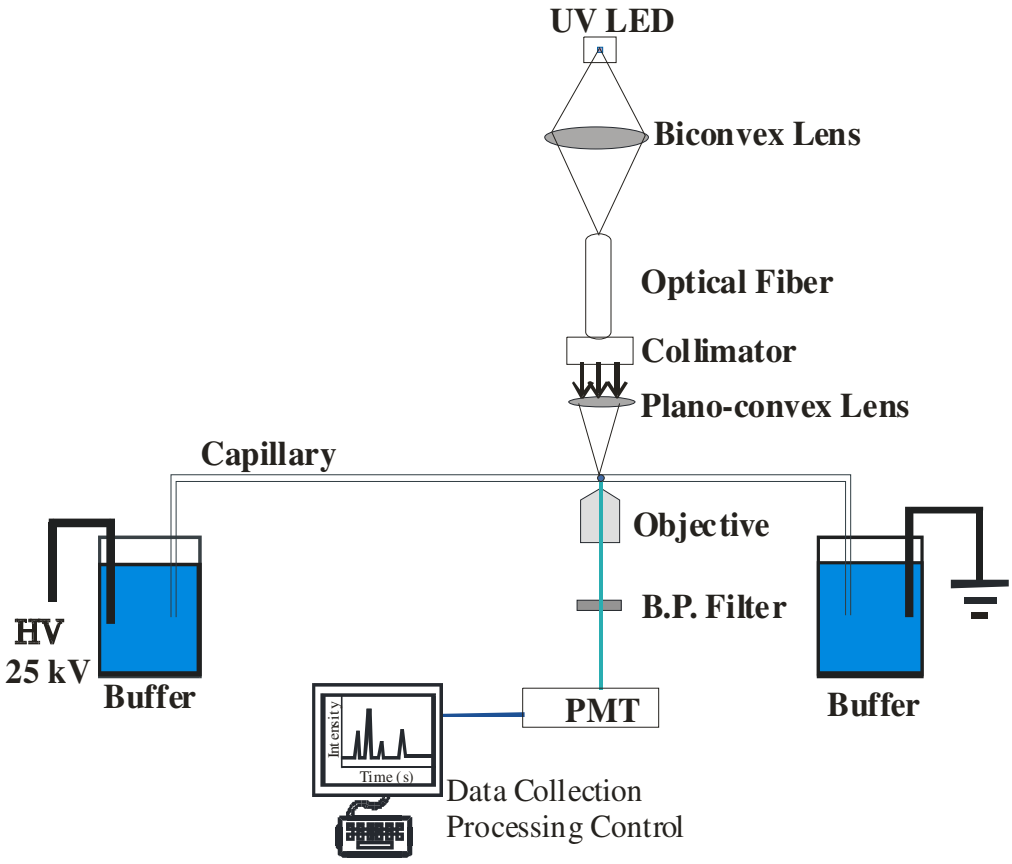

Figure A-1. Schematic diagram of the UV light emitting diode induced-fluorescence detection system, in which optical fiber was used to improve the light quality.

APPENDIX B. POG-CE-LIF CHIP INSTRUMENT

POG-CE-LIF chip instrument was built in house for the future use. This system can hold a microfluidic chip in the dimensions of 2" x 2" that can be used for electrophoretic separations. Chips can be fabricated using lithographic techniques[189] and more detail information on chip fabrication was discussed by Braun and Aspinwall[293]. A schematic diagram of the chip instrument is shown in Figure B-1. The output of an Ar^+ laser (Innova 70C series, Coherent, Inc., Santa Clara, CA) operating at 3 W total power was split into UV and visible wavelengths using a dichroic mirror (LWP-45-RS 355-TS 488-PW-1025-UV, CVI Laser, Albuquerque, NM). The UV lines were passed through two UV band pass filters (U-330, Edmund Industrial Optics, Barrington, NJ) to further remove visible light in the photolysis beam. The photolysis beam, comprised of the combined 351-364 nm lines, was focused into the center of the separation channel using a fused silica biconvex lens (f = 25 mm, Melles Griot, Irvine, CA). Sample injection is accomplished by photolysis beam, which was controlled using a LS3 mechanical shutter with VMM-T1 control (Unibitz LS3, Vincent Associates, Rochester, NY). For detection, the visible wavelengths of the laser were dispersed using a prism (Melles Griot) and the 488 nm laser-line was isolated using spatial filters, reflected off by a dichroic mirror (Z488RDC, Chroma Technology, Rockingham, VT) and focused into the center of the separation channel using a microscope objective (20x, 0.4 N.A., Melles Griot). For the detection, fluorescence was collected by the same microscope objective. Collected light was passed through the same dichroic mirror, a band pass filter (D525/25 M, Chroma Technology, Rockingham, VT) and a spatial filter. The signal was detected by a PMT

(H957, Hamamatsu Photonics, Bridgewater, NJ), the current from which was amplified (Model 428, Keithley Instruments, Cleveland, OH), low pass filtered (950, Frequency Devices, Haverhill, MA) and collected with an A/D converter (PCI-MIO-16E-4, National Instruments, Austin, TX) using in-house software written in LabView (National Instruments). Electric fields were applied using a 30 kV power supply (CZE-1000, Spellman High Voltage Corporation, Hauppauge, NY).

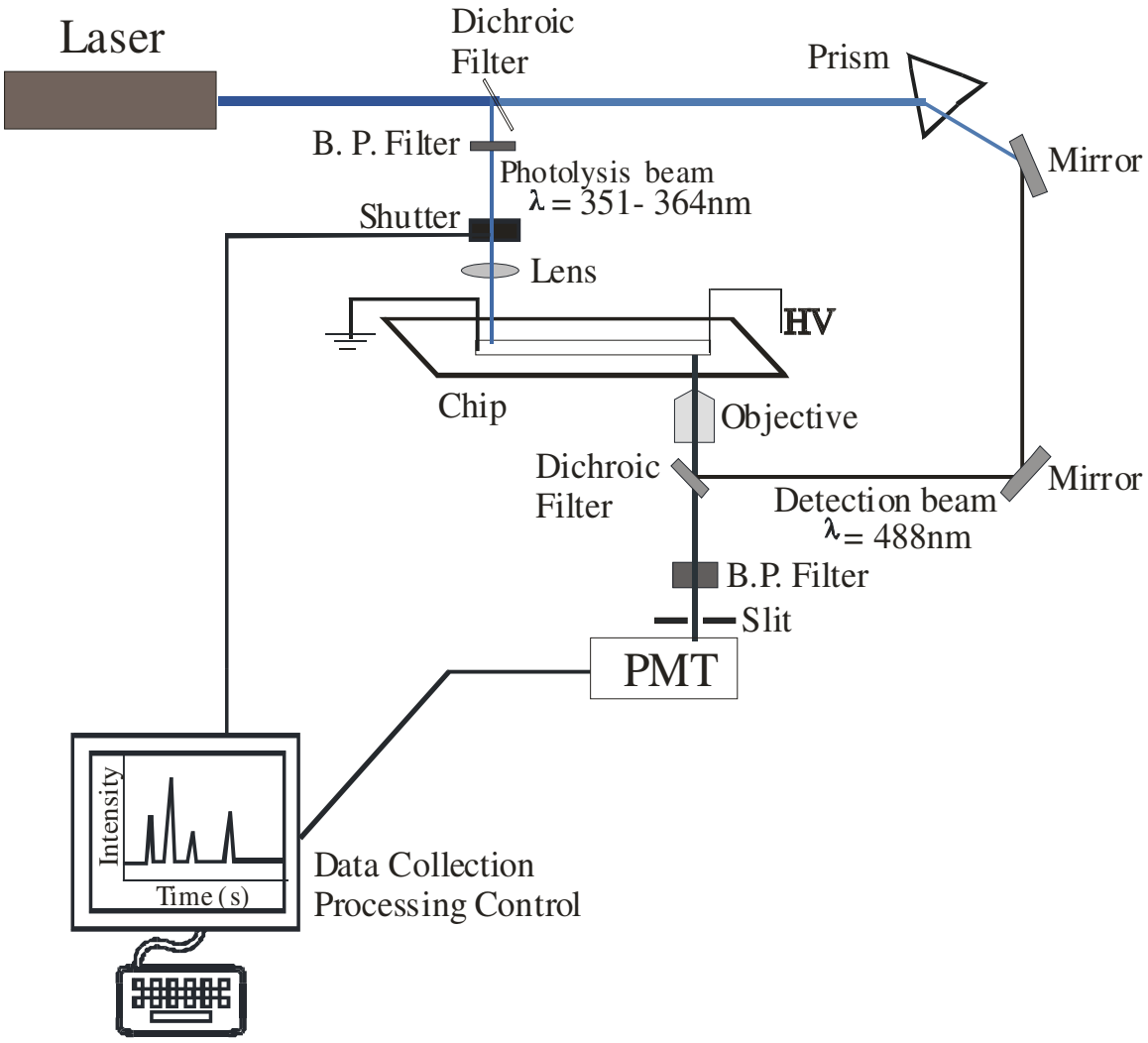

Figure B-1. POG-CE-LIF Chip instrument.

APPENDIX C. PERMISSIONS

Karen Buehler

-From: suminda@email.arizona.edu
\,.ent: Tuesday, March 06, 2007 5:07 PM
To: Copyright
Subject: Copy right request

PERMISSION REQUEST FORM Date;03/06/2007

To: Copyright Office
Publications Division
American Chemical Society
1155 Sixteenth Street, N.W.
Washington, DC 20036

From; Suminda Hapuarachchi
University of Arzona
Department of Chemistry
1306 E. University Blvd
Tucson AZ 85721-0041
Your Phone No,520-626-1335
Your Pax No. 520-621-8407

I am preparing a paper entitled:
(Phd Dissertation) Rapid, High *sensitivity* capillary separations for the analysis of biologically active species to appear in a (circle one) other entitled; to be published by; ProQuest Information and Learning Company

- I would appreciate your permission to use the following ACS material in print and other formats with the understanding that the required ACS copyright credit line will appear with each item and that this permission is for only the requested work listed above;

From ACS journals or magazines (for ACS magazines, also include issue no.):

ACS publication Title	Issue Date	Vol.	No.	Page(s)	Material to be used*
Analytical Chemistry		70	13	2463 and 2465	(Figure 3 and Figure 5)

If you use more than three figures/tables from any article and/or chapter, the author's permission will also be required.
Questions? Please call Arleen Courtney at (202) 872-4368 or use the FAX number above.

This space is reserved for
ACS Copyright Office Use

PERMISSION TO REPRINT IS GRANTED BY THE AMERICAN CHEMICAL SOCIETY

ACS CREDIT LINE REQUIRED. *Please* follow *this* sample:
Reprinted with permission from (reference citation). Copyright (year) American Chemical Society.

APPROVED BY: _ *C. Arleen Courtney*
ACS Copyright Office

0 If box is checked, author permission is also required. Sec original article for address.

BIOGRAPHICAL SKETCH

Suminda Hapuarachchi was born in Kurunegala, Sri Lanka, in 1972. He attended the Dharmaraja College and graduated in 1991. He received a Bachelor of Science in Special Degree in Chemistry in 1998. After two years working in the private sector, he entered Sam Houston State University in 2000 and received his Masters Degree in Chemistry in 2002. In 2002, he came to University of Arizona and started his Ph.D. work with Dr. Craig A. Aspinwall. He received his Doctor of Philosophy degree in 2007, May. He then pursues his career in industry and joined Amgen, Thousand Oaks, California.

REFERENCES

1. Banks, P. R.; Paquette, D. M. *Bioconjugate Chemistry* **1995,** *6*, 447-58.
2. Paul, P. H.; Garguilo, M. G.; Rakestraw, D. J. *Anal.Chem.* **1998,** *70*, 2459-67.
3. Trepman, E.; Chen, R. F. *Archives of Biochemistry and Biophysics* **1980,** *204*, 524-32.
4. Chen, R. F.; Scott, C.; Trepman, E. *Biochimica et Biophysica Acta* **1979,** *576*, 440-55.
5. Weber, G.; Teale, F. W. J. *Transactions of the Faraday Society* **1957,** *53*, 646-55.
6. Hjerten, S. *Arkiv for Kemi* **1958,** *13*, 151-52.
7. Hjerten, S. *Chromatogr.Rev.* **1967,** *9*, 122.
8. Mikkers, F. E. P.; Everaerts, F. M.; Verheggen, T. P. E. M. *Journal of Chromatography* **1979,** *169*, 11-20.
9. Neuhoff, V.; Weise, M.; Sternbac, H. *Hoppe-Seylers Zeitschrift fur Physiologische Chemie* **1970,** *351*, 1395-&.
10. Neuhoff, V.; Schill, W. B.; Sternbac, H. *Biochemical Journal* **1970,** *117*, 623-&.
11. Jorgenson, J. W.; Lukacs, K. D. *Anal.Chem.* **1981,** *53*, 1298-302.
12. Jorgenson, J. W.; Lukacs, K. D. *Science* **1983,** *222*, 266-72.
13. Camilleri, P *Capillary Electrophoresis : Theory and Practice;CRC press: Boca Raton* **1993**.
14. Beale, S. C. *Anal.Chem.* **1998,** *70*, 279R-300R.
15. Cannon, D. M.; Winograd, N.; Ewing, A. G. *Annual Review of Biophysics and Biomolecular Structure* **2000,** *29*, 239-63.
16. Huck, C. W.; Stecher, G.; Bakry, R.; Bonn, G. K. *Electrophoresis* **2003,** *24*, 3977-97.
17. Johnson, M. E.; Landers, J. P *Electrophoresis* **2004,** *25*, 3513-27.
18. Kennedy, R. T. *Analytica Chimica Acta* **1999,** *400*, 163-80.

19. Kennedy, R. T.; German, I.; Thompson, J. E.; Witowski, S. R. *Chem.Rev.* **1999,** *99*, 3081-+.

20. Kraly, J.; Fazal, M. A.; Schoenherr, R. M.; Bonn, R.; Harwood, M. M.; Turner, E.; Jones, M.; Dovichi, N. J. *Anal.Chem.* **2006**.

21. Quigley, W. W. C.; Dovichi, N. J. *Anal.Chem.* **2004,** *76*, 4645-58.

22. Krylov, S. N.; Dovichi, N. J. *Anal.Chem.* **2000,** *72*, 111R-28R.

23. Schmitt-Kopplin, P.; Frommberger, M. *Electrophoresis* **2003,** *24*, 3837-67.

24. Swinney, K.; Bornhop, D. J. *Electrophoresis* **2000,** *21*, 1239-50.

25. Padarauskas, A. *Analytical and Bioanalytical Chemistry* **2006,** *384*, 132-44.

26. Little, M. J.; Paquette, D. M.; Roos, P. K. *Electrophoresis* **2006,** *27*, 2477-85.

27. Patrick, J. S.; Lagu, A. L. *Electrophoresis* **2001,** *22*, 4179-96.

28. Lagu, A. L. *Electrophoresis* **1999,** *20*, 3145-55.

29. Zagursky, R. J.; Mccormick, R. M. *Biotechniques* **1990,** *9*, 74-&.

30. Scherer, J. R.; Kheterpal, I.; Radhakrishnan, A.; Ja, W. W.; Mathies, R. A. *Electrophoresis* **1999,** *20*, 1508-17.

31. Yeung, W. S. B.; Luo, G. A.; Wang, Q. G.; Ou, J. P. *Journal of Chromatography B-Analytical Technologies in the Biomedical and Life Sciences* **2003,** *797*, 217-28.

32. Huck, C. W.; Stecher, G.; Bakry, R.; Bonn, G. K. *Electrophoresis* **2003,** *24*, 3977-97.

33. Krylov, S. N.; hmadzadeh, H. *Methods Mol.Biol.* **2004,** *276*, 29-38.

34. Miao, H.; Rubakhin, S. S.; Sweedler, J. V. *Anal.Chem.* **2005,** *77*, 7190-94.

35. Gunasekera, N.; Olson, K. J.; Musier-Forsyth, K.; Arriaga, E. A. *Anal.Chem.* **2004,** *76*, 655-62.

36. Ma, S.; Nashabeh, W. *Anal.Chem.* **1999,** *71*, 5185-92.

37. Wan, H.; Blomberg, L. G.; Hamberg, M. *Electrophoresis* **1999,** *20*, 132-37.

38. Jussila, M.; Sundberg, S.; Hopia, A.; Makinen, M.; Riekkola, M. L. *Electrophoresis* **1999,** *20*, 111-17.

39. Hu, S.; Zhang, L.; Dovichi, N. J. *Journal of Chromatography A* **2001,** *924*, 369-75.

40. Lucangioli, S.; Rodriguez, V.; Carducci, C. N. *Boll.Chim.Farm.* **1999,** *138*, 7-11.

41. Lada, M. W.; Kennedy, R. T. *Journal of Neuroscience Methods* **1997,** *72*, 153-59.

42. Lada, M. W.; Vickroy, T. W.; Kennedy, R. T. *Anal.Chem.* **1997,** *69*, 4560-65.

43. Bowser, M. T.; Kennedy, R. T. *Electrophoresis* **2001,** *22*, 3668-76.

44. Lada, M. W.; Kennedy, R. T. *Journal of Neuroscience Methods* **1995,** *63*, 147-52.

45. Shou, M.; Smith, A. D.; Shackman, J. G.; Peris, J.; Kennedy, R. T. *Journal of Neuroscience Methods* **2004,** *138*, 189-97.

46. Bushey, M. M.; Jorgenson, J. W. *Anal.Chem.* **1990,** *62*, 978-84.

47. Hooker, T. F.; Jorgenson, J. W. *Anal.Chem.* **1997,** *69*, 4134-42.

48. Lemmo, A. V.; Jorgenson, J. W. *Journal of Chromatography* **1993,** *633*, 213-20.

49. Moore, A. W.; Jorgenson, J. W. *Anal.Chem.* **1995,** *67*, 3448-55.

50. Choudhary, G.; Hancock, W.; Witt, K.; Rozing, G.; Torres-Duarte, A.; Wainer, I. *Journal of Chromatography A* **1999,** *857*, 183-92.

51. Moore, A. W.; Jorgenson, J. W. *Anal.Chem.* **1993,** *65*, 3550-60.

52. Monnig, C. A.; Jorgenson, J. W. *Anal.Chem.* **1991,** *63*, 802-07.

53. Lemmo, A. V.; Jorgenson, J. W. *Anal.Chem.* **1993,** *65*, 1576-81.

54. Fung, E. N.; Yeung, E. S. *Anal.Chem.* **1995,** *67*, 1913-19.

55. Guttman, A.; Nelson, R. J.; Cooke, N. *Journal of Chromatography* **1992,** *593*, 297-303.

56. Hjerten, S.; Zhu, M. D. *Journal of Chromatography* **1985,** *346*, 265-70.

57. Foret, F.; Szoko, E.; Karger, B. L. *Journal of Chromatography* **1992,** *608*, 3-12.

58. Wu, J. Q.; Li, S. C.; Watson, A. *Journal of Chromatography A* **1998,** *817*, 163-71.

59. Gebauer, P.; Bocek, P. *Electrophoresis* **2002,** *23*, 3858-64.

60. Gebauer, P.; Caslavska, J.; Thormann, W. *Journal of Biochemical and Biophysical Methods* **1991,** *23*, 97-105.

61. Everaert, F. M. *Journal of Chromatography* **1972,** *65*, 3-&.

62. Terabe, S.; Otsuka, K.; Ichikawa, K.; Tsuchiya, A.; Ando, T. *Anal.Chem.* **1984,** *56*, 111-13.

63. Bao, J. J. *Journal of chromatography B* **1997,** *699*, 463-80.

64. Powell, P. R.; Ewing, A. G. *Analytical and Bioanalytical Chemistry* **2005,** *382*, 581-91.

65. Liu, X.; Sosic, Z.; Krull, I. S. *Journal of Chromatography A* **1996,** *735*, 165-90.

66. Chen, S. M.; Wiktorowicz, J. E. *Analytical Biochemistry* **1992,** *206*, 84-90.

67. Hjerten, S.; Liao, J. L.; Yao, K. *Journal of Chromatography* **1987,** *387*, 127-38.

68. Kilar, F.; Hjerten, S. *Electrophoresis* **1989,** *10*, 23-29.

69. Verheggen, T. P. E. M.; Beckers, J. L.; Everaerts, F. M. *Journal of Chromatography* **1988,** *452*, 615-22.

70. Korir, A. K.; Almeida, V. K.; Malkin, D. S.; Larive, C. K. *Anal.Chem.* **2005,** *77*, 5998-6003.

71. Wolters, A. M.; Jayawickrama, D. A.; Larive, C. K.; Sweedler, J. V. *Anal.Chem.* **2002,** *74*, 2306-13.

72. Hjerten, S.; Elenbring, K.; Kilar, F.; Liao, J. L.; Chen, A. J. C.; Siebert, C. J.; Zhu, M. D. *Journal of Chromatography* **1987,** *403*, 47-61.

73. Cohen, A. S.; Karger, B. L. *Journal of Chromatography* **1987,** *397*, 409-17.

74. Cohen, A. S.; Paulus, A.; Karger, B. L. *Chromatographia* **1987,** *24*, 15-24.

75. Pappas, T. J.; Gayton-Ely, M.; Holland, L. A. *Electrophoresis* **2005,** *26*, 719-34.

76. Hu, S.; Jiang, J.; Cook, L. M.; Richards, D. P.; Horlick, L.; Wong, B.; Dovichi, N. J. *Electrophoresis* **2002,** *23*, 3136-42.

77. Imasaka, T.; Nishitani, K.; Ishibashi, N. *Analytica Chimica Acta* **1992,** *256*, 3-7.

78. Hapuarachchi, S.; Janaway, G. A.; Aspinwall, C. A. *Electrophoresis* **2006,** *27*, 4052-59.

79. Otsuka, K.; Terabe, S. *Trac-Trends in Analytical Chemistry* **1993,** *12*, 125-30.

80. Swinney, K.; Bornhop, D. J. *Electrophoresis* **2000,** *21*, 1239-50.

81. Giddings, J. C. *Separation Science* **1969,** *4*, 181-&.

82. Salomon, K.; Burgi, D. S.; Helmer, J. C. *Journal of Chromatography* **1991,** *559*, 69-80.

83. Pretoriu, V.; Hopkins, B. J.; Schieke, J. D. *Journal of Chromatography* **1974,** *99*, 23-30.

84. Stevens, T. S.; Cortes, H. J. *Anal.Chem.* **1983,** *55*, 1365-70.

85. Vandeemter, J. J.; Zuiderweg, F. J.; Klinkenberg, A. *Chemical Engineering Science* **1956,** *5*, 271-89.

86. Moody, H. W. *Journal of Chemical Education* **1982,** *59*, 290-91.

87. Weinberger, R. *Practical Capillary Electrophoresis, Academic Press, Boston* **1993**.

88. Hjerten, S.; Valtcheva, L.; Elenbring, K.; Liao, J. L. *Electrophoresis* **1995,** *16*, 584-94.

89. Liu, J. P.; Dolnik, V.; Hsieh, Y. Z.; Novotny, M. *Anal.Chem.* **1992,** *64*, 1328-36.

90. Gelfi, C.; Curcio, M.; Righetti, P. G.; Sebastiano, R.; Citterio, A.; Ahmadzadeh, H.; Dovichi, N. J. *Electrophoresis* **1998,** *19*, 1677-82.

91. Gilges, M.; Kleemiss, M. H.; Schomburg, G. *Anal.Chem.* **1994,** *66*, 2038-46.

92. Righetti, P. G.; Gelfi, C.; Verzola, B.; Castelletti, L. *Electrophoresis* **2001,** *22*, 603-11.

93. Grossman, P. D.; Colburn, J. C.; Lauer, H. H.; Nielsen, R. G.; Riggin, R. M.; Sittampalam, G. S.; Rickard, E. C. *Anal.Chem.* **1989,** *61*, 1186-94.

94. Towns, J. K.; Regnier, F. E. *Anal.Chem.* **1992,** *64*, 2473-78.

95. Green, J. S.; Jorgenson, J. W. *Journal of Chromatography* **1989,** *478*, 63-70.

96. Bushey, M. M.; Jorgenson, J. W. *Journal of Chromatography* **1989,** *480*, 301-10.

97. Wiktorowicz, J. E.; Colburn, J. C. *Electrophoresis* **1990,** *11*, 769-73.

98. Emmer, A.; Jansson, M.; Roeraade, J. *Hrc-Journal of High Resolution Chromatography* **1991,** *14*, 738-40.

99. Oda, R. P.; Madden, B. J.; Spelsberg, T. C.; Landers, J. P. *Journal of Chromatography A* **1994,** *680*, 85-92.

100. Yeung, W. S. B.; Luo, G. A.; Wang, J. P.; Ou, J. P. *Journal of chromatography B* **2003,** *797*, 217-28.

101. Erim, F. B.; Cifuentes, A.; Poppe, H.; Kraak, J. C. *Journal of Chromatography A* **1995,** *708*, 356-61.

102. Busch, M. H. A.; Kraak, J. C.; Poppe, H. *Journal of Chromatography A* **1995,** *695*, 287-96.

103. Rose, D. J.; Jorgenson, J. W. *Anal.Chem.* **1988,** *60*, 642-48.

104. Ermakov, S. V.; Zhukov, M. Y.; Capelli, L.; Righetti, P. G. *Electrophoresis* **1994,** *15*, 1158-66.

105. Huang, X. H.; Gordon, M. J.; Zare, R. N. *Anal.Chem.* **1988,** *60*, 375-77.

106. Tao, L.; Thompson, J. E.; Kennedy, R. T. *Anal.Chem.* **1998,** *70*, 4015-22.

107. Meyer, R. *Journal of Chromatography A* **1985,** *334*, 197-209.

108. Li, M. W.; Huynh, B. H.; Hulvey, M. K.; Lunte, S. M.; Martin, R. S. *Anal.Chem.* **2006,** *78*, 1042-51.

109. Mesaros, J. M.; Luo, G.; Roeraade, J.; Ewing, A. G. *Anal.Chem.* **1993,** *65*, 3313-19.

110. Effenhauser, C. S.; Manz, A.; Widmer, H. M. *Anal.Chem.* **1993,** *65*, 2637-42.

111. Jacobson, S. C.; Koutny, L. B.; Hergenroder, R.; Moore, A. W.; Ramsey, J. M. *Anal.Chem.* **1994,** *66*, 3472-76.

112. Chen, S. H.; Lin, Y. H.; Wang, L. Y.; Lin, C. C.; Lee, G. B. *Anal.Chem.* **2002,** *74*, 5146-53.

113. Huynh, B. H.; Fogarty, B. A.; Martin, R. S.; Lunte, S. M. *Anal.Chem.* **2004,** *76*, 6440-47.

114. Effenhauser, C. S.; Bruin, G. J. M.; Paulus, A. *Electrophoresis* **1997,** *18*, 2203-13.

115. Lada, M. W.; Kennedy, R. T. *Anal.Chem.* **1996,** *68*, 2790-97.

116. Ciriacks, C. M.; Bowser, M. T. *Anal.Chem.* **2004,** *76*, 6582-87.

117. O'Brien, K. B.; Esguerra, M.; Klug, C. T.; Miller, R. F.; Bowser, M. T. *Electrophoresis* **2003,** *24*, 1227-35.

118. Lada, M. W.; Schaller, G.; Carriger, M. H.; Vickroy, T. W.; Kennedy, R. T. *Analytica Chimica Acta* **1995,** *307*, 217-25.

119. Harrison, D. J.; Fluri, K.; Seiler, K.; Fan, Z. H.; Effenhauser, C. S.; Manz, A. *Science* **1993,** *261*, 895-97.

120. Seiler, K.; Harrison, D. J.; Manz, A. *Anal.Chem.* **1993,** *65*, 1481-88.

121. Plenert, M. L.; Shear, J. B. *Proceedings of the National Academy of Sciences of the United States of America* **2003,** *100*, 3853-57.

122. Moore, A. W.; Jorgenson, J. W. *Anal.Chem.* **1995,** *67*, 3464-75.

123. Lapos, J. A.; Ewing, A. G. *Anal.Chem.* **2000,** *72*, 4598-602.

124. Xu, X. M.; Roddy, T. P.; Lapos, J. A.; Ewing, A. G. *Anal.Chem.* **2002,** *74*, 5517-22.

125. Thompson, J. E.; Vickroy, T. W.; Kennedy, R. T. *Anal.Chem.* **1999,** *71*, 2379-84.

126. Hapuarachchi, S.; Premeau, S. P.; Aspinwall, C. A. *Anal.Chem.* **2006,** *78*, 3674-80.

127. Jacobson, S. C.; Culbertson, C. T.; Daler, J. E.; Ramsey, J. M. *Anal.Chem.* **1998,** *70*, 3476-80.

128. Landers, J. P. Ed *Handbook of Capillary Electrophoresis, CRC Press, New York* **1997**.

129. Xi, X. B.; Yeung, E. S. *Applied Spectroscopy* **1991,** *45*, 1199-203.

130. Yeung, E. S. *Accounts of Chemical Research* **1989,** *22*, 125-30.

131. Weston, A.; Brown, P. R.; Jandik, P.; Jones, W. R.; Heckenberg, A. L. *Journal of Chromatography* **1992,** *593*, 289-95.

132. Jandik, P.; Jones, W. R.; Weston, A.; Brown, P. R. *Lc Gc-Magazine of Separation Science* **1991,** *9*, 634-&.

133. Grill, E.; Huber, C.; Oefner, P.; Vorndran, A.; Bonn, G. *Electrophoresis* **1993,** *14*, 1004-10.

134. Wang, T.; Hartwick, R. A. *Journal of Chromatography* **1992,** *589*, 307-13.

135. Bornhop, D. J.; Hankins, J. *Anal.Chem.* **1996,** *68*, 1677-84.

136. Krattiger, B.; Bruin, G. J. M.; Bruno, A. E. *Anal.Chem.* **1994,** *66*, 1-8.

137. Bornhop, D. J. *Applied Optics* **1995,** *34*, 3234-39.

138. Mikkers, F. E. P.; Everaerts, F. M.; Verheggen, T. P. E. M. *Journal of Chromatography* **1979,** *169*, 11-20.

139. Huang, X. H.; Pang, T. K. J.; Gordon, M. J.; Zare, R. N. *Anal.Chem.* **1987,** *59*, 2747-49.

140. Zemann, A. J.; Schnell, E.; Volgger, D.; Bonn, G. K. *Anal.Chem.* **1998,** *70*, 563-67.

141. da Silva, J. A. F.; do Lago, C. L. *Anal.Chem.* **1998,** *70*, 4339-43.

142. Wallingford, R. A.; Ewing, A. G. *Anal.Chem.* **1988,** *60*, 1972-75.

143. Wallingford, R. A.; Ewing, A. G. *Anal.Chem.* **1987,** *59*, 1762-66.

144. Powell, P. R.; Paxon, T. L.; Han, K. A.; Ewing, A. G. *Anal.Chem.* **2005,** *77*, 6902-08.

145. Paxon, T. L.; Powell, P. R.; Lee, H. G.; Han, K. A.; Ewing, A. G. *Anal.Chem.* **2005,** *77*, 5349-55.

146. Shamsi, S. A.; Miller, B. E. *Electrophoresis* **2004,** *25*, 3927-61.

147. Servais, A. C.; Crommen, J.; Fillet, M. *Electrophoresis* **2006,** *27*, 2616-29.

148. Wei, H.; Nolkrantz, K.; Parkin, M. C.; Chisolm, C. N.; O'Callaghan, J. P.; Kennedy, R. T. *Anal.Chem.* **2006,** *78*, 4342-51.

149. Gassmann, E.; Kuo, J. E.; Zare, R. N. *Science* **1985,** *230*, 813-14.

150. Wu, S. L.; Dovichi, N. J. *Journal of Chromatography* **1989,** *480*, 141-55.

151. Dovichi, N. J.; Martin, J. C.; Jett, J. H.; Trkula, M.; Keller, R. A. *Anal.Chem.* **1984,** *56*, 348-54.

152. Dovichi, N. J.; Martin, J. C.; Jett, J. H.; Keller, R. A. *Science* **1983,** *219*, 845-47.

153. Swerdlow, H; Wu, S; Harke, H; Dovichi, N. J. *Journal of Chromatography* **1990,** *516*, 61-67.

154. Kuhr, W. G.; Yeung, E. S. *Anal.Chem.* **1988,** *60*, 1832-43.

155. Kuhr, W. G.; Yeung, E. S. *Anal.Chem.* **1988,** *60*, 2642-46.

156. Walrafen, G. E; Blatz, L. A. *Jouran of chemistry and physics* **1973,** 2646.

157. Bruno, A. E.; Maystre, F.; Krattiger, B.; Nussbaum, P.; Gassmann, E. *Trac-Trends in Analytical Chemistry* **1994,** *13*, 190-98.

158. Chabinyc, M. L.; Chiu, D. T.; McDonald, J. C.; Stroock, A. D.; Christian, J. F.; Karger, A. M.; Whitesides, G. M. *Anal.Chem.* **2001,** *73*, 4491-98.

159. Kuo, J. S.; Kuyper, C. L.; Allen, P. B.; Fiorini, G. S.; Chiu, D. T. *Electrophoresis* **2004,** *25*, 3796-804.

160. Macka, M.; Andersson, P.; Haddad, P. R. *Electrophoresis* **1996,** *17*, 1898-905.

161. Sluszny, C.; He, Y.; Yeung, E. S. *Electrophoresis* **2005,** *26*, 4197-203.

162. Yeung, E. S.; Wang, P. G.; Li, W. N.; Giese, R. W. *Journal of Chromatography* **1992,** *608*, 73-77.

163. Oldenburg, K. E.; Xi, X. Y.; Sweedler, J. V. *Journal of Chromatography A* **1997,** *788*, 173-83.

164. Lee, T. T.; Yeung, E. S. *Anal.Chem.* **1992,** *64*, 3045-51.

165. Timperman, A. T.; Oldenburg, K. E.; Sweedler, J. V. *Anal.Chem.* **1995,** *67*, 3421-26.

166. Waterval, J. C. M.; ingeman, H.; Bult, A.; Underberg, W. J. M. *Electrophoresis* **2000,** *23*, 4029-45.

167. Underberg, W. J. M.; Waterval, J. C. M. *Electrophoresis* **2002,** *23*, 3922-33.

168. Albin, M.; Weinberger, R.; Sapp, E.; Moring, S. *Anal.Chem.* **1991,** *63*, 417-22.

169. Molina, M.; Silva, M. *Electrophoresis* **2002,** *23*, 1096-103.

170. Kei Lau, Shung; Zaccardo, Fabian; Little, Michael; Banks, Peter *Journal of Chromatography A* **1998,** *809*, 203-10.

171. Zhao, Jian Ying; Chen, Da Yong; Dovichi, Norman J. *Journal of Chromatography A* **1992,** *608*, 117-20.

172. Liu, X.; Hu, Y. Q.; Ma, L.; Lu, Y. T. *Journal of Chromatography A* **2004,** *1049*, 237-42.

173. Molina, M.; Silva, M. *Electrophoresis* **2002,** *23*, 2333-40.

174. Beard, N. P.; Edel, J. B.; deMello, A. J. *Electrophoresis* **2004,** *25*, 2363-73.

175. Cao, L. W.; Wang, H.; Zhang, H. S. *Electrophoresis* **2005,** *26*, 1954-62.

176. Hogan, B. L.; Lunte, S. M.; Stobaugh, J. F.; Lunte, C. E. *Anal.Chem.* **1994,** *66*, 596-602.

177. Zhou, S. Y.; Zuo, H.; Stobaugh, J. F.; Lunte, C. E.; Lunte, S. M. *Anal.Chem.* **1995,** *67*, 594-99.

178. Liu, J. P.; Hsieh, Y. Z.; Wiesler, D.; Novotny, M. *Anal.Chem.* **1991,** *63*, 408-12.

179. Chen, Z.; Wu, J.; Baker, G. B.; Parent, M.; Dovichi, N. J. *Journal of Chromatography A* **2001,** *914*, 293-98.

180. Arriaga, E. A.; Zhang, Y. N.; Dovichi, N. J. *Analytica Chimica Acta* **1995,** *299*, 319-26.

181. Dovichi, N. J.; Hu, S. *Current Opinion in Chemical Biology* **2003,** *7*, 603-08.

182. Krylov, S. N.; Arriaga, E. A.; Chan, N. W. C.; Dovichi, N. J.; Palcic, M. M. *Analytical Biochemistry* **2000,** *283*, 133-35.

183. Lee, I. H.; Pinto, D.; Arriaga, E. A.; Zhang, Z. R.; Dovichi, N. J. *Anal.Chem.* **1998,** *70*, 4546-48.

184. Sims, C. E.; Meredith, G. D.; Krasieva, T. B.; Berns, M. W.; Tromberg, B. J.; Allbritton, N. L. *Anal.Chem.* **1998,** *70*, 4570-77.

185. Li, H.; Wu, H. Y.; Wang, Y.; Sims, C. E.; Allbritton, N. L. *Journal of chromatography B* **2001,** *757*, 79-88.

186. Li, H.; Sims, C. E.; Kaluzova, M.; Stanbridge, E. J.; Allbritton, N. L. *Biochemistry* **2004,** *43*, 1599-608.

187. Meredith, G. D.; Sims, C. E.; Soughayer, J. S.; Allbritton, N. L. *Nature Biotechnology* **2000,** *18*, 309-12.

188. Kristensen, H. K.; Lau, Y. Y.; Ewing, A. G. *Journal of Neuroscience Methods* **1994,** *51*, 183-88.

189. Roper, M. G.; Shackman, J. G.; Dahlgren, G. M.; Kennedy, R. T. *Anal.Chem.* **2003,** *75*, 4711-17.

190. Tao, L.; Kennedy, R. T. *Anal.Chem.* **1996,** *68*, 3899-906.

191. German, I.; Kennedy, R. T. *Journal of Chromatography B-Analytical Technologies in the Biomedical and Life Sciences* **2000,** *742*, 353-62.

192. Miao, H.; Rubakhin, S. S.; Sweedler, J. V. *Analytical and Bioanalytical Chemistry* **2003,** *377*, 1007-13.

193. Stuart, J. N.; Sweedler, J. V. *Analytical and Bioanalytical Chemistry* **2003,** *375*, 28-29.

194. Garguilo, M. G.; Michael, A. C. *Journal of Neuroscience Methods* **1996,** *70*, 73-82.

195. Liu, Y. M.; Sweedler, J. V. *Journal of the American Chemical Society* **1995,** *117*, 8871-72.

196. Fluri, K.; Fitzpatrick, G.; Chiem, N.; Harrison, D. J. *Anal.Chem.* **1996,** *68*, 4285-90.

197. Alarie, J. P.; Jacobson, S. C.; Culbertson, C. T.; Ramsey, J. M. *Electrophoresis* **2000,** *21*, 100-06.

198. Jacobson, S. C.; Hergenroder, R.; Moore, A. W.; Ramsey, J. M. *Anal.Chem.* **1994,** *66*, 4127-32.

199. Moore, A. W.; Jorgenson, J. W. *Anal.Chem.* **1995,** *67*, 3456-63.

200. Roddy, E. S.; Lapos, J. A.; Ewing, A. G. *Journal of Chromatography A* **2003,** *1004*, 217-24.

201. Rainelli, A.; Hauser, P. C. *Analytical and Bioanalytical Chemistry* **2005,** *382*, 789-94.

202. Kaneta, T. *Anal.Chem.* **2001,** *73*, 540A-7A.

203. Kaneta, T.; Yamaguchi, Y.; Imasaka, T. *Anal.Chem.* **1999,** *71*, 5444-46.

204. Xu, H. W.; Roddy, E. S.; Roddy, T. P.; Lapos, J. A.; Ewing, A. G. *Journal of Separation Science* **2004,** *27*, 7-12.

205. Xu, H. W.; Ewing, A. G. *Analytical and Bioanalytical Chemistry* **2004,** *378*, 1710-15.

206. Mitchison, T. J. *Journal of Cell Biology* **1989,** *109*, 637-52.

207. Dang, F.; Zhang, L.; Hagiwara, H.; Mishina, Y.; Baba, Y. *Electrophoresis* **2003,** *24*, 714-21.

208. Chamow, S. M.; Kogan, T. P.; Peers, D. H.; Hastings, R. C.; Byrn, R. A.; Ashkenazi, A. *Journal of Biological Chemistry* **1992,** *267*, 15916-22.

209. Tsai, S. C.; Klinman, J. P. *Bioorganic Chemistry* **2003,** *31*, 172-90.

210. Stoddard, B. L.; Cohen, B. E.; Brubaker, M.; Mesecar, A. D.; Koshland, D. E. *Nature Structural Biology* **1998,** *5*, 891-97.

211. Sanchez, J. A.; Vergara, J. *American Journal of Physiology* **1994,** *266*, C1291-C1300.

212. Ross, D.; Locascio, L. E. *Anal.Chem.* **2003,** *75*, 1218-20.

213. Johnson, T. J.; Ross, D.; Gaitan, M.; Locascio, L. E. *Anal.Chem.* **2001,** *73*, 3656-61.

214. Ross, D.; Johnson, T. J.; Locascio, L. E. *Anal.Chem.* **2001,** *73*, 2509-15.

215. Molho, J. I.; Herr, A. E.; Mosier, B. P.; Santiago, J. G.; Kenny, T. W.; Brennen, R. A.; Gordon, G. B.; Mohammadi, B. *Anal.Chem.* **2001,** *73*, 1350-60.

216. Herr, A. E.; Molho, J. I.; Santiago, J. G.; Mungal, M. G.; Kenny, T. W.; Garguilo, M. G. *Anal.Chem.* **2000,** *72*, 1053-57.

217. Schrum, K. F.; Lancaster, J. M.; Johnston, S. E.; Gilman, S. D. *Anal.Chem.* **2000,** *72*, 4317-21.

218. Braun, K. L.; Hapuarachchi, S.; Fernandez, F. M.; Aspinwall, C. A. *Anal.Chem.* **2006,** *78*, 1628-35.

219. Chen, D. Y.; Adelhelm, K.; Cheng, X. L.; Dovichi, N. J. *Analyst* **1994,** *119*, 349-52.

220. Cheng, Y. F.; Dovichi, N. J. *Science* **1988,** *242*, 562-64.

221. Shackman, J. G.; Watson, C. J.; Kennedy, R. T. *Journal of Chromatography A* **2004,** *1040*, 273-82.

222. Underberg, W. J. M.; Waterval, J. C. M. *Electrophoresis* **2002,** *23*, 3922-33.

223. Stobaugh, J. F.; Repta, A. J.; Sternson, L. A.; Garren, K. W. *Analytical Biochemistry* **1983,** *135*, 495-504.

224. Simons, Jr. S. Stoney; Johnson, David F. *Analytical Biochemistry* **1978,** *90*, 705-25.

225. Simons, Jr. S. Stoney; Johnson, David F. *Analytical Biochemistry* **1977,** *82*, 250-54.

226. Fan, L. Y.; Cheng, Y. Q.; Chen, H. L.; Liu, L. H.; Chen, X. G.; Hu, Z. D. *Electrophoresis* **2004,** *25*, 3163-67.

227. Bardelmeijer, H. A.; Waterval, J. C. M.; Lingeman, H.; van't Hof, R.; Bult, A.; Underberg, W. J. M. *Electrophoresis* **1997,** *18*, 2214-27.

228. Strong, R. A.; Cho, B. Y.; Fate, G. D.; Krull, I. S. *Journal of Chromatography A* **1998,** *824*, 25-33.

229. Hill, D. W.; Walters, F. H.; Wilson, T. D.; Stuart, J. D. *Anal.Chem.* **1979,** *51*, 1338-41.

230. Lindroth, P.; Mopper, K. *Anal.Chem.* **1979,** *51*, 1667-74.

231. Oguri, S.; Yokoi, K.; Motohase, Y. *Journal of Chromatography A* **1997,** *787*, 253-60.

232. Roth, M. *Anal.Chem.* **1971,** *43*, 880-&.

233. Fan, L. Y.; Chen, H. L.; Zhang, J. Y.; Chen, X. G.; Hu, Z. D. *Analytica Chimica Acta* **2004,** *501*, 129-35.

234. Sovocool, G. W.; Brumley, W. C.; Donnelly, J. R. *Electrophoresis* **1999,** *20*, 3297-310.

235. Dasgupta, P. K.; Eom, I. Y.; Morris, K. J.; Li, J. Z. *Analytica Chimica Acta* **2003,** *500*, 337-64.

236. Tong, W.; Yeung, E. S. *Journal of Chromatography A* **1995,** *718*, 177-85.

237. Wang, S. L.; Huang, X. J.; Fang, Z. L.; Dasgupta, P. K. *Anal.Chem.* **2001,** *73*, 4545-49.

238. Guo, Y. L.; Uchiyama, K.; Nakagama, T.; Shimosaka, T.; Hobo, T. *Electrophoresis* **2005,** *26*, 1843-48.

239. Chen, S. J.; Chen, M. J.; Chang, H. T. *Journal of Chromatography A* **2003,** *1017*, 215-24.

240. Lu, Q.; Collins, G. E. *Analyst* **2001,** *126*, 429-32.

241. Ye, M. L.; Hu, S.; Quigley, W. W. C.; Dovichi, N. J. *Journal of Chromatography A* **2004,** *1022*, 201-06.

242. Lu, M. J.; Chiu, T. C.; Chang, P. L.; Ho, H. T.; Chang, H. T. *Analytica Chimica Acta* **2005,** *538*, 143-50.

243. Wang, Chunling; Zhao, Shulin; Yuan, Hongyan; Xiao, Dan *Journal of chromatography B* **2006,** *833*, 129-34.

244. Zhao, S. L.; Yuan, H. Y.; Xiao, D. *Electrophoresis* **2006,** *27*, 461-67.

245. Sandlin, Z. D.; Shou, M. S.; Shackman, J. G.; Kennedy, R. T. *Anal.Chem.* **2005,** *77*, 7702-08.

246. Otsuka, K.; Higashimori, M.; Koike, R.; Karuhaka, K.; Okada, Y.; Terabe, S. *Electrophoresis* **1994,** *15*, 1280-83.

247. Lee, Thomas T.; Yeung, Edward S. *Journal of Chromatography A* **1992,** *595*, 319-25.

248. Kaneta, T.; Yamashita, T.; Imasaka, T. *Analytica Chimica Acta* **1995,** *299*, 371-75.

249. Nickerson, B.; Jorgenson, J. W. *Journal of Chromatography* **1989,** *480*, 157-68.

250. Ramsey, J. D.; Jacobson, S. C.; Culbertson, C. T.; Ramsey, J. M. *Anal.Chem.* **2003,** *75*, 3758-64.

251. Hu, K.; Zarrine-Afsar, A.; Ahmadzadeh, H.; Krylov, S. N. *Instrumentation Science & Technology* **2004,** *32*, 31-41.

252. Krylov, S. N.; Starke, D. A.; Arriaga, E. A.; Zhang, Z. R.; Chan, N. W. C.; Palcic, M. M.; Dovichi, N. J. *Anal.Chem.* **2000,** *72*, 872-77.

253. Soughayer, J. S.; Wang, Y.; Li, H. A.; Cheung, S. H.; Rossi, F. M.; Stanbridge, E. J.; Sims, C. E.; Allbritton, N. L. *Biochemistry* **2004,** *43*, 8528-40.

254. Turner, E. H.; Lauterbach, K.; Pugsley, H. R.; Palmer, V. R.; Dovichi, N. J. *Anal.Chem.* **2007,** *79*, 778-81.

255. Tong, W.; Yeung, E. S. *Journal of chromatography B* **1997,** *689*, 321-25.

256. Le, X. C.; Scaman, C.; Zhang, Y. N.; Zhang, J. H.; Dovichi, N. J.; Hindsgaul, O.; Palcic, M. M. *Journal of Chromatography A* **1995,** *716*, 215-20.

257. Zhang, Y. N.; Le, X. C.; Dovichi, N. J.; Compston, C. A.; Palcic, M. M.; Diedrich, P.; Hindsgaul, O. *Analytical Biochemistry* **1995,** *227*, 368-76.

258. Chen, D. Y.; Dovichi, N. J. *Anal.Chem.* **1996,** *68*, 690-96.

259. Krylov, S. N.; Arriaga, E.; Zhang, Z. R.; Chan, N. W. C.; Palcic, M. M.; Dovichi, N. J. *Journal of chromatography B* **2000,** *741*, 31-35.

260. Sims, C. E.; Allbritton, N. L. *Current Opinion in Biotechnology* **2003,** *14*, 23-28.

261. Meredith, G. D.; Sims, C. E.; Soughayer, J. S.; Allbritton, N. L. *Nature Biotechnology* **2000,** *18*, 309-12.

262. Zarrine-Afsar, A.; Krylov, S. N. *Anal.Chem.* **2003,** *75*, 3720-24.

263. Yoon, S.; Han, K. Y.; Nam, H. S.; Nga, L. V.; Yoo, Y. S. *Journal of Chromatography A* **2004,** *1056*, 237-42.

264. Chauhan, A.; Tikoo, A.; Kapur, A. K.; Singh, M. *Journal of Controlled Release* **2007,** *117*, 148-62.

265. Tunnemann, G.; Martin, R. M.; Haupt, S.; Patsch, C.; Edenhofer, F.; Cardoso, M. C. *Faseb Journal* **2006,** *20*, 1775-84.

266. Fittipaldi, A.; Ferrari, A.; Zoppe, M.; Arcangeli, C.; Pellegrini, V.; Beltram, F.; Giacca, M. *Journal of Biological Chemistry* **2003,** *278*, 34141-49.

267. Caron, Nicolas J.; Torrente, Yvan; Camirand, Geoffrey; Bujold, Mathieu; Chapdelaine, Pierre; Leriche, Karine; Bresolin, Nereo; Tremblay, Jacques P. *Mol Ther* **2001,** *3*, 310-18.

268. Peitz, M.; Pfannkuche, K.; Rajewsky, K.; Edenhofer, F. *Proceedings of the National Academy of Sciences of the United States of America* **2002,** *99*, 4489-94.

269. Tyagi, M.; Rusnati, M.; Presta, M.; Giacca, M. *Journal of Biological Chemistry* **2001,** *276*, 3254-61.

270. Krylov, S. N.; Dovichi, N. J. *Electrophoresis* **2000,** *21*, 767-73.

271. Pang, Z. L.; Al Mahrouki, A.; Berezovski, M.; Krylov, S. N. *Electrophoresis* **2006,** *27*, 1489-94.

272. Malek, A. H.; Khaledi, M. G. *Electrophoresis* **2003,** *24*, 1054-62.

273. Suzuki, T.; Futaki, S.; Niwa, M.; Tanaka, S.; Ueda, K.; Sugiura, Y. *Journal of Biological Chemistry* **2002,** *277*, 2437-43.

274. Orchard, I.; Ramirez, J. M.; Lange, A. B. *Annual Review of Entomology* **1993,** *38*, 227-49.

275. Geng, C. X.; Sparks, T. C.; Skomp, J. R.; Gajewski, R. P. *Comparative Biochemistry and Physiology C-Pharmacology Toxicology & Endocrinology* **1993,** *106*, 275-84.

276. Kingan, T. G.; Hishinuma, A. *Comparative Biochemistry and Physiology C-Pharmacology Toxicology & Endocrinology* **1987,** *87*, 9-14.

277. Christensen, T. A.; Hildebrand, J. G. *Current Opinion in Neurobiology* **2002,** *12*, 393-99.

278. Maxwell, G. D.; Tait, J. F.; Hildebrand, J. G. *Comparative Biochemistry and Physiology C-Pharmacology Toxicology & Endocrinology* **1978,** *61*, 109-19.

279. Otsuka, M.; Iversen, L. L.; Hall, Z. W.; Kravitz, E. A. *Proceedings of the National Academy of Sciences of the United States of America* **1966,** *56*, 1110-&.

280. Kingan, T. G.; Hildebrand, J. G. *Insect Biochemistry* **1985,** *15*, 667-75.

281. Waldrop, B.; Christensen, T. A.; Hildebrand, J. G. *Journal of Comparative Physiology A-Sensory Neural and Behavioral Physiology* **1987,** *161*, 23-32.

282. Sparks, T. C.; Geng, C. X. *Analytical Biochemistry* **1992,** *205*, 319-25.

283. Sanes, J. R.; Hildebrand, J. G. *Developmental Biology* **1976,** *51*, 282-99.

284. Truman, J. W. *Journal of Experimental Biology* **1973,** *58*, 821-29.

285. Kloppenburg, P.; Ferns, D.; Mercer, A. R. *Journal of Neuroscience* **1999,** *19*, 8172-81.

286. Wu, Jin; Chen, Zhaohui; Dovichi, Norman J. *Journal of Chromatography B: Biomedical Sciences and Applications* **2000,** *741*, 85-88.

287. Hapuarachchi, S.; Aspinwall, C. A. *Electrophoresis* **2007,** *28*, 1100-06.

288. Gross, Larry; Yeung, Edward S. *Anal.Chem.* **1990,** *62*, 427-31.

289. Belder, D.; Schomburg, G. *Hrc-Journal of High Resolution Chromatography* **1992,** *15*, 686-93.

290. Bernardinelli, Y.; Haeberli, C.; Chatton, J. Y. *Cell Calcium* **2005,** *37*, 565-72.

291. Kottegoda, S.; Shaik, I.; Shippy, S. A. *Journal of Neuroscience Methods* **2002,** *121*, 93-101.

292. Kennedy, R. T.; Thompson, J. E.; Vickroy, T. W. *Journal of Neuroscience Methods* **2002,** *114*, 39-49.

293. Braun, K. L.; Aspinwall, C. A. *Dissertation, University of Arizona, Tucson* **2005**.